VAPOR-LIQUID EQUILIBRIUM IN THE THREE BINARY MIXTURES OF HEXANE, BENZENE, AND ETHANOL AT 25° C

By

VINSON C. SMITH

Bachelor of Science

Oklahoma State University

Stillwater, Oklahoma

1967

Submitted to the Faculty of the Graduate College
of the Oklahoma State University
in partial fulfillment of the requirements
for the Degree of
MASTER OF SCIENCE
May, 1970

VAPOR-LIQUID EQUILIBRIUM IN THE THREE BINARY MIXTURES OF HEXANE, BENZENE, AND ETHANOL AT 25° C

Thesis Approved:

Robert L. Robinson, Jr.
Thesis Adviser

John H. Erbar

J. Dunham
Dean of the Graduate College

PREFACE

Vapor-liquid equilibrium at 25° C was studied for the binary mixtures hexane-benzene, benzene-ethanol, and hexane-ethanol. An apparatus for measurement of solution vapor pressure was designed, constructed and tested with the mixtures mentioned. Vapor compositions were calculated from experimental measurements of solution vapor pressure and liquid composition. The significance of these calculated results has been discussed.

I am indebted to my adviser, Dr. R. L. Robinson, Jr., for his technical advice and guidance and his sincere interest for the duration of this project.

Discussions with my fellow graduate students were most beneficial in this study. Messers. C. J. Mundis and D. D. Dillard deserve special thanks for their help.

Phillips Petroleum Co. donated the research grade chemicals used in the project. Financial support during this study was gratefully received from Continental Oil Co., the National Science Foundation and the School of Chemical Engineering.

I express sincere appreciation to my wife, Anna Beth, for her patience and encouragement during my graduate studies.

TABLE OF CONTENTS

LIST OF TABLES

LIST OF FIGURES

NOMENCLATURE

A, B = van Laar constants in equations II-31 and II-32

A', B', C' = Redlich-Kister constants in equations II-33, II-34, and II-35

a, b, c, d = constants in equation II-53

C = condensation of variables defined by equations V-3 and V-4

D = number of data points

E_m = measured transducer output

E_i = voltage drop across the 1 ohm resistor

E^o = transducer output at full vacuum

F = condensation of variables defined by equation II-12

f = fugacity

f^o = standard state fugacity

G = molal Gibbs free energy

$\overline{G}_i^E$ = partial molal excess Gibbs free energy of component i

g^E = correction to excess Gibbs free energy defined by equation II-50

H = molal enthalpy

N = mole fraction

n = number of components

n_i = moles of component i

n_T = total number of moles in a mixture

P = pressure

P^* = pure component vapor pressure

R = Universal gas law constant

S = molal entropy

T = absolute temperature

v = molar volume

x = liquid phase mole fraction

y = vapor phase mole fraction

Greek Symbols

α = a specific value of x_1

β = second virial coefficient

β_{mix} = second virial coefficient of the mixture defined by equation II-16

γ = activity coefficient

Δ = spacing between adjacent values of x_1

Λ = Wilson parameters defined by equations II-37 and II-38

λ = Wilson parameters

ν_i^* = fugacity coefficient of pure i at pressure P_i^*

Π = mixture vapor pressure

Π_{calc} = calculated mixture vapor pressure

Σ = summation sign

σ = standard error of estimate as defined by equation V-7

ϕ = fugacity coefficient

Superscripts

E = excess thermodynamic property

L = liquid phase

M = thermodynamic mixing property

V = vapor phase

Subscripts

i	= component i
j	= component j
ii	= denotes pure i
jj	= denotes pure j
ij	= denotes interaction between components i and j
1	= component 1
2	= component 2

Miscellaneous

d	= differential operator
∂	= partial operator
exp	= exponential operator for e, the base of natural logarithms
ln	= natural logarithm
$\int$	= integral sign

CHAPTER I

INTRODUCTION

The complete identification of the thermodynamic mixing properties of a mixture requires a knowledge of both the heat of mixing and the excess Gibbs free energy of the mixture. Literature provides large amounts of both isothermal vapor-liquid equilibrium data (from which excess Gibbs energy may be calculated) and heat of mixing data. However, recent work at Oklahoma State University by Chao, Robinson, Smith, and Kuo (7) on solution theory has resulted in an awareness that systematic studies of the vapor-liquid equilibrium and heat of mixing in binary systems at the same temperature conditions are scarce. The lack of vapor-liquid equilibrium data on systems for which heat of mixing data are already available has led to the major objective of this study: to design, construct, and test a simplified apparatus for vapor-liquid equilibrium measurements.

In this study, vapor-liquid equilibrium data were determined from the measurements of mixture vapor pressure and liquid composition. The static vapor pressure method was chosen to avoid the tedious and often inaccurate experimental analysis of the vapor phase composition. Vapor pressure measurements at 25° C were taken over the entire composition range of the following systems:

1. normal hexane-benzene
2. benzene-ethanol

3. normal hexane-ethanol

These three non-ideal binary mixtures are combinations of organic compounds from the three groups: alkanes, aromatics, and alcohols.

Several authors report isothermal vapor-liquid equilibrium data for each of these systems at several temperatures (2, 3, 16, 19, 33, 35, 40), but no authors report equilibrium data for these systems at 25° C. However, heat of mixing data for each of these systems at 25° C has been reported (18). The systems used for testing the apparatus were chosen because they would yield excess Gibbs energy data which could be combined with existing heat of mixing data to complete the identification of pertinent mixing properties for each system at 25° C.

CHAPTER II

LITERATURE REVIEW

In the early stages of this study, a review of literature pertinent to the present work was undertaken. Literature concerning experimental apparatus, equilibrium data for the systems studied, thermodynamic principles of vapor-liquid equilibrium, and methods of data reduction were given special attention. Each of these topics will be discussed in this chapter.

Experimental Apparatus

Descriptions of apparatus used in previous vapor pressure studies were investigated for ideas which could be used in the present apparatus design.

Ljunglin (20) describes the apparatus which he used for solution vapor pressure measurements. His successful use of an absolute pressure transducer for pressure measurement led to the use of a transducer in the present study. Ljunglin's pressure transducer was connected to a 140 ml glass equilibrium cell. As in the present design, the entire apparatus was submerged in a controlled-temperature bath. A disadvantage of Ljunglin's design was his degassing apparatus. Ljunglin degassed pure materials by intermittent withdrawal of vapor from a storage flask over the period of a week. He then transferred the pure materials to the glass cell by distillation under vacuum.

The complicated transfer of degassed materials was avoided by Davison, Smith, and Chun (9). These authors describe an equilibrium cell with a built-in condenser that enables the mixture to be thoroughly degassed after it has been loaded in the equilibrium cell. This condenser feature has been used in the present study. Davison and co-workers used mercury-in-glass manometers for pressure measurement. A disadvantage of their apparatus was the use of two greased ball joints and a greased vacuum stopcock between the equilibrium cell and the manometer. In the present study, a greaseless high-vacuum stopcock was used to regulate flow from the equilibrium cell to the pressure transducer.

An apparatus described by Hermsen (14) consists of a metallic vapor pressure cell, sampling bulb, and null manometer. Pressure was measured with a mercury barometer. Additional degassing and sample loading equipment were used. Large laboratory jacks were used to raise and lower a thermostated bath beneath the equilibrium cell and null manometer. Hermsen's successful use of this equipment led to its further use by Harris (13).

Another successful vapor pressure apparatus is described by Scatchard, Wilson, and Satkiewicz (31). These authors use a glass equilibrium cell in conjunction with a null manometer and a main manometer. The equilibrium apparatus was maintained in an air thermostat.

The apparatus described by Hermsen and by Scatchard and co-workers were more complicated than desired in the present study. As previously stated, the apparatus used in this study was designed for simplicity without sacrifice of experimental accuracy.

Experimental Data

Chemical Abstracts from 1907 to July, 1968 and compilations of vapor-liquid equilibrium data by Chu (8) and Timmermans (34) were used to locate published equilibrium data for the systems studied. Although the literature provides no equilibrium data at 25° C, several authors report data for these systems at other temperatures. Available isothermal vapor-liquid equilibrium data for these systems are summarized in Table I.

TABLE I

SUMMARY OF AVAILABLE EQUILIBRIUM DATA

System	Temperatures, °C	Reference No.
Hexane-Benzene	55	(16)
Hexane-Benzene	60	(2)
Hexane-Benzene	70	(33)
Benzene-Ethanol	40, 50, 60	(35)
Benzene-Ethanol	45	(5)
Benzene-Ethanol	50	(40)
Benzene-Ethanol	55	(16)
Hexane-Ethanol	35, 45, 55	(19)
Hexane-Ethanol	55	(16)
Hexane-Benzene-Ethanol	55	(16)

Heat of mixing data for each of the binary mixtures and for the ternary mixture at 25° C have been measured and reported by Jones and Lu (18). For comparison with their data, these authors present the results of all previous heat of mixing studies for these systems at 25° C.

Thermodynamic Principles of Vapor-Liquid Equilibrium

A review of thermodynamic principles relevent to vapor-liquid equilibrium is presented in this section.

The fundamental criterion for phase equilibrium is the equality of the fugacity of each component in every phase. For vapor-liquid equilibrium,

$$f_i^L = f_i^V \tag{II-1}$$

where f_i = fugacity of component i, mm Hg.

The definition of the fugacity of a component in a mixture requires that,

$$\lim_{P \to 0} (\phi_i) = 1.0 \tag{II-2}$$

where $\phi_i = f_i/N_iP$ = fugacity coefficient of component i

and N_i = mole fraction of component i

P = system pressure, mm Hg.

An ideal solution may be defined as one which obeys the Lewis-Randall fugacity rule,

$$f_i = N_i f_i^\circ \tag{II-3}$$

where f_i° = fugacity of component i at a designated standard state.

For completely miscible mixtures, the standard state fugacity, f_i°, is chosen to be the fugacity of the pure component at the temperature and pressure of the mixture. Departures from ideal solution behavior are accounted for by defining the activity coefficient. For a component

in the liquid phase

$$\gamma_i^L = \frac{f_i^L}{x_i f_i^{\circ L}} \qquad \text{(II-4)}$$

where γ_i^L = liquid phase activity coefficient of component i.

x_i = mole fraction of component i in the liquid phase.

Equation II-1 may be substituted into equation II-4 to give

$$\gamma_i^L = \frac{f_i^V}{x_i f_i^{\circ L}} \qquad \text{(II-5)}$$

For mixtures at low pressures, the vapor phase is often assumed to behave as an ideal solution and as an ideal gas. At these conditions, equation II-2 is applicable. Therefore,

$$f_i^V = y_i \Pi \qquad \text{(II-6)}$$

where Π = mixture vapor pressure, mm Hg.

y_i = mole fraction of component i in the vapor phase

and,

$$f_i^{\circ L} = P_i^* \qquad \text{(II-7)}$$

where P_i^* = vapor pressure of pure component i at system temperature, mm Hg.

With these restrictions, equation II-5 may be written as

$$\gamma_i^L = \frac{y_i \Pi}{x_i P_i^*} \qquad \text{(II-8)}$$

Equation II-8 may be rearranged to give,

$$\sum_{i=1}^{n} y_i \Pi = \Pi = \sum_{i=1}^{n} \gamma_i^L x_i P_i^* \qquad \text{(II-9)}$$

where n = number of components in the mixture.

For a binary mixture,

$$\Pi = \gamma_1^L x_1 P_1^* + \gamma_2^L x_2 P_2^* \qquad \text{(II-10)}$$

If the liquid phase is assumed to be incompressible, equation II-8 may be modified in the following manner when vapor phase non-idealities are significant,

$$\gamma_i^L = \frac{y_i \Pi \phi_i^V}{x_i P_i^* \nu_i^* \exp\left[\frac{v_i^L(\Pi - P_i^*)}{RT}\right]} \qquad \text{(II-11)}$$

where $\phi_i^V = f_i^V/(y_i\Pi)$ = vapor phase fugacity coefficient of component i

$\nu_i^* = f_i^*/P_i^*$ = fugacity coefficient of pure i at system temperature and pressure P_i^*

$\exp\left[\frac{v_i^L(\Pi - P_i^*)}{RT}\right]$ = Poynting correction factor to the standard state fugacity of an incompressible liquid component i.

v_i^L = molar volume of component i at the system temperature, cc/gram mole

R = Universal gas law constant

T = absolute temperature, °K.

For convenience, the fugacity coefficients and Poynting correction factor are combined in the form

$$F_i = \frac{\phi_i^V}{\nu_i^* \exp\left[\frac{v_i^L(\Pi - P_i^*)}{RT}\right]} \qquad \text{(II-12)}$$

With this simplification, equation II-11 is rearranged to give equations analogous to equation II-9 and II-10.

$$\sum_{i=1}^{n} y_i \Pi = \Pi = \sum_{i=1}^{n} \frac{\gamma_i^L x_i P_i^*}{F_i} \qquad \text{(II-13)}$$

For a binary mixture,

$$\Pi = \frac{\gamma_1^L x_1 P_1^*}{F_1} + \frac{\gamma_2^L x_2 P_2^*}{F_2} \qquad \text{(II-14)}$$

Equation II-14 is the basic equation for indirect calculations of vapor-liquid equilibrium values from Π-x data.

When vapor phase non-idealities are significant, fugacity coefficients, ϕ_i^V and ν_i^*, may be calculated from an equation of state that expresses pressure-volume-temperature (PvT) behavior. For vapors at low to moderate pressures, the virial equation of state may be used. This equation, truncated after the second term, is

$$\Pi v/RT = 1 + \beta/v + \ldots\ldots \qquad \text{(II-15)}$$

where v = molar volume of the vapor phase, cc/gram mole

β = second virial coefficient, cc/gram mole.

When the virial equation is applied to a mixture, the virial coefficient,

β_{mix} must be calculated by the relationship

$$\beta_{mix} = \sum_{i=1}^{n} \sum_{j=1}^{n} y_i y_j \beta_{ij} \qquad \text{(II-16)}$$

where β_{ii} and β_{jj} = pure component second virial coefficients

$\beta_{ij(i\neq j)}$ = second interaction virial coefficient of components i and j.

For a binary mixture,

$$\beta_{mix} = y_1^2 \beta_{11} + 2y_1 y_2 \beta_{12} + y_2^2 \beta_{22} \qquad \text{(II-17)}$$

O'Connell and Prausnitz (23) show that the relation of fugacity coefficient to the virial equation, truncated after the β term, is

$$\ln \phi_i^V = (2/v) \sum_{j=1}^{n} y_j \beta_{ij} - \ln(\Pi v/RT) \qquad \text{(II-18)}$$

For a binary mixture, equation II-18 gives,

$$\ln \phi_1^V = (2/v)(y_2 \beta_{12} + y_1 \beta_{11}) - \ln(\Pi v/RT) \qquad \text{(II-19)}$$

$$\ln \phi_2^V = (2/v)(y_1 \beta_{12} + y_2 \beta_{22}) - \ln(\Pi v/RT) \qquad \text{(II-20)}$$

Equation II-18, simplified for calculating fugacity coefficients of pure components, gives

$$\ln \nu_i^* = (2/v_i)(\beta_{ii}) - \ln(P_i^* v_i/RT) \qquad \text{(II-21)}$$

Use of the virial equation for calculating fugacity coefficients by the above equation is dependent on the availability of pure component

and interaction virial coefficients. Several correlations for the calculation of second virial coefficients have been reported. A correlation by O'Connell and Prausnitz (23) was used in this study.

A brief discussion of thermodynamic mixing properties is now presented. Chao (6) defines mixing properties as, "the change in properties accompanying the formation of the mixture from its pure components at the same temperature and pressure as the mixture." For example,

$$H^M = H - \sum_{i=1}^{n} x_i H_i \qquad \text{(II-22)}$$

where H^M = molal heat of mixing, cal/gram mole

H = molal enthalpy of the mixture, cal/gram mole

H_i = molal enthalpy of pure component i, cal/gram mole.

Other thermodynamic mixing properties may be defined by similar equations. Hougen and co-workers (17) show that for an ideal solution,

$$H^M = 0 \qquad \text{(II-23)}$$

and

$$G^M = -TS^M = RT \sum_{i=1}^{n} x_i \ln(x_i) \qquad \text{(II-24)}$$

where G^M = molal Gibbs free energy of mixing, cal/gram mole

S^M = molal entropy of mixing, cal/(gram mole)(°K).

Excess properties of mixing may be defined as the difference in actual mixing properties and the mixing properties of an ideal solution. Applying this definition and equations II-23 and II-24

$$H^E = H^M \qquad \text{(II-25)}$$

$$G^E = G^M - RT \sum_{i=1}^{n} x_i \ln(x_i) \qquad \text{(II-26)}$$

and

$$TS^E = TS^M + RT \sum_{i=1}^{n} x_i \ln(x_i) \qquad \text{(II-27)}$$

where the superscript E denotes an excess molal property of mixing. If two of the above three excess properties are known, the third property can be calculated by the relationship defining Gibbs free energy,

$$G^E = H^E - TS^E \qquad \text{(II-28)}$$

Excess Gibbs free energy of mixing is related to activity coefficient by the useful relationships

$$G^E = RT \sum_{i=1}^{n} x_i \ln(\gamma_i^L) \qquad \text{(II-29)}$$

and

$$RT\ln(\gamma_i^L) = \left[\frac{\partial(n_T G^E)}{\partial n_i}\right]_{T,P,n_{j\neq i}} = \overline{G}_i^E \qquad \text{(II-30)}$$

where $\overline{G}_i^E$ = partial molal excess Gibbs energy of component i, cal/gram mole

n_i = moles of component i

$n_T = \sum_{i=1}^{n} n_i$ = total moles in the mixture.

The reader is referred to the text by Hougen and co-workers (17) for the derivation of these relationships.

Methods for Data Reduction

Several methods have been proposed for the calculation of vapor-liquid equilibrium data from experimental liquid composition-vapor pressure data. Ljunglin and Van Ness (20) classify these methods as being either direct or indirect. A brief discussion of the direct method is followed by a more detailed discussion of two indirect methods.

Direct Method

The direct method presented by Ljunglin involves integration of the coexistence equation, a first order differential equation which must be satisfied when phases coexist at equilibrium. Starting with a general form of the Gibbs-Duhem equation, Ljunglin derives a completely general form of the coexistence equation. Simplification of the general equation for either a constant temperature or a constant pressure case and the use of an equation of state result in a form of the equation suitable for numerical integration.

The main disadvantage of Ljunglin's direct method is that the calculation cannot be carried through an azeotrope point where the derivative of vapor pressure with respect to liquid composition, $d\Pi/dx = 0$. One must work from both ends of the Π-x curve toward the azeotrope.

Indirect Methods

The indirect methods involve the calculation of liquid phase activity coefficients from which vapor phase compositions are calculated. Barker (1) proposed the use of a model relating activity coefficient to liquid composition. Parameters for the selected model must be calculated to give the best fit to the experimental vapor pressure data.

Three different models expressing the composition dependence of activity coefficient were used in this study. Van Laar (36) proposed equations of the form

$$\ln(\gamma_1) = \frac{Ax_2^2}{(Ax_1/B + x_2)^2} \qquad \text{(II-31)}$$

and

$$\ln(\gamma_2) = \frac{Bx_1^2}{(Bx_2/A + x_1)^2} \qquad \text{(II-32)}$$

where the parameters A and B are characteristic van Laar constants for each binary mixture.

Redlich and Kister relate excess Gibbs free energy to liquid composition by a series function,

$$G^E/RT = x_1x_2[A' + B'(x_1-x_2) + C'(x_1-x_2)^2 + ..] \qquad \text{(II-33)}$$

where A', B', C' .... = Redlich-Kister constants for the mixture. Several terms may be used in this series function to accurately fit the experimental data. Redlich-Kister equations with two, three, and four parameters were used in this study. Equation II-33 may be differentiated according to equation II-30 to obtain expressions for binary mixture activity coefficients,

$$\ln(\gamma_1) = x_1x_2[A' + B'(x_1-x_2) + C'(x_1-x_2)^2 + ...]$$

$$+ x_2[A'(x_2-x_1) + B'(6x_1x_2-1) \qquad \text{(II-34)}$$

$$+ C'(x_1-x_2)(8x_1x_2-1) + ..]$$

and $$\ln(\gamma_2) = x_1 x_2[A' + B'(x_1-x_2) + C'(x_1-x_2)^2 + \ldots]$$

$$- x_1[A'(x_2-x_1) + B'(6x_1x_2-1) \qquad \text{(II-35)}$$

$$+ C'(x_1-x_2)(8x_1x_2-1) + ..]$$

Wilson (31) derived an expression for excess Gibbs energy applicable to multicomponent mixtures. The equation is

$$G^E/RT = - \sum_{i=1}^{n} x_i \ln[\sum_{j=1}^{n} x_j \Lambda_{ij}] \qquad \text{(II-36)}$$

where $$\Lambda_{ij} = v_j^L/v_i^L \exp -[(\lambda_{ij}-\lambda_{ii})/RT] \qquad \text{(II-37)}$$

and $$\Lambda_{ji} = v_i^L/v_j^L \exp -[(\lambda_{ij}-\lambda_{jj})/RT] \qquad \text{(II-38)}$$

The physical significance of Wilson's parameters λ_{ij} and λ_{ii} is explained by Orye and Prausnitz (24). They point out that whereas $\lambda_{ij} = \lambda_{ji}$, $\Lambda_{ij} \neq \Lambda_{ji}$. Activity coefficients may be obtained from equation II-36 by applying equation II-30. The result is

$$\ln(\gamma_k) = -\ln[\sum_{j=1}^{n} x_j \Lambda_{kj}] + 1 - \sum_{i=1}^{n} \frac{x_i \Lambda_{ik}}{\sum_{j=1}^{n} x_j \Lambda_{ij}} \qquad \text{(II-39)}$$

Equation II-39 may be used with equation II-11 to predict multicomponent vapor-liquid equilibrium data if the constants Λ_{ij} and Λ_{ji} are known for each pair of components in the multicomponent mixture. For binary mixtures equation II-39 reduces to

$$\ln(\gamma_1) = -\ln(x_1 + \Lambda_{12}x_2) + x_2\left[\frac{\Lambda_{12}}{x_1 + \Lambda_{12}x_2} - \frac{\Lambda_{21}}{\Lambda_{21}x_1 + x_2}\right] \quad \text{(II-40)}$$

and $$\ln(\gamma_2) = -\ln(x_2 + \Lambda_{21}x_1) - x_1\left[\frac{\Lambda_{12}}{x_1 + \Lambda_{12}x_2} - \frac{\Lambda_{21}}{\Lambda_{21}x_1 + x_2}\right] \quad \text{(II-41)}$$

The main disadvantage of Barker's indirect method is that some model must be chosen to express the activity coefficient-composition relationship. For some mixtures, no activity coefficient expression results in a good fit of experimental Π-x data.

This disadvantage may be avoided by an indirect method described by Mixon, Gumowski, and Carpenter (22). Instead of using a model for activity coefficient, these authors use an iterative numerical calculation of activity coefficient. This numerical calculation is based on equations for the partial molal excess Gibbs free energy developed by Dodge (10). For a binary mixture these equations are

$$\overline{G}_1^E = G^E + \left(\frac{\partial G^E}{\partial x_1}\right)_{T,P} - x_1\left(\frac{\partial G^E}{\partial x_1}\right)_{T,P} \quad \text{(II-42)}$$

and $$\overline{G}_2^E = G^E - x_1\left(\frac{\partial G^E}{\partial x_1}\right)_{T,P} \quad \text{(II-43)}$$

Substitution of equations II-42 and II-43 into equation II-30 gives

$$RT\ln(\gamma_1^L) = G^E + \left(\frac{\partial G^E}{\partial x_1}\right)_{T,P} - x_1\left(\frac{\partial G^E}{\partial x_1}\right)_{T,P} \quad \text{(II-44)}$$

and $$RT\ln(\gamma_2^L) = G^E - x_1\left(\frac{\partial G^E}{\partial x_1}\right)_{T,P} \quad \text{(II-45)}$$

Equations II-44 and II-45 may be solved for activity coefficients to give

$$\gamma_1^L = \exp\left[\frac{G^E + (\partial G^E/\partial x_1)_{T,P} - x_1(\partial G^E/\partial x_1)_{T,P}}{RT}\right] \quad \text{(II-46)}$$

and

$$\gamma_2^L = \exp\left[\frac{G^E - x_1(\partial G^E/\partial x_1)_{T,P}}{RT}\right] \quad \text{(II-47)}$$

In Mixon's method, equally spaced values of x_1 are used. For every value of x_1 there are corresponding values of Π and G^E. With this restriction, values of $(\partial G^E/\partial x_1)_{T,P}$ may be calculated by the finite difference expression

$$\left(\frac{\partial G^E}{\partial x_1}\right)_{x_1 = \alpha} = \frac{G^E_{(\alpha + \Delta)} - G^E_{(\alpha - \Delta)}}{2\Delta} \quad \text{(II-48)}$$

where α = value of x_1 for which $\partial G^E/\partial x_1$ is evaluated

Δ = spacing between adjacent values of x_1.

Equations II-46, II-47, and II-48 may be substituted into equation II-10 to give

$$\Pi = x_1 P_1^* \exp\left[\frac{1}{RT}\left(G^E_\alpha + \frac{G^E_{\alpha+\Delta} - G^E_{\alpha-\Delta}}{2\Delta} - x_1\left\{\frac{G^E_{\alpha+\Delta} - G^E_{\alpha-\Delta}}{2\Delta}\right\}\right)\right] + x_2 P_2^* \exp\left[\frac{1}{RT}\left(G^E - x_1\left\{\frac{G^E_{\alpha+\Delta} - G^E_{\alpha-\Delta}}{2\Delta}\right\}\right)\right] \quad \text{(II-49)}$$

With the initial assumption that $G^E = 0$ at each of the equally spaced values of x_1, equation II-49 is used to calculate a value of Π corresponding to each value of x_1. Calculated values of Π are compared with the experimental values. Mixon outlines a technique by which

improved values of G^E are calculated as

$$G^E_{new} = G^E_{old} + g^E \qquad \text{(II-50)}$$

where g^E = correction to previous value of G^E.

Values of G^E_{new} are then used in equation II-49 for the calculation of Π. This iterative procedure of improving the values of G^E and calculating values of Π is repeated until calculated pressures agree with experimental values within a specified tolerance.

After the pressure calculations converge, vapor compositions are calculated by arranging equation II-8 in the form

$$y_1 = \frac{\gamma_1^L x_1 P_1^*}{\Pi} \qquad \text{(II-51)}$$

The values of y_1 calculated by equation II-51 are based on the assumption of an ideal vapor phase.

The Mixon method may be extended to include corrections for a non-ideal vapor phase. Values of y_1 calculated by equation II-51 are used to calculate fugacity coefficients from equations II-19 and II-20. These values of ϕ_1 and ϕ_2 are used with values of pure component fugacity coefficients and Poynting correction factors for the calculation of Π by equation II-14. If these values of Π differ from the experimental values, Mixon's iterative process of improving G^E must be repeated. After pressure calculations converge again, new values of y_1 are calculated by a form of equation II-11

$$y_1 = \frac{\gamma_1^L x_1 P_1^*}{F_1 \Pi} \qquad \text{(II-52)}$$

The entire iterative procedure is continued until all values of y_1 agree with previous values of y_1 within a specified tolerance.

The method developed by Mixon and co-workers has one disadvantage. The experimental data must be smoothed for the determination of Π values at equally spaced intervals of x_1. Mixon suggests that the Π-x data can be smoothed by a polynomial

$$\Pi = a + bx_1 + cx_1^2 + dx_1^3 + ex_1^4 + ... \qquad \text{(II-53)}$$

where the constants a, b, etc. are determined by statistical methods. This author believes that use of equation II-53 cancels the main advantage of Mixon's method which was to avoid using a model in fitting the Π-x data. For this reason, values of Π at mole fraction intervals of 0.05 were determined from large plots of the experimental Π-x data in this study.

All methods for calculating equilibrium data from solution vapor pressures have one common disadvantage. Since each method depends on some form of the Gibbs-Duhem equation, this cannot be used to test the experimental data for thermodynamic consistency. Other techniques must be used to determine the consistency of the data.

CHAPTER III

APPARATUS AND MATERIALS

The measurement of mixture vapor pressure was accomplished by using a glass equilibrium cell connected to an absolute pressure transducer. A vacuum system was used for degassing the cell, transducer, and materials. Isothermal equilibrium was attained by submerging the cell and transducer in a constant temperature bath. Additional equipment was used for preparation and analysis of each liquid mixture. The details of these apparatus and the materials used are discussed in this chapter.

Vapor Pressure Apparatus

Equilibrium Cell

An equilibrium cell was constructed from pyrex glass. Each mixture was introduced into the cell before the degassing phase of the experimental procedure. By using a single cell for both degassing and pressure measurement, the construction of a separate degassing apparatus was not required. The tedious process of transferring "degassed" materials to the vapor pressure cell was also avoided. The cell is illustrated in Figure 1. (Letters used below refer to Figure 1.)

Stopcock A controlled flow to and from sidearms B and C and compartment D. The stopcock was a greaseless, high vacuum, 3-way stopcock. (See Appendix A for catalog numbers and specifications of all

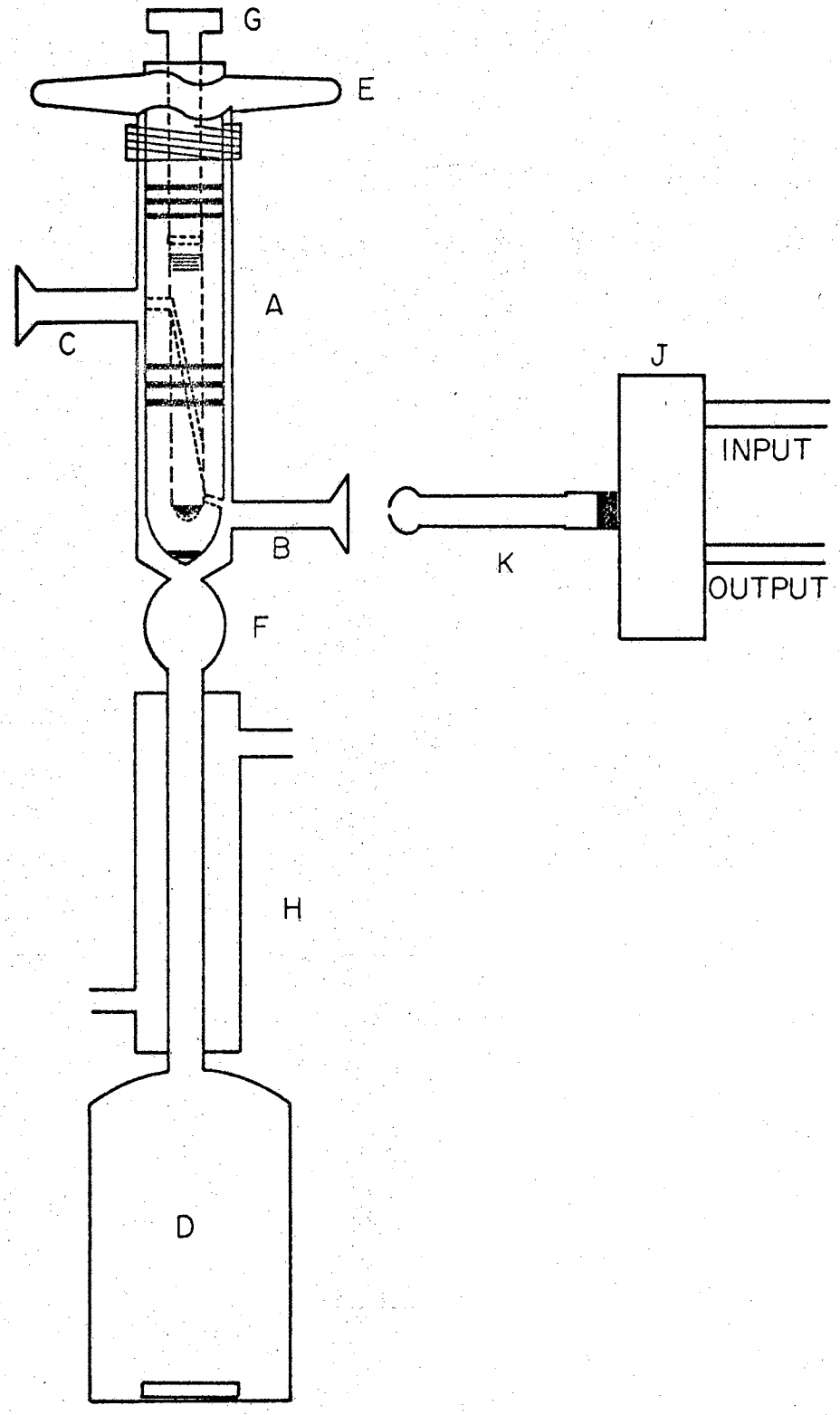

Figure 1. Equilibrium Cell

commercial items such as the 3-way stopcock.) Three O-rings above sidearm C and three O-rings above sidearm B provide vacuum tight seals between the teflon plug E and the glass walls of the stopcock. Plug E can be screwed up and down to open or close compartment D to sidearm B. When the plug is all the way in the down position, a small O-ring seats directly above expansion F to form a vacuum tight seal. Inside of the plug is a valve G which opens sidearm B to sidearm C. O-rings are used for vacuum seals between the valve and the inside of the plug. When both the plug and the valve are in the up position, both sidearms and the compartment are simultaneously open.

Each of the two sidearms is five cm long and has an 18/9 pyrex socket attached at its end. Compartment D was constructed from cylindrical glass tubing and has a volume of 42 cc. A small glass encapsulated magnetic spinbar rests in the bottom of the compartment. Compartment D is connected to expansion F by condenser H. The condenser which is twelve cm long has an inner tube of ten mm diameter and an outer tube of 25 mm diameter.

Transducer and Electrical Circuit

Vapor pressures were measured with an absolute pressure transducer, J. (See Appendix A for transducer specifications.) The transducer was installed in a waterproof adapter. The kovar end of a kovar to pyrex seal was connected to the transducer adapter by a Swagelok male connector. An 18/9 ball member was attached to the pyrex end of the kovar seal. Total length of the extension K from the transducer adapter was five cm. During the final degassing and pressure measurement phases of the experimental procedure, the ball member of extension K was

clamped to the socket member of sidearm B.

Figure 2 shows a schematic diagram of the electrical circuit used with the pressure transducer. (Letters used below now refer to Figure 2.) The pressure transducer A required an excitation of 5 volts dc which was supplied by power supply B. Output from the transducer ranged from about -4 mv at vacuum to about 11 mv at atmospheric pressure. This output was read to the nearest 0.0001 mv on potentiometer C. Power supply E provided 2 volts dc input to the potentiometer. Galvanometer D was used as a null indicator.

A 1 ohm precision resistor and a 2000 ohm precision resistor were connected in series. This resistor circuit was connected in parallel with the input leads of the transducer. Therefore, the voltage drop across the resistor circuit equaled the voltage supplied to the pressure transducer. Output leads were connected to the 1 ohm resistor so that the voltage drop across this resistor could be monitored. The output leads from the transducer and the output leads from the 1 ohm resistor were connected at different positions of a two gang multiple selector switch F. Leads from the common terminal of the switch led to the load terminals of the potentiometer.

A potential drop of 5 volts across each branch of the parallel circuit is equivalent to a drop of 2.5 mv across the 1 ohm resistor. Before each run, the power supply was adjusted so that the galvanometer indicated a null when the potentiometer indicated a 2.5 mv drop across the 1 ohm resistor. Before each pressure reading, the voltage drop across the 1 ohm resistor was measured. This voltage drop had normally drifted from the initial setting of 2.5 mv. (Deviations from 2.5 mv were always less than ±0.001 mv.) To correct for this slight drift,

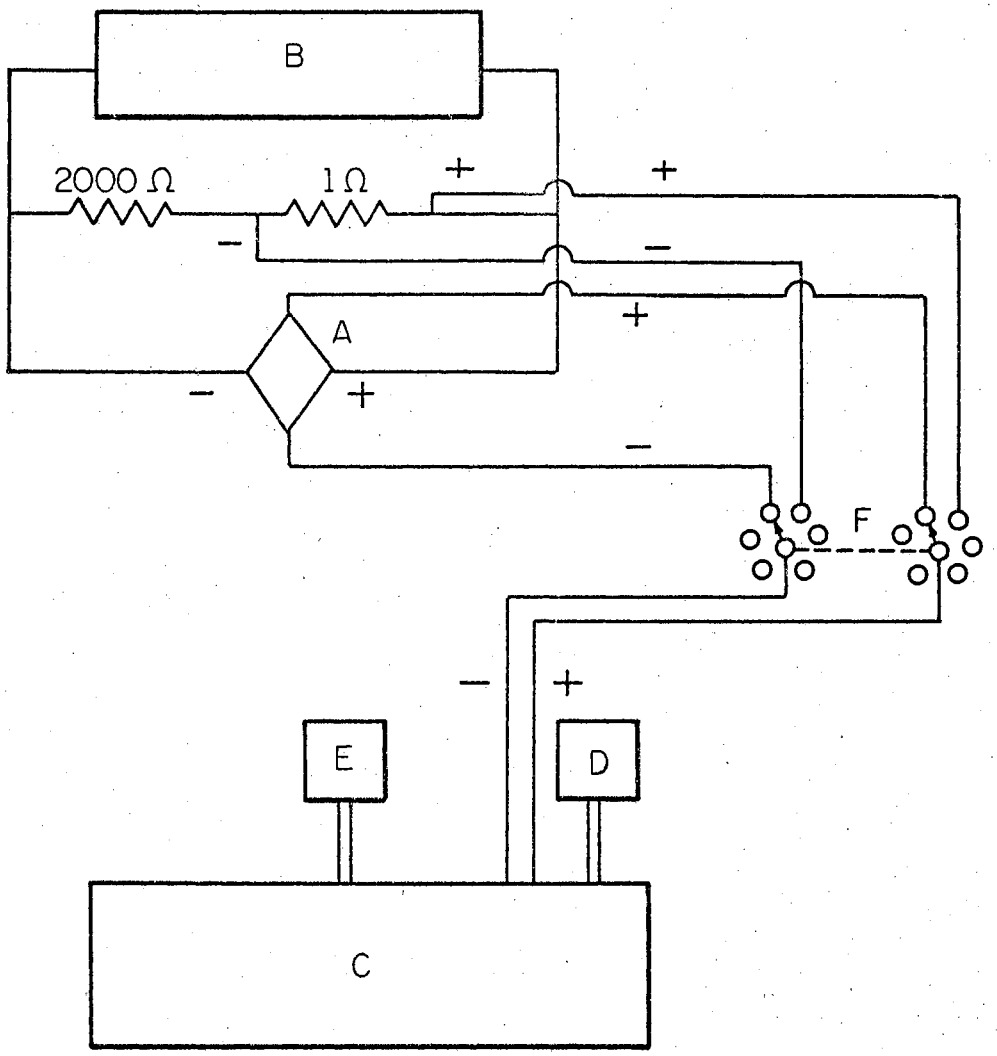

Figure 2. Schematic Diagram of Electrical Circuit

the following correction formula was used for each pressure reading:

$$E_c = E_m(E_i/2.5 \text{ mv}) \qquad \text{(III-1)}$$

where E_c = corrected transducer output, mv

E_m = measured transducer output, mv

E_i = voltage drop across the 1 ohm resistor, mv

This correction formula results from the proportional relationship between the output of the transducer and its excitation.

The transducer was calibrated at 25° C against a Texas Instruments fused quartz precision pressure gage which had been calibrated by the manufacturer. The precision gage could be read to the nearest 0.01 mm Hg. Due to drift in the transducer output at full vacuum (1 micron) the transducer was calibrated relative to its output at full vacuum. Evaluation of the calibration data resulted in the following polynomial:

$$\Pi = 0.0132 + 48.9091(E_c - E_c^\circ) - 0.01537\ (E_c - E_c^\circ)^2 \qquad \text{(III-2)}$$

where E_c° = corrected transducer output at full vacuum, mm Hg.

Values of Π calculated from this polynomial deviated from the true pressures as indicated by the quartz tube gage by an average of less than 0.04 mm Hg.

Degassing Apparatus

A leak tight vacuum system was constructed for degassing the apparatus and materials. A vacuum manifold with two greased stopcocks was constructed from glass tubing. Flexible rubber vacuum tubing connected the "left" stopcock of the manifold to the "low pressure" side of a

cartesian manostat. On the "high pressure" side of the manostat, vacuum tubing led to a glass "T" which was connected to (1) a Bourdon vacuum guage and (2) an 18/9 glass ball. The manostat was used to regulate the degree of vacuum in the equilibrium cell during the first phase of degassing. The "right" stopcock was connected directly to an 18/9 ball member by vacuum tubing. A full vacuum of 1 micron could be pulled on the equilibrium cell through the "right" stopcock by clamping its ball member to one of the sidearms of the equilibrium cell.

Pressure in the vacuum system was measured with a McLeod gage. A cold trap immersed in liquid nitrogen was used to trap condensable materials before they reached the pump. A schematic diagram of the vacuum system appears in Figure 3 below.

Constant Temperature Bath

The constant temperature bath was a commercial unit. Dimensions of the bath were 15 in. by 12 in. by 13 in. Water was the bath fluid. Heat was supplied to the bath by two immersion heaters. One of the heaters was intermittent and one was auxiliary. Both heaters were controlled by a thermoregulator operating in conjunction with a relay. Water chilled to 40° F by a commercial water chiller was pumped through a coil of copper tubing submerged in the bath. The flow rate of the cooling water was regulated so that the off-on cycle of the intermittent heater had a period of approximately two minutes. The bath fluid was mixed by a heavy duty stirrer driven by a 1/30 hp motor.

The temperature of the bath was measured with a mercury-in-glass thermometer which had divisions of 0.01° C. The mercury thermometer was calibrated against a platinum resistance thermometer which had been

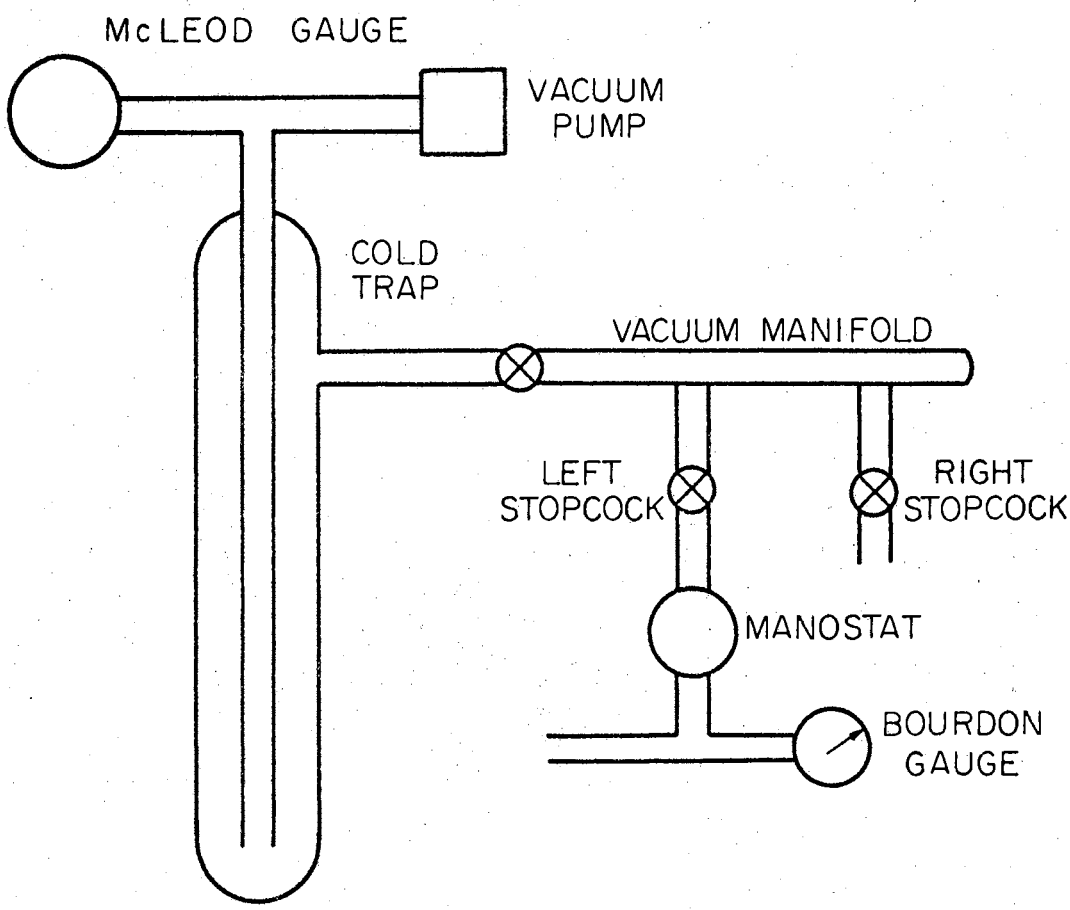

Figure 3. Schematic Diagram of Vacuum System

calibrated by the National Bureau of Standards. When operating at 25° C, the bath temperature could be controlled to within ±0.015° C.

A water driven magnetic stirrer which rested in the bottom of the bath was used to turn the spinbar in the equilibrium cell while the mixture was reaching isothermal equilibrium.

Support Frame and Table

The temperature bath, equilibrium cell, and vacuum manifold were mounted on a frame and table which were constructed from slotted angle iron and plywood. Dimensions of the frame were 3 ft by 2 ft. by 2.5 ft. A plywood backboard which had a height of 2.5 ft. extended vertically at the rear of the frame.

A sheet of plywood bolted to the frame 9 inches above the floor supported the temperature bath. The top of the bath was flush with the top of the frame. The main working table extended from the left edge of the frame to the top left edge of the temperature bath.

Two aluminum rods attached to the plywood backboard extended horizontally above the temperature bath. Another aluminum rod was clamped vertically to the horizontal rods. A clamp was also provided to secure the equilibrium cell in its position with the transducer. The cell and transducer could be lowered into the bath by loosening the clamps which held the vertical rod.

The vacuum manifold was supported by clamps and rods extending from the backboard. The equilibrium cell was supported in a similar manner during the first phase of degassing.

Mixture Preparation and Transfer Apparatus

Small glass bottles were used to hold the pure components and the liquid mixture before each run. Glass syringes were used to transfer the pure components to the mixture bottle and to transfer the mixture to the equilibrium cell.

A Metler balance was used for the gravimetric preparation of each liquid mixture. The balance could be read to the nearest 0.01 mg and it had a rated accuracy of ±0.02 mg.

Liquid Composition Analysis Apparatus

A refractometer was used to compare the liquid composition before and after each run for the systems hexane-benzene and benzene-ethanol. The refractometer had a rated accuracy of ±0.00003 units. Conventional temperature control equipment was used to maintain the prisms of the refractometer at 25° C.

Materials

The organic chemicals used in this study are listed below with the manufacturer's specified minimum purity:

Normal hexane	Phillips Petroleum Co.	99.99 mole %
Benzene	Phillips Petroleum Co.	99.91 mole %
Ethanol	U. S. Industrial Chem. Co.	Reagent Quality

All chemicals were used as received. Phillips Petroleum Company indicated that the impurities in the normal hexane were methylcyclopentane and 3-methylpentane and that the impurity in benzene was most

probably toluene. The chemicals were stored over molecular sieve to remove water which might have been absorbed from the atmosphere.

CHAPTER IV

EXPERIMENTAL PROCEDURE AND RESULTS

The experimental methods used to obtain data for this study are described below. A tabulation of experimental results is included in this chapter.

Mixture Preparation and Composition Analysis

At the beginning of each experimental run, a mixture having a desired overall composition was prepared gravimetrically. Details of the mixture preparation and composition analysis are as follows.

To begin the preparation of each binary mixture, portions of each pure component were transferred through funnels to separate 60 cc bottles. The volume of each component necessary for the preparation of a binary mixture having a total volume of 45 ml and a known molar composition had been calculated.

A clean, dry glass bottle and its attached lid were placed on the pan of the Metler balance. The mass of the bottle as indicated by the balance was recorded. The bottle was removed from the pan, and the desired volume of component 1 was delivered to the bottle through a hypodermic syringe. The lid was screwed on and the bottle and its contents were weighed on the balance. This weight was recorded. In like manner, the desired volume of component 2 was delivered to the mixture bottle. Again the bottle and its contents were weighed and the weight

was recorded. The mass of each component in the mixture was calculated by difference. The number of moles of each component and the mole fraction of each component were calculated by the usual methods.

The gravimetric determination of liquid composition as described above was chosen for its simplicity and high accuracy. However, a major concern was whether or not this liquid composition remained constant during the experimental procedure, which included degassing. To determine whether or not a composition change occurred, the refractive index of each mixture was measured before and after each run. By assuming that refractive index is a linear function of mole fraction, an estimate of the change in mole fraction of the mixture could be determined from the difference in refractive index before and after each run. If the change in composition had been appreciable, the true mixture composition could have been determined directly from the refractive index of the mixture after the run by using an experimentally determined index of refraction-liquid composition relationship.

The refractometer described in the previous chapter was used according to the manufacturer's instruction manual. The maximum change in mole fraction for 21 runs with the systems hexane-benzene and benzene-ethanol was 0.002. The average change in mole fraction was less than 0.001. Since this change was not considered appreciable, refractive index was not measured for the hexane-ethanol runs.

Loading the Cell

The equilibrium cell was secured in its clamp above the table. A 12 inch length of teflon "spaghetti" tubing was pushed through sidearm B into the condenser until one end of the tubing reached the bottom

of compartment D. (See Figure 1.) The other end of the tubing remained outside sidearm B. A total of 38 ml of the mixture was transferred by a syringe through the teflon tubing into the cell. After the cell was loaded, plug E and valve G were both closed to prevent further contact of the mixture with the atmosphere.

Degassing the Mixture and Apparatus

Degassing was one of the most critical phases of the experimental procedure. The elimination of all air from the mixture and apparatus was essential for the accurate measurement of mixture vapor pressure. The degassing procedure was divided into two phases; each phase will be described separately.

Boiling-Condensation

The boiling-condensation procedure for degassing the mixture was an adaptation of the method described by Davison, Smith, and Chun (9).

Immediately after the cell was loaded, the 18/9 ball member connected to the glass "T" was clamped to the socket of sidearm B. A 100 ml glass beaker wrapped with electrical heating tape was brought up around the compartment of the cell. The beaker was held in this position while an electrical magnetic stirrer was brought into position beneath the beaker. Water was poured into the beaker submerging the compartment. The leads from the heating tape were plugged into the receptacle of a variable powerstat. Water at 40° F was pumped from the water chiller through tygon tubing and circulated through the condenser above compartment D.

With the degassing apparatus in the position described, the left stopcock of the vacuum manifold was opened and the manostat was adjusted for the desired pressure in the equilibrium cell. The desired pressure was 200 mm Hg for the less volatile mixtures and ranged up to 300 mm Hg for the more volatile mixtures. By opening plug E of the equilibrium cell the pressure in the compartment was lowered to the pressure indicated by the gauge. Air bubbles could be seen rising to the surface of the mixture. The magnetic stirrer was adjusted so that the spinbar stirred the mixture at a moderate rate.

Heat was supplied through the electrical heating tape until the mixture reached its boiling temperature. By adjusting the variable powerstat the mixture received just enough heat to boil smoothly. As the mixture boiled, the vapors condensed in the lower portion of the condenser and returned to the cell.

After boiling with complete condensation had continued for about one hour, the flow of cooling water was discontinued; the tygon tubing was disconnected from the condenser, and the water was drained from the condenser. Air was forced out of the system as the ring of condensation progressed up the inner condenser tube. When the first vapors were observed condensing above the bottom O-ring, plug E was tightly closed to prevent appreciable change in mixture composition by loss of vapors from the system. The manostat was fully opened to allow the small amount of condensed material to be removed from the stopcock portion of the equilibrium cell. With this final step, the first phase of degassing was complete.

Pumping Above Frozen Mixture

The left stopcock of the manifold was closed and the cell was removed from its position above the table. The ground glass socket on sidearm B and the ball extending from the transducer adapter were lightly lubricated with stopcock grease. The cell was then clamped in position with the transducer above the water bath. The ball member connected to the right stopcock of the manifold was clamped to the socket of sidearm C. This stopcock and valve G were opened. A full vacuum resulted in thorough degassing of the 3-way stopcock and the glass tubing which led to the transducer.

A piece of plywood was supported on the front and back edges of the water bath. A dewar flask was brought up around the compartment of the equilibrium cell and supported by the plywood. Liquid nitrogen was poured into the dewar flask until the compartment was submerged.

After the mixture was completely frozen (30 minutes was allowed for freezing) plug E was opened so that a full vacuum was attained above the frozen mixture. Ideally, any air which remained in the system after the boiling phase of degassing was removed by pumping above the solid for a period of about one hour. Care was taken to keep the compartment submerged in liquid nitrogen during this one hour period.

Hermsen and Prausnitz (14) state that an indication of complete degassing of a mixture is the absence of bubbles leaving the solid as it thaws. This criterion for complete degassing was used in this study.

Plug E was shut and the dewar was removed from its position. A

stream of dry compressed air was sprayed on the compartment of the cell to remove frost which formed on the cold glass cell. The removal of frost was essential for clear observation of the melting process. Observation of a single bubble during melting indicated incomplete degassing.

The freezing-pumping process was repeated at least one time to check for complete degassing. If no bubbles were observed during the second thaw, degassing was considered complete. If less than three bubbles were observed during the second thaw, an attempt was made to complete the degassing by repeating the freezing technique. If more than three bubbles were observed during the second thaw, the boiling phase was repeated before further freezings were attempted. It was necessary to repeat the boiling phase for four of the 33 experimental runs.

Establishing Equilibrium and Pressure Measurement

Isothermal equilibrium between liquid and vapor phases is easily established when static rather than dynamic methods (such as circulating stills) are used. Details of this step are described below.

After the mixture had been thoroughly degassed, valve G of the equilibrium cell was tightly closed to prevent loss of the vacuum which had been established in sidearm B and extension K. The right stopcock of the manifold was closed and the ball joint at sidearm C was disconnected.

The equilibrium cell-transducer assembly was lowered into the constant temperature bath by loosening the clamps which held the vertical support rod. The rod was lowered until the transducer was completely

submerged and the bottom of the cell touched the water powered magnetic stirrer. The assembly was held in this position by tightening the clamps on the support rod.

The vacuum tubing which held the glass ball member was removed from the right stopcock of the manifold. This tubing was replaced with a short section of vacuum tubing which led through a 20 inch piece of 3/8 in. o.d. copper tubing to another section of rubber tubing which held an 18/9 ball member. This new extension from the stopcock was exactly long enough to reach the socket of sidearm C after the cell was submerged. The ball joint was tightly clamped in this new position. The stopcock at the manifold and the valve on the equilibrium cell were opened so that degassing of the apparatus could continue.

The solution was stirred at a moderate rate by circulating tap water through the magnetic stirrer. The temperature of the bath was checked and the temperature controller was adjusted if necessary. One hour was allowed for the mixture and transducer to reach the bath temperature of 25° C. During this one hour period, the output voltage of the transducer at full vacuum was observed. This output and the corresponding voltage drop across the one ohm resistor were recorded. The corrected transducer output, E_c°, would be used in the calculation of pressure by equation III-2.

After the system reached the bath temperature, valve G was closed so that the vacuum pump did not pull on any portion of the apparatus below sidearm C. Plug E was opened 1 1/2 turns so that the vapor phase of the mixture could expand above the bottom O-ring and into the evacuated glass tubing leading to the transducer.

Preliminary experimental runs showed that heat added to the mixture by movement of the magnetic spinbar caused a slight increase in mixture temperature and a slightly inaccurate vapor pressure. Therefore, flow of water through the magnetic stirrer was discontinued five minutes after plug E was opened. Five minutes later, the first pressure reading was taken. The voltage output of the transducer and the voltage drop across the 1 ohm resistor were recorded. These measurements were repeated at five minute intervals until the pressure changed not more than 0.02 mm Hg during a ten minute period, i. e., the transducer output varied not more than 0.0004 mv for three successive pressure readings. The time required for equilibrium and constant vapor pressure to occur varied for different runs. For pure ethanol and mixtures with high ethanol concentrations, equilibrium was attained about 15 minutes after plug E was opened. Mixtures high in benzene and/or hexane required up to 50 minutes to reach a constant vapor pressure.

After the mixture vapor pressure was determined, plug E was closed and valve G was opened so that the glass tubing leading to the transducer could be evacuated. After fifteen minutes had been allowed for evacuation of this portion of the apparatus, E_m° and E_i were again measured and recorded. If E_c° differed from the value determined before the pressure measurements began, the more recent value was used in the calculation of Π by equation III-2.

At this time during each run, the bath temperature could have been changed if measurements at more than one temperature had been desired. After sufficient time had been allowed for the mixture and transducer to reach the new temperature, vapor pressure measurements would have been repeated. This procedure could have been repeated several times

for the determination of vapor pressure at several temperatures.

Since pressure measurements were desired only at 25° C in the present study, the ball joint at sidearm C was disconnected, and the equilibrium cell-transducer assembly was removed from the bath.

Apparatus Maintenance

At the completion of each run, the equilibrium cell and other glass equipment were cleaned to prevent contamination of the next mixture. Details of the apparatus maintenance will be briefly described.

The equilibrium cell was disconnected from its assembly with the transducer. The cell was then clamped in its original position above the table. The 20 cc syringe and teflon "spaghetti" tubing were used to remove the mixture from the compartment of the cell. The first 20 ml to be removed were saved in one of the small glass bottles. The remainder of the mixture was discarded. The 20 ml sample was taken to the refractometer. The refractive index of the mixture after the run was measured and recorded. (See Chapter III, Vapor Pressure Apparatus.)

Disposable Kimwipes were used to clean stopcock grease from the socket of sidearm B and from the ball member of the extension K. Removal of grease from these portions of the apparatus was essential to minimize contamination of the next run due to stopcock grease. The socket at sidearm B was connected to the ball member at the glass "T", and the left stopcock of the manifold was opened. The cell was evacuated and quickly dried. The organic vapors condensed in the cold trap before they could reach the vacuum pump.

The glass bottles and the funnels were washed with soap and water. After being thoroughly rinsed with tap water, these items were rinsed

with distilled water and acetone. The bottles and funnels were allowed to dry by evaporation at room temperature. The cold trap was removed from the vacuum line, cleaned and replaced in its position.

Experimental Results

The experimental procedure described above was used over the entire composition range for each of the three binary systems at 25° C. Experimental results of this study are given in Tables II, III, and IV. Graphical presentation of the experimental data is shown in Figures 4, 5, and 6. Plotted with the experimental Π-x data are vapor compositions calculated by Mixon's Method. These calculations are discussed in the next chapter.

TABLE II

EXPERIMENTAL VAPOR PRESSURE DATA AT 25° C FOR THE SYSTEM N-HEXANE-BENZENE

Liquid Mole Fraction n-Hexane, X_1	Vapor Pressure, Π, mm Hg
0.0	95.24
0.1085	116.84
0.2053	126.87
0.2991	134.67
0.3810	139.75
0.5019	144.57
0.5940	147.44
0.7003	150.50
0.7991	152.89
0.8977	154.18
1.0	152.99

TABLE III

EXPERIMENTAL VAPOR PRESSURE DATA AT 25° C FOR THE SYSTEM BENZENE-ETHANOL

Liquid Mole Fraction Benzene, X_1	Vapor Pressure, Π, mm Hg
0.0	59.36
0.1015	89.50
0.1998	106.37
0.2994	115.59
0.4101	120.92
0.4981	123.37
0.5959	124.47
0.6922	124.76
0.8072	124.29
0.8990	121.66

TABLE IV

EXPERIMENTAL VAPOR PRESSURE DATA AT 25° C FOR THE SYSTEM N-HEXANE-ETHANOL

Liquid Mole Fraction Hexane, X_1	Vapor Pressure, Π, mm Hg
0.0	58.90
0.1006	145.15
0.2051	173.42
0.2921	182.20
0.4035	188.17
0.4906	188.84
0.6031	189.86
0.7359	190.77
0.8943	189.53
0.9456	187.66
0.9733	183.85
1.0	152.69

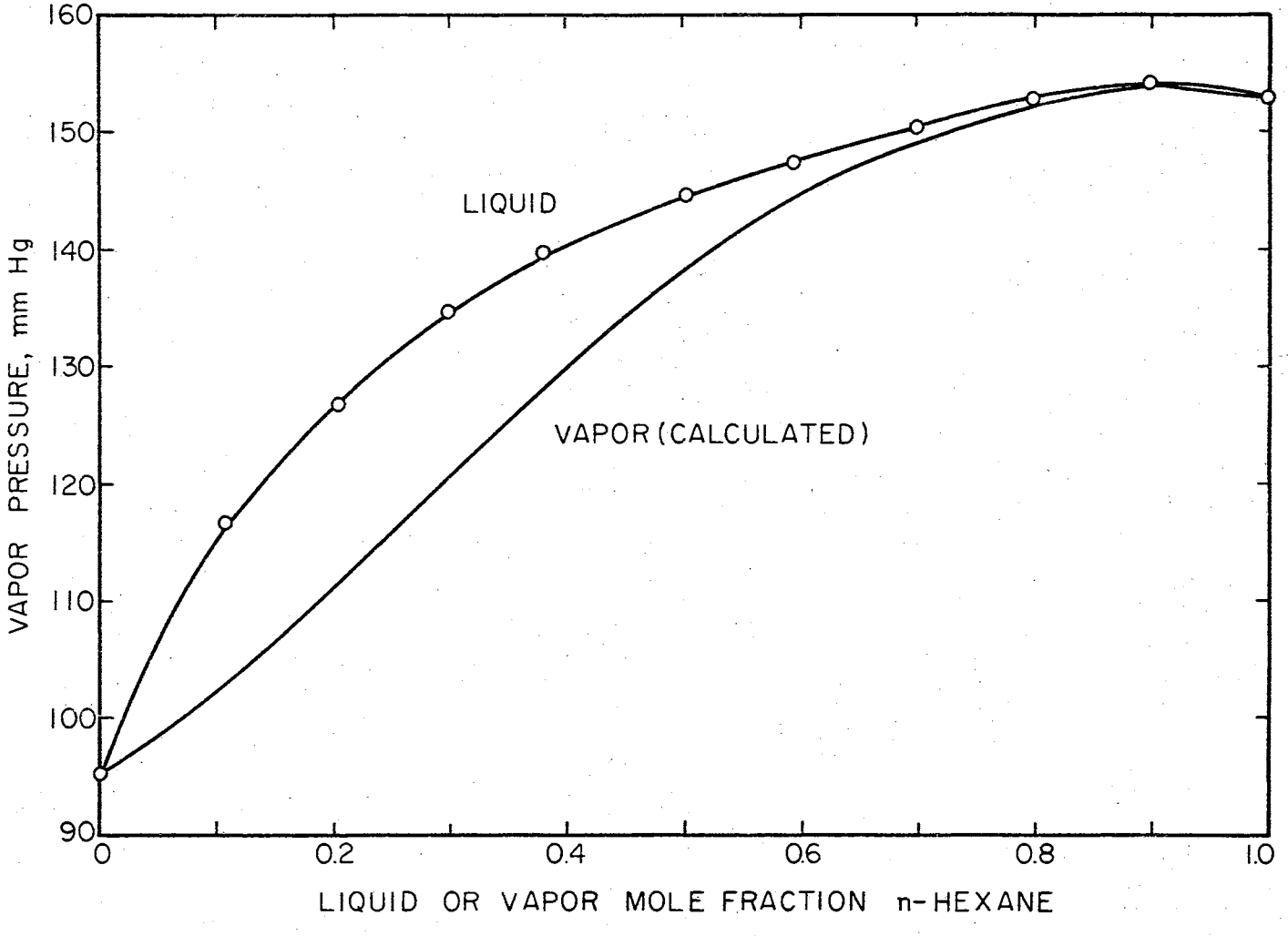

Figure 4. Vapor Pressure at 25° C for the System n-Hexane-Benzene

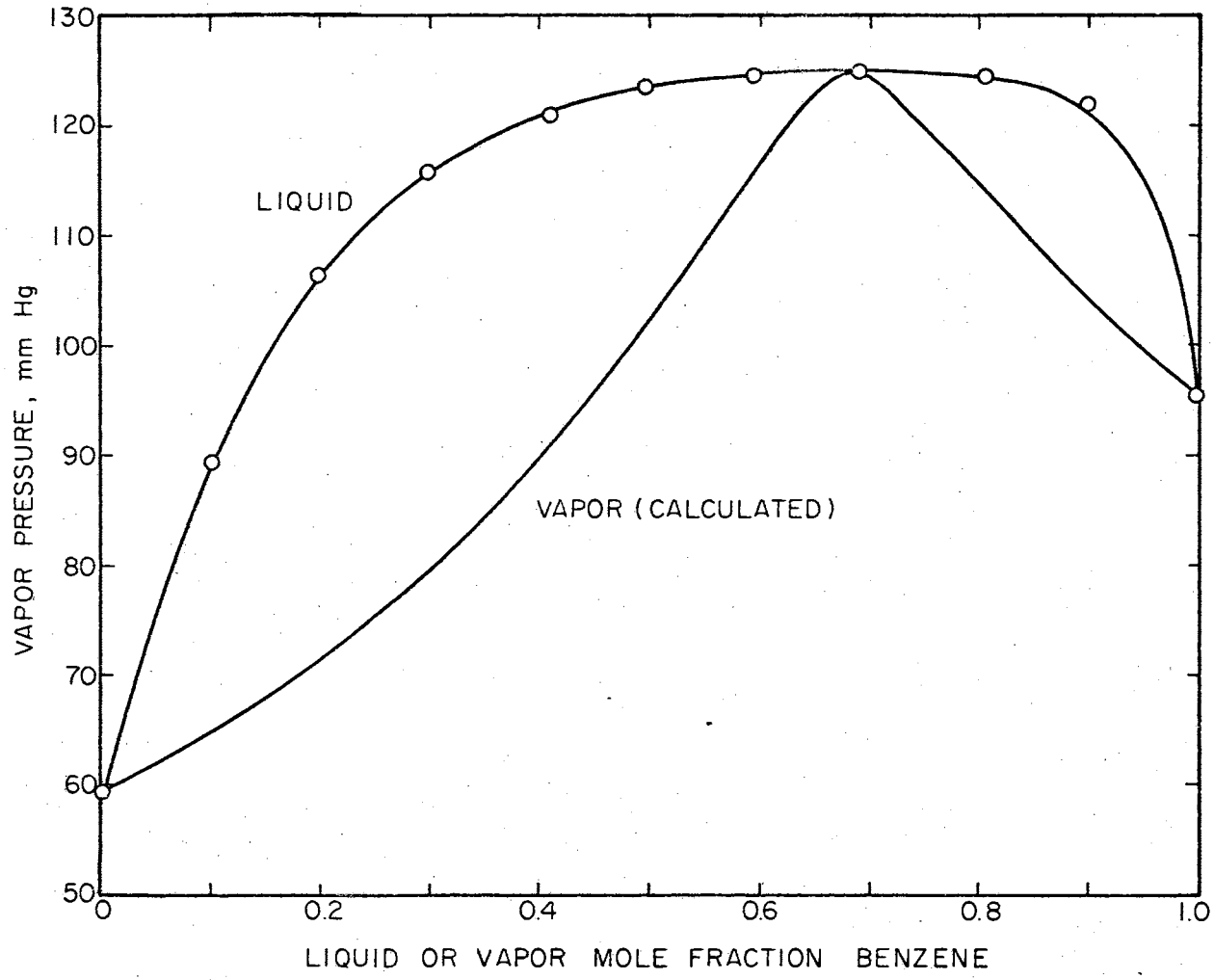

Figure 5. Vapor Pressure at 25° C for the System Benzene-Ethanol

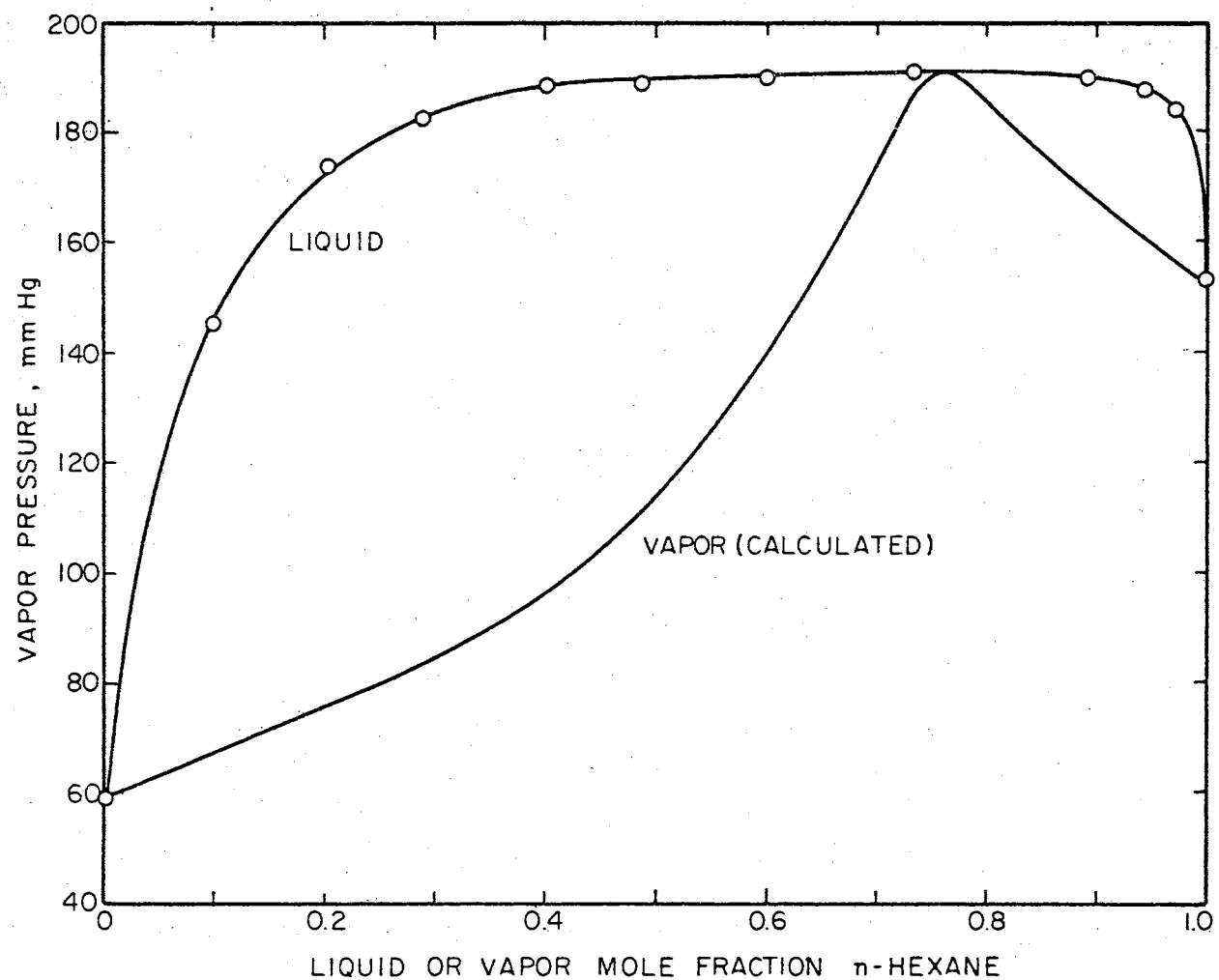

Figure 6. Vapor Pressure at 25° C for the System n-Hexane-Ethanol

CHAPTER V

DISCUSSION OF RESULTS

The experimental data from this study have been tabulated in the previous chapter. In this chapter, the significance of these data will be discussed.

First, the accuracy of the experimental pressure measurements is discussed. Several models for expressing the composition dependence of activity coefficient are then compared for each system studied. Vapor-liquid equilibrium data calculated from the best model for each system are compared with results from the Mixon exact method. Next, the use of Wilson's equation for prediction of heat of mixing data from vapor-liquid equilibrium (VLE) data is discussed. Tabulation of excess temperature-entropy product completes the thermodynamic mixing data for each system at 25° C. An analysis of the consistency of the experimental data with literature data concludes this chapter.

Accuracy of the Experimental Data

Possible sources of experimental error are discussed in this section. Also included is a comparison of pure component vapor pressures with literature values.

Experimental Error

The most probable cause of experimental error in the measurement

of solution vapor pressure is incomplete degassing, which would result in a measured pressure greater than the actual pressure. As previously mentioned, the absence of bubbles during melting was the criterion for complete degassing in this study.

Another cause for experimental error in this study might have been the use of a lubricated ball and socket between the equilibrium cell and the transducer. The organic vapors may have been slightly contaminated by the lubricant. Ball members utilizing teflon cladding and O-rings were originally used instead of a lubricated joint. However, leaks in the system resulted in use of the lubricated joint. At the completion of each run, there was visual evidence that the lubricant had been attacked by the organic vapors. No estimate of the degree of error caused by this contamination can be made, but a significant contribution to the overall error is deemed highly unlikely.

Pure Component Vapor Pressures

A comparison of experimental pure component vapor pressures with literature values gives an indication of the accuracy of the experimental measurements. The vapor pressure of pure ethanol at 25° C was measured four times before any mixture data were taken, once at the beginning of the benzene-ethanol runs and once at the beginning of the hexane-ethanol runs. The vapor pressure of pure benzene was measured once, and the vapor pressure of pure hexane was measured twice. Results of these measurements are compared with literature values in Table V. Literature values were calculated using Antoine constants tabulated by Prausnitz and co-workers (25).

For ethanol and benzene the measured vapor pressures are close to the literature values. For hexane, the deviation from the literature

value is significant; however, the two experimental measurements agree within 0.3 mm Hg.

TABLE V

PURE COMPONENT VAPOR PRESSURES AT 25° C

P^*_{exptl}, mm Hg	P^*_{lit}, mm Hg (a)	$P^*_{exptl} - P^*_{lit}$, mm Hg
	Ethanol	
58.86	59.17	-0.31
58.89	59.17	-0.28
59.47	59.17	+0.30
58.90	59.17	-0.27
59.36	59.17	+0.19
58.90	59.17	-0.27
	Benzene	
95.24	95.18	+0.06
	n-Hexane	
152.99	151.33	+1.66
152.69	151.33	+1.35

(a) Calculated by Antoine equation (25).

On the basis of these pure component data, the mixture vapor pressure are estimated within ±0.3 mm Hg.

Vapor-Liquid Equilibrium Data by Barker's Method

As discussed in Chapter II, Barker's method involves the calculation of parameters for an activity coefficient model which result in the best fit to the experimental Π-x data. In this study, a computer program (12) for the estimation of non-linear parameters was used to minimize

$$\sum_{i=1}^{D} (\Pi - \Pi_{calc})_i^2$$

where Π = experimental vapor pressures

Π_{calc} = calculated vapor pressures

D = number of data points

A brief explanation of how values of Π_{calc} were determined is pertinent. Equation II-13 can be rearranged for a binary mixture as

$$y_1 \Pi = \frac{\gamma_1^L x_1 P_1^*}{F_1} \qquad \text{(V-1)}$$

and

$$(1 - y_1)\Pi = \frac{\gamma_2^L (1 - x_1) P_2^*}{F_2} \qquad \text{(V-2)}$$

Dividing equation V-1 by equation V-2 gives

$$\frac{y_1}{1 - y_1} = \left(\frac{\gamma_1^L x_1 P_1^*}{F_1} \right) \left(\frac{F_2}{\gamma_2^L (1 - x_1) P_2^*} \right) \qquad \text{(V-3)}$$

If values of all the terms on the right side of equation V-3 are known,

$$\frac{y_1}{1 - y_1} = C \qquad \text{(V-4)}$$

and

$$y_1 = \frac{C}{1 + C} \qquad \text{(V-5)}$$

Using equation V-5 in equation V-1,

$$\Pi_{calc} = \frac{\gamma_1^L x_1 P_1^*}{F_1 (\frac{C}{1 + C})} \qquad \text{(V-6)}$$

The computer program uses initially assumed parameter values to calculate γ_2 and γ_1. With the assumption that $F_1 = F_2 = 1.0$, values of y_1 and Π_{calc} are calculated by equations V-5 and V-6 respectively. These values of y_1 and Π_{calc} are used to calculate new values of F_1 and F_2 by methods discussed in Chapter II. The calculation of y_1 and Π_{calc} by equations V-5 and V-6 is repeated until convergence occurs. Next, the program compares values of Π_{calc} with experimental values so that improved estimates of the parameters can be made. This iterative procedure is repeated until the least squares criterion is satisfied.

Parameters for the van Laar equation, the Wilson equation, and three forms of the Redlich-Kister equation were calculated for each system. The model which gave the lowest standard error of estimate, σ, where

$$\sigma = \sqrt{\frac{\sum_{i=1}^{D} (\Pi - \Pi_{calc})_i^2}{D}} \qquad \text{(V-7)}$$

is the model which best fit the experimental data. Table VI gives the value of σ for each model and each system. Also tabulated are maximum errors and the value of x_1 where the maximum error occurred.

Table VI shows that for each system the Wilson equation gives the best fit for 2-parameter expressions. For the hexane-ethanol system, Wilson's equation fits the experimental data better than the 3 and 4-parameter Redlich-Kister equations. For the benzene-ethanol system, Wilson's equation is significantly better than the 3-parameter Redlich-Kister (R-K) equation. However, the 4-parameter R-K equation gives a slightly improved fit. For the hexane-benzene system, both the 3 and 4-parameter R-K equations fit the data better than the Wilson equation. Notice, however, that for this system all five models have approximately the same value of σ.

These observations support the conclusion of Orye and Prausnitz (24) that the Wilson equation "appears to be the best 2-parameter equation suitable for a wide variety of mixtures." Harris (13) found that in his studies, "significant improvement . . . was obtained by using the 3-parameter Redlich-Kister expression."

Table VI may be used to estimate the precision of the experimental data. The standard error for the Wilson equation fit to the benzene-ethanol data is 0.17 mm Hg; the maximum error is 0.34 mm Hg. These deviations result from both data scatter and lack of fit to the experimental data by the Wilson equation. Assuming that the larger deviations for the other systems are due primarily to lack of fit, these observations support the estimate that the precision of the experimental data is ± 0.3 mm Hg.

TABLE VI

STANDARD ERROR OF ESTIMATE AND MAXIMUM ABSOLUTE ERROR FOR EACH SYSTEM WITH EACH MODEL

	(1) Hexane-Benzene	(2) Hexane-Benzene	(1) Benzene-Ethanol	(2) Benzene-Ethanol	(1) Hexane-Ethanol	(2) Hexane-Ethanol
Model	Standard Error, σ, mm Hg	Max. Abs. Error, mm Hg	Standard Error, σ, mm Hg	Max. Abs. Error, mm Hg	Standard Error, σ, mm Hg	Max. Abs. Error, mm Hg
van Laar	.4965[a]	.9928[b] (.8977)[c]	.9491	1.758 (.8990)	7.7565	15.65 (.9733)
Wilson	.4807	.9472 (.8977)	.1697	.3421 (.1015)	1.5633	3.20 (.9733)
2 Parameter Redlich-Kister	.6325	1.194 (.8977)	1.4156	2.90 (.8990)	8.3644	17.598 (.9733)
3 Parameter Redlich-Kister	.4252	.6514 (.3810)	.4341	.7476 (.8990)	3.8119	9.088 (.9733)
4 Parameter Redlich-Kister	.3829	.7016 (.2053)	.0711	.1439 (.4981)	2.3616	4.874 (.9733)

(a) Standard Error of Estimate = σ, defined by equation V-7.

(b) Maximum Absolute Error = maximum value of $|(\Pi - \Pi_{calc})|$, mm Hg

(c) Numbers in parentheses are the values of x_1 at which the maximum error occurs.

Notice that for the system hexane-ethanol, the standard error for the best fit expression is greater than the standard error of the worst fit for the other two systems. The poor fit for this system can be partially explained. Hougen and co-workers (17) state that in the evaluation of R-K constants, "more weight should be assigned to data in the middle concentration range than is given by the method of least squares." Excluding end points, three of the ten data points for the hexane-ethanol mixture are in the high hexane concentration range, where a sharp break in the Π-x curve occurs. (See Figure 6.) Therefore, rather than assigning more weight to the middle concentration range, undo weight was given the high hexane composition range in the least squares determination of R-K constants.

Wilson parameters and 4-parameter R-K constants for each system are shown below in Tables VII and VIII. Liquid molar volume data tabulated by Prausnitz and co-workers (25) were used in the calculation of Wilson parameters, Λ_{ij}.

Vapor compositions, excess Gibbs free energy and activity coefficients calculated using the best model for each system are tabulated with results from Mixon's method in the next section.

Vapor-Liquid Equilibrium Data by Mixon's Method

Mixon's method for calculating vapor-liquid equilibrium data from Π-x data as outlined in Chapter II was programmed for computer use. A listing of the program, a block diagram of the iterative procedure, and information concerning program input and output are presented in Appendix C.

The program worked very well for the system hexane-benzene. How-

TABLE VII

WILSON PARAMETERS FOR EACH SYSTEM AT 25° C

System **	$\lambda_{12} - \lambda_{11}$ cal/g-mole	Λ_{12} *	$\lambda_{21} - \lambda_{22}$ cal/g-mole	Λ_{21}
Hexane-Benzene	384.47	.3607	148.42	1.1278
Benzene-Ethanol	154.89	.5058	1621.00	.0987
Hexane-Ethanol	354.79	.2489	2209.77	.0530

$$*\Lambda_{ij} = \frac{v_j^L}{v_i^L} \exp-\left[\frac{(\lambda_{ij} - \lambda_{ii})}{RT}\right]$$

** Component 1 is the first component listed for each system.

TABLE VIII

4-PARAMETER REDLICH-KISTER CONSTANTS FOR EACH SYSTEM AT 25° C

System	A'	B'	C'	D'
Hexane-Benzene	.6403	-.1871	.0832	.0737
Benzene-Ethanol	1.7633	.3548	.2543	.1608
Hexane-Ethanol	2.1933	.2083	.5320	.4003

ever, the program failed to converge for the benzene-ethanol and hexane-ethanol systems. The program also failed to converge for the 55° C Π-x data for these two systems reported by Ho and Lu (16). Private communications with Gumowski, a co-author of the Mixon method, revealed that these authors had also found systems for which their method failed to converge. A combination manual-computer "strong arm" technique was used to force the program to converge. First, the program was modified to receive values of G^E corresponding to each value of x_1 as data. Values of G^E predicted by the 4-parameter Redlich-Kister equation were initially used. The program was allowed to proceed through only one iteration. Based on printed results after this iteration, values of G^E_{new} were estimated by this author and entered as new data in the program. This "strong arm" technique was repeated several times before all values of $(\Pi - \Pi_{calc})$ were less than 0.05 mm Hg. Even with this complication, the Mixon method resulted in a much better fit to the Π-x data than did the best model for each system. Table IX compares σ values for the Mixon method and the best model for each system.

Because the Mixon method results in a negligible standard error of estimate, vapor compositions calculated by this method were plotted with the experimental Π-x data for each system in Figures 4, 5, and 6 of Chapter IV.

Table X summarizes vapor compositions, excess Gibbs free energy and activity coefficients calculated by both methods for the system hexane-benzene. Tables XI and XII give the same information for the systems benzene-ethanol and hexane-ethanol respectively. This information is shown graphically in Figures 7 through 15. In these graphs,

values calculated by Mixon's method have been shown as specific points. Values calculated by Barker's method have been shown as smooth curves. Figures 7 through 15 show that there is excellent agreement between VLE data calculated by the Mixon and Barker methods.

TABLE IX

COMPARISON OF STANDARD ERROR FOR THE MIXON METHOD AND BEST MODEL, 25° C

System	Standard Error of Estimate-Mixon Method, mm Hg	Barker Method, Best Model	Standard Error of Estimate-Best Model, mm Hg
Hexane-Benzene	.0014	4-parameter R-K Equation	.3829
Benzene-Ethanol	.0133	4-Parameter R-K Equation	.0711
Hexane-Ethanol	.0212	Wilson Equation	1.5633

Figures 7, 10, and 13 show that each system has an azeotrope point at 25° C. For the hexane-benzene system, the azeotrope occurs at a hexane mole fraction of 0.920. Benzene-ethanol has an azeotrope at a benzene mole fraction of 0.688. The azeotrope for hexane-ethanol occurs at a hexane mole fraction of 0.755.

Heat of Mixing Data

Heat of mixing is related to excess Gibbs free energy by the relationship

TABLE X

VAPOR-LIQUID EQUILIBRIUM DATA AT 25° C
FOR THE SYSTEM N-HEXANE-BENZENE

Liquid Mole Fraction Hexane, x_1	Smoothed Vapor Pressure, Π, mm Hg	Vapor Mole Fraction Hexane, y_1		Excess Gibbs Free Energy, G^E, cal/g-mole		Activity** Coefficient, γ_1		Activity Coefficient, γ_2	
		I*	II	I	II	I	II	I	II
.0500	107.68	0.1542	0.1479	26.24	23.14	2.1811	2.0709	1.0056	1.0028
.1000	115.42	0.2420	0.2466	45.85	42.95	1.8336	1.8655	1.0188	1.0113
.1500	121.40	0.3084	0.3175	61.02	59.43	1.6372	1.6924	1.0348	1.0255
.2000	126.39	0.3634	0.3719	73.05	72.67	1.5053	1.5489	1.0532	1.0449
.2500	130.68	0.4117	0.4164	82.17	82.81	1.4102	1.4317	1.0729	1.0690
.3000	134.51	0.4556	0.4550	89.22	90.04	1.3380	1.3371	1.0946	1.0971
.3500	137.70	0.4940	0.4904	94.08	94.61	1.2725	1.2616	1.1214	1.1281
.4000	140.39	0.5288	0.5245	96.75	96.75	1.2149	1.2021	1.1530	1.1612
.4500	142.63	0.5610	0.5584	97.16	96.74	1.1635	1.1557	1.1905	1.1954
.5000	144.51	0.5921	0.5928	95.38	94.84	1.1197	1.1200	1.2323	1.2298
.5500	146.15	0.6243	0.6281	91.53	91.28	1.0851	1.0926	1.2756	1.2638
.6000	147.69	0.6608	0.6645	85.78	86.28	1.0638	1.0717	1.3091	1.2972
.6500	149.18	0.6992	0.7020	79.21	80.01	1.0494	1.0555	1.3398	1.3304
.7000	150.61	0.7438	0.7403	71.33	72.60	1.0464	1.0427	1.3438	1.3647
.7500	151.90	0.7733	0.7792	64.40	64.07	1.0239	1.0320	1.4391	1.4023
.8000	153.04	0.8200	0.8189	51.13	54.40	1.0188	1.0227	1.4293	1.4467
.8500	153.93	0.8691	0.8594	44.31	43.46	1.0286	1.0145	1.4036	1.5032
.9000	154.31	0.9039	0.9018	32.76	31.01	1.0128	1.0074	1.5497	1.5793
.9500	154.40	0.9459	0.9475	19.14	16.69	1.0047	1.0022	1.7459	1.6862

*I Mixon's Method
II Barker's Method with 4-Parameter Redlich-Kister Equation

**Component 1 is n-hexane.

TABLE XI

VAPOR-LIQUID EQUILIBRIUM DATA AT 25° C
FOR THE SYSTEM BENZENE-ETHANOL

Liquid Mole Fraction Benzene, x_1	Smoothed Vapor Pressure, Π, mm Hg	Vapor Mole Fraction Benzene, y_1		Excess Gibbs Free Energy, G^E, cal/g-mole		Activity** Coefficient, γ_1		Activity Coefficient, γ_2	
		I*	II	I	II	I	II	I	II
0.0500	75.40	0.2499	0.2547	40.72	43.13	3.9857	4.0929	1.0008	1.0025
0.1000	89.50	0.3972	0.3922	80.50	83.17	3.7496	3.6880	1.0067	1.0110
0.1500	99.50	0.4787	0.4751	117.32	119.67	3.3443	3.3059	1.0242	1.0270
0.2000	106.50	0.5301	0.5291	149.41	152.34	2.9696	2.9618	1.0498	1.0513
0.2500	111.80	0.5666	0.5662	177.90	180.99	2.6637	2.6610	1.0839	1.0845
0.3000	115.70	0.5940	0.5933	201.78	205.50	2.4070	2.4036	1.1258	1.1273
0.3500	118.70	0.6154	0.6139	222.17	225.80	2.1918	2.1828	1.1784	1.1807
0.4000	120.80	0.6320	0.6305	237.96	241.88	2.0038	1.9955	1.2429	1.2460
0.4500	122.40	0.6458	0.6444	249.96	253.69	1.8435	1.8357	1.3228	1.3252
0.5000	123.50	0.6576	0.6563	257.29	261.15	1.7044	1.6981	1.4193	1.4221
0.5500	124.10	0.6641	0.6668	260.61	264.14	1.5721	1.5781	1.5548	1.5422
0.6000	124.40	0.6720	0.6759	257.94	262.43	1.4617	1.4721	1.7117	1.6946
0.6500	124.80	0.6838	0.6837	251.41	255.67	1.3772	1.3773	1.8944	1.8938
0.7000	124.90	0.6877	0.6905	239.35	243.37	1.2870	1.2919	2.1833	2.1635
0.7500	124.80	0.6929	0.6965	220.65	224.87	1.2093	1.2152	2.5729	2.5433
0.8000	124.50	0.7000	0.7032	195.37	199.29	1.1425	1.1473	3.1399	3.1023
0.8500	123.50	0.7137	0.7137	161.76	165.53	1.0875	1.0893	3.9586	3.9669
0.9000	121.20	0.7398	0.7366	120.11	122.22	1.0447	1.0431	5.3029	5.3832
0.9500	115.30	0.7952	0.7970	67.11	67.70	1.0122	1.0118	7.9578	7.8669

*I Mixon's Method
II Barker's Method with 4-Parameter Redlich-Kister Equation

**Component 1 is benzene

TABLE XII

VAPOR-LIQUID EQUILIBRIUM DATA AT 25° C
FOR THE SYSTEM N-HEXANE-ETHANOL

Liquid Mole Fraction Hexane, x_1	Smoothed Vapor Pressure, Π, mm Hg	Vapor Mole Fraction Hexane, y_1		Excess Gibbs Free Energy, G^E, cal/g-mole		Activity** Coefficient, γ_1		Activity Coefficient, γ_2	
		I*	II	I	II	I	II	I	II
0.0500	117.50	0.5165	0.5026	65.88	64.34	8.0087	7.5605	1.0096	1.0079
0.1000	145.20	0.6202	0.6183	120.64	119.82	5.9185	5.8461	1.0331	1.0289
0.1500	161.80	0.6674	0.6682	167.53	167.56	4.7211	4.7116	1.0666	1.0610
0.2000	172.10	0.6937	0.6954	207.31	208.36	3.9096	3.9163	1.1095	1.1033
0.2500	178.60	0.7098	0.7122	240.93	242.77	3.3181	3.3336	1.1638	1.1561
0.3000	182.80	0.7206	0.7234	268.30	271.21	2.8715	2.8913	1.2287	1.2202
0.3500	185.70	0.7282	0.7314	290.38	293.96	2.5257	2.5459	1.3073	1.2972
0.4000	187.50	0.7337	0.7373	306.69	311.20	2.2478	2.2699	1.4014	1.3896
0.4500	188.60	0.7371	0.7419	317.88	323.05	2.0186	2.0450	1.5182	1.5010
0.5000	189.10	0.7393	0.7455	323.29	329.52	1.8269	1.8587	1.6608	1.6365
0.5500	189.70	0.7418	0.7484	323.47	330.56	1.6716	1.7022	1.8330	1.8037
0.6000	190.00	0.7437	0.7509	317.93	326.03	1.5386	1.5692	2.0505	2.0137
0.6500	190.20	0.7441	0.7532	306.69	315.68	1.4225	1.4550	2.3395	2.2844
0.7000	190.40	0.7486	0.7553	288.92	299.15	1.3302	1.3560	2.6849	2.6447
0.7500	190.60	0.7526	0.7575	265.80	275.89	1.2493	1.2698	3.1821	3.1460
0.8000	190.40	0.7579	0.7603	234.46	245.07	1.1782	1.1944	3.8826	3.8877
0.8500	189.80	0.7699	0.7643	196.31	205.45	1.1228	1.1285	4.9077	5.0891
0.9000	189.40	0.7764	0.7723	148.54	154.95	1.0671	1.0716	7.1381	7.3406
0.9500	187.0	0.7931	0.7963	85.63	89.66	1.0197	1.0251	13.0593	12.8756

*I Mixon's Method
II Barker's Method with Wilson's Equation

**Component 1 is n-hexane.

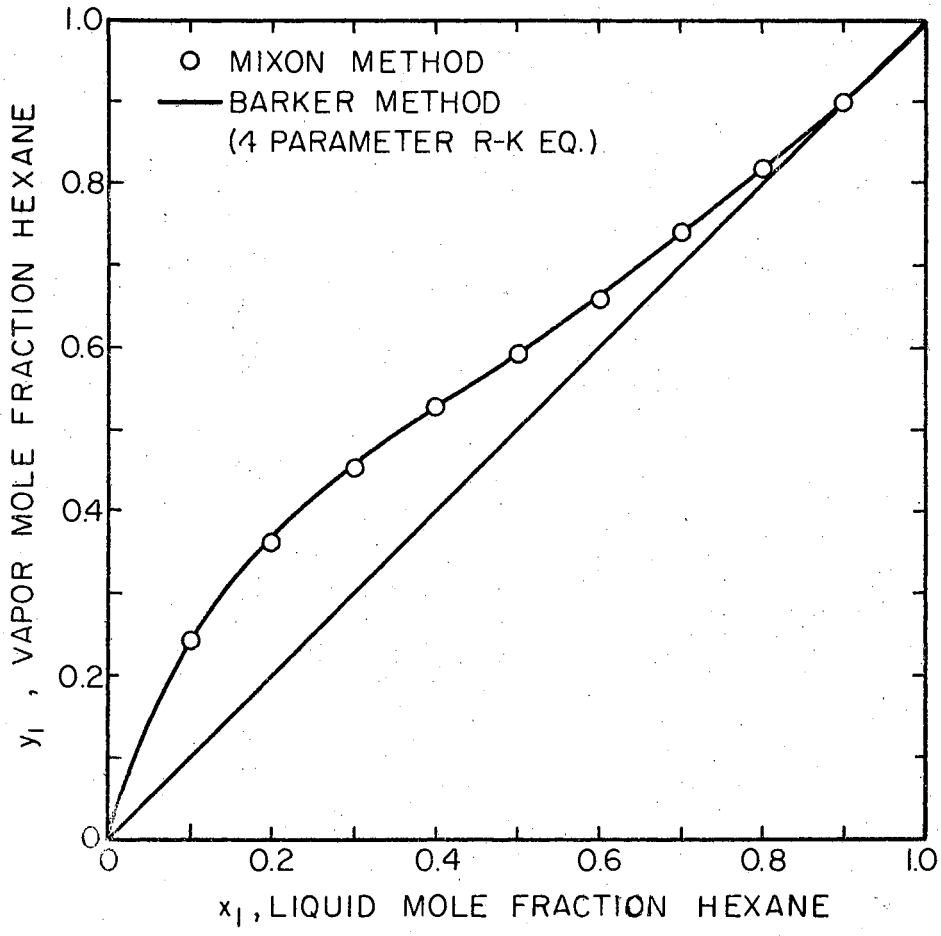

Figure 7. Vapor Composition at 25° C for the System n-Hexane-Benzene

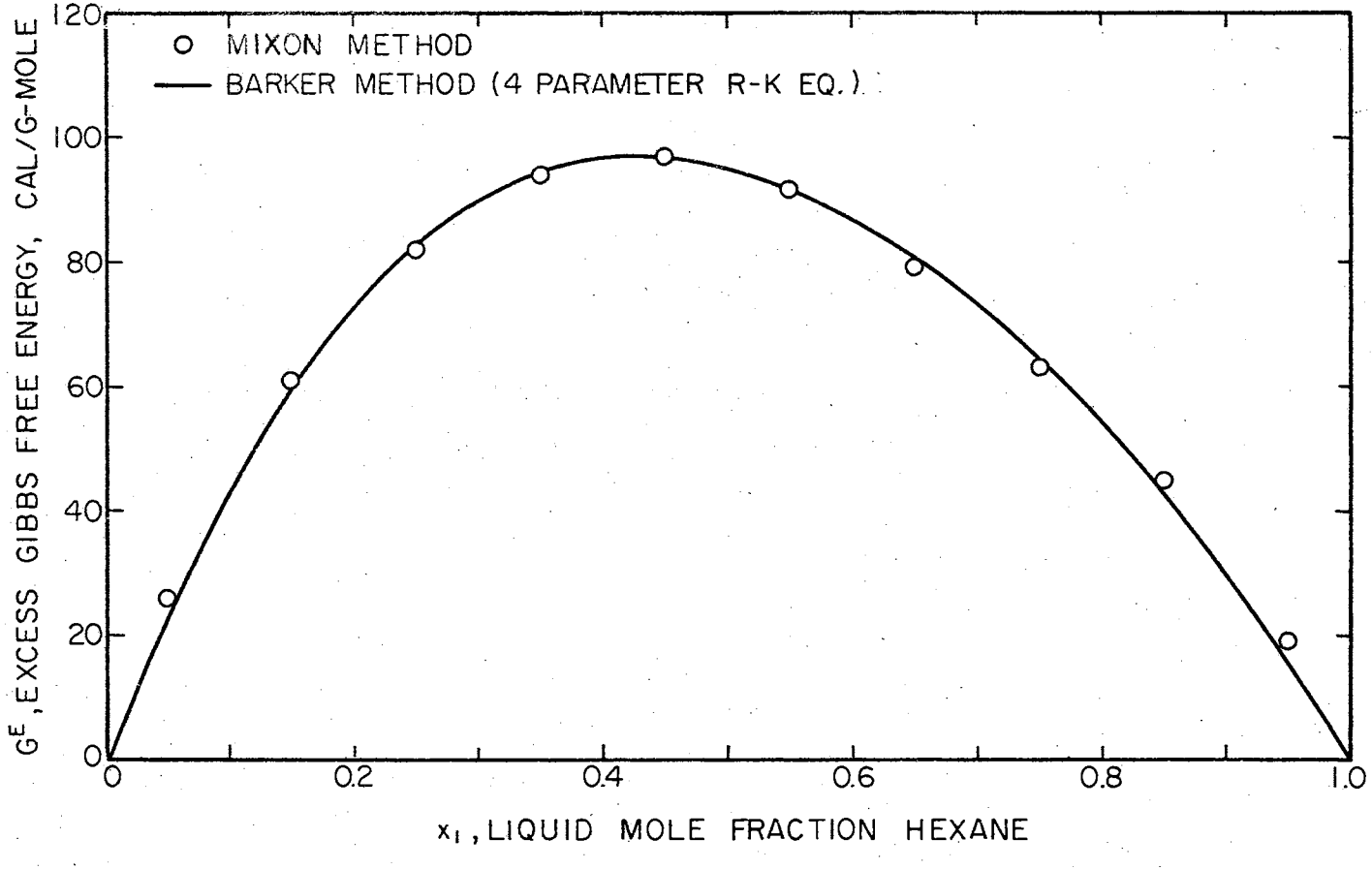

Figure 8. Excess Gibbs Free Energy at 25° C for the System n-Hexane-Benzene

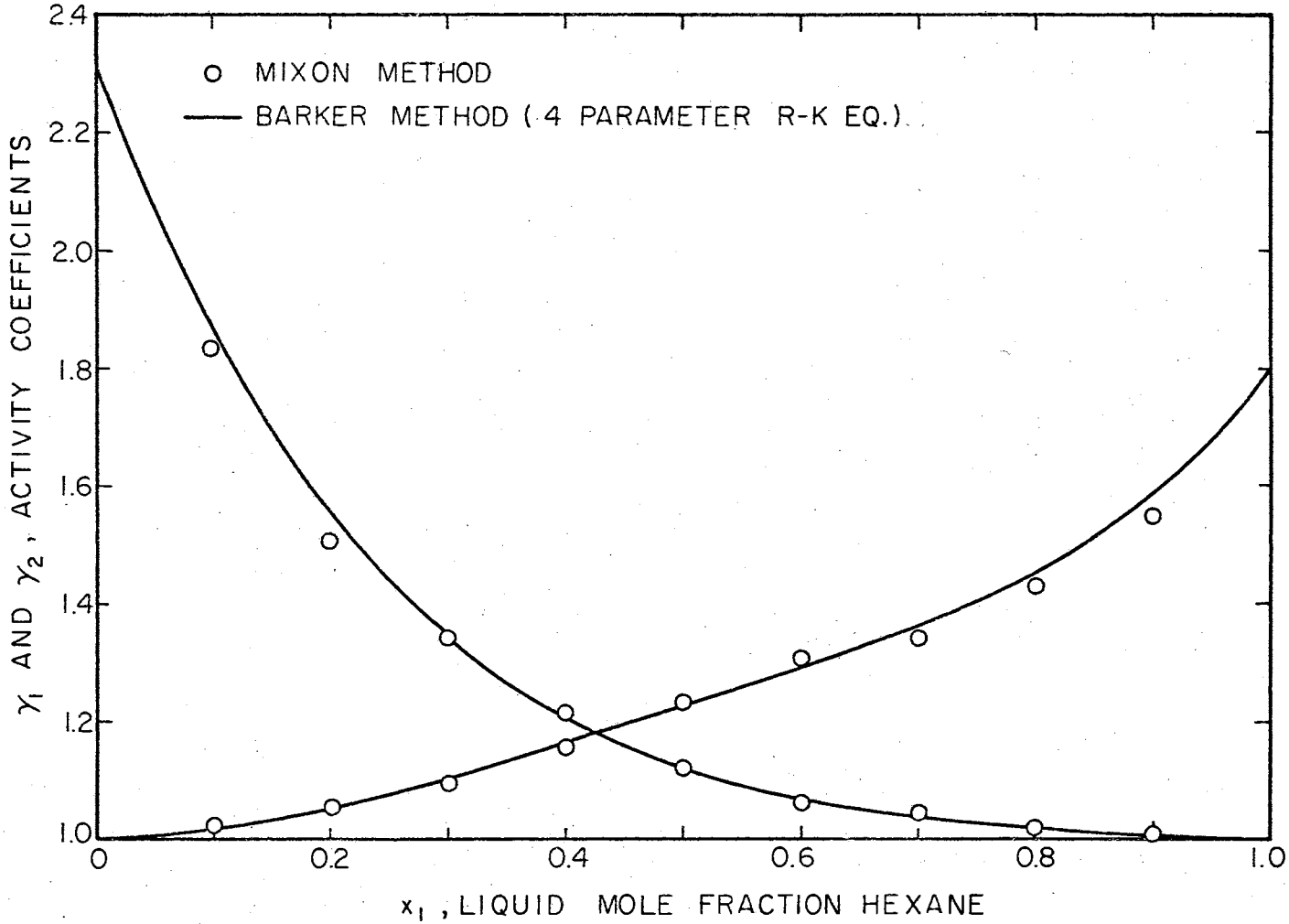

Figure 9. Activity Coefficients at 25° C for the System n-Hexane-Benzene

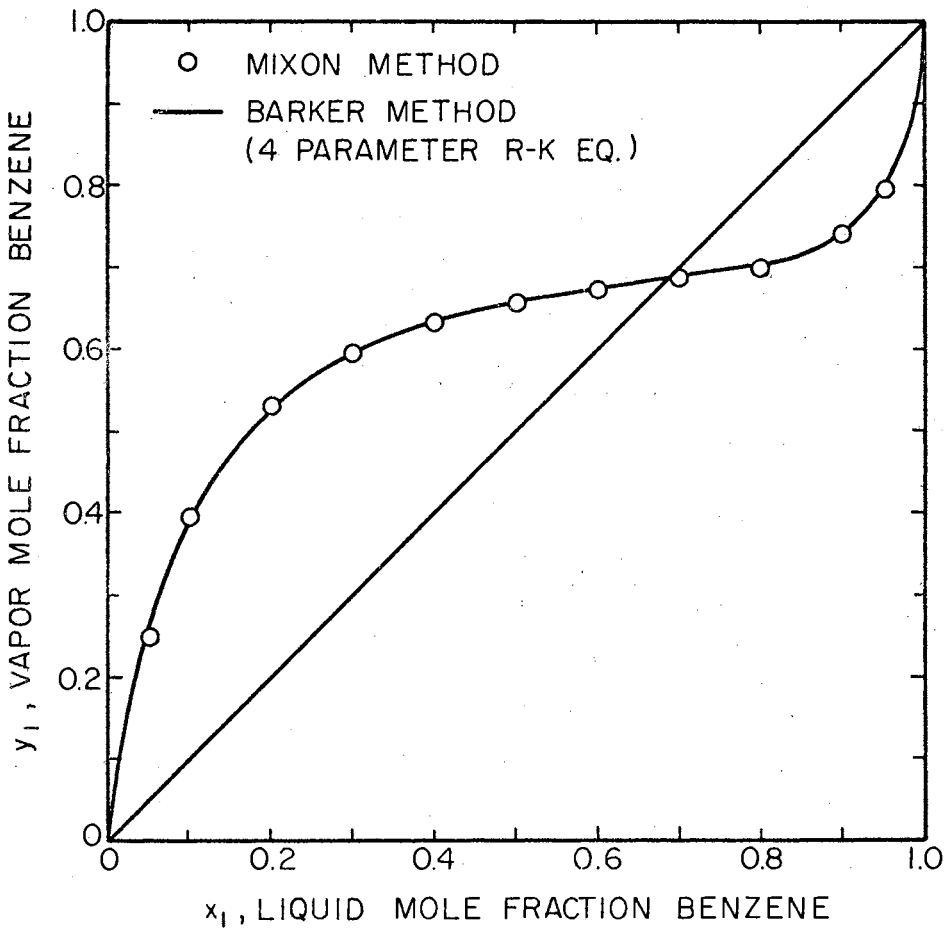

Figure 10. Vapor Composition at 25° C for the System Benzene-Ethanol

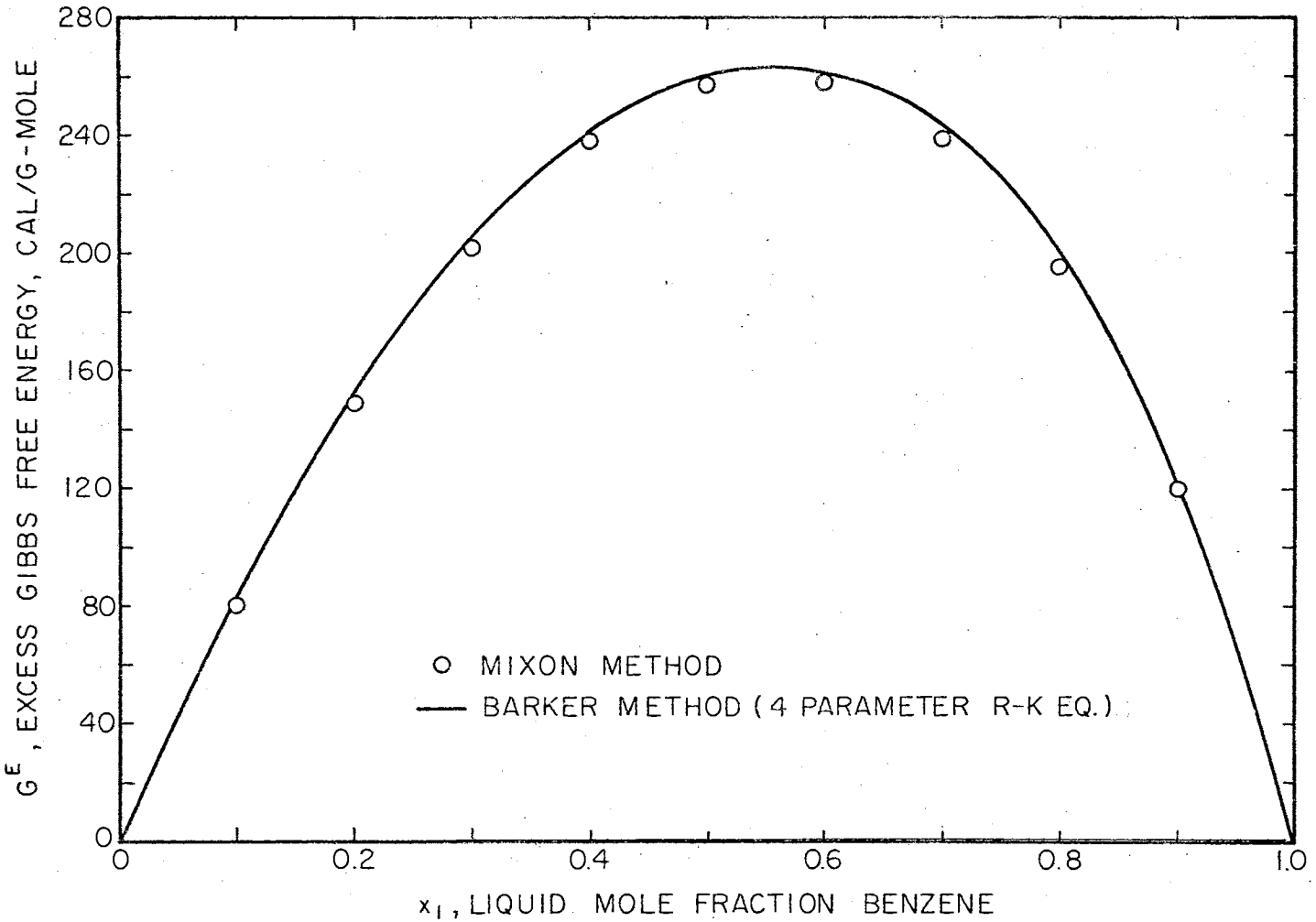

Figure 11. Excess Gibbs Free Energy at 25° C for the System Benzene-Ethanol

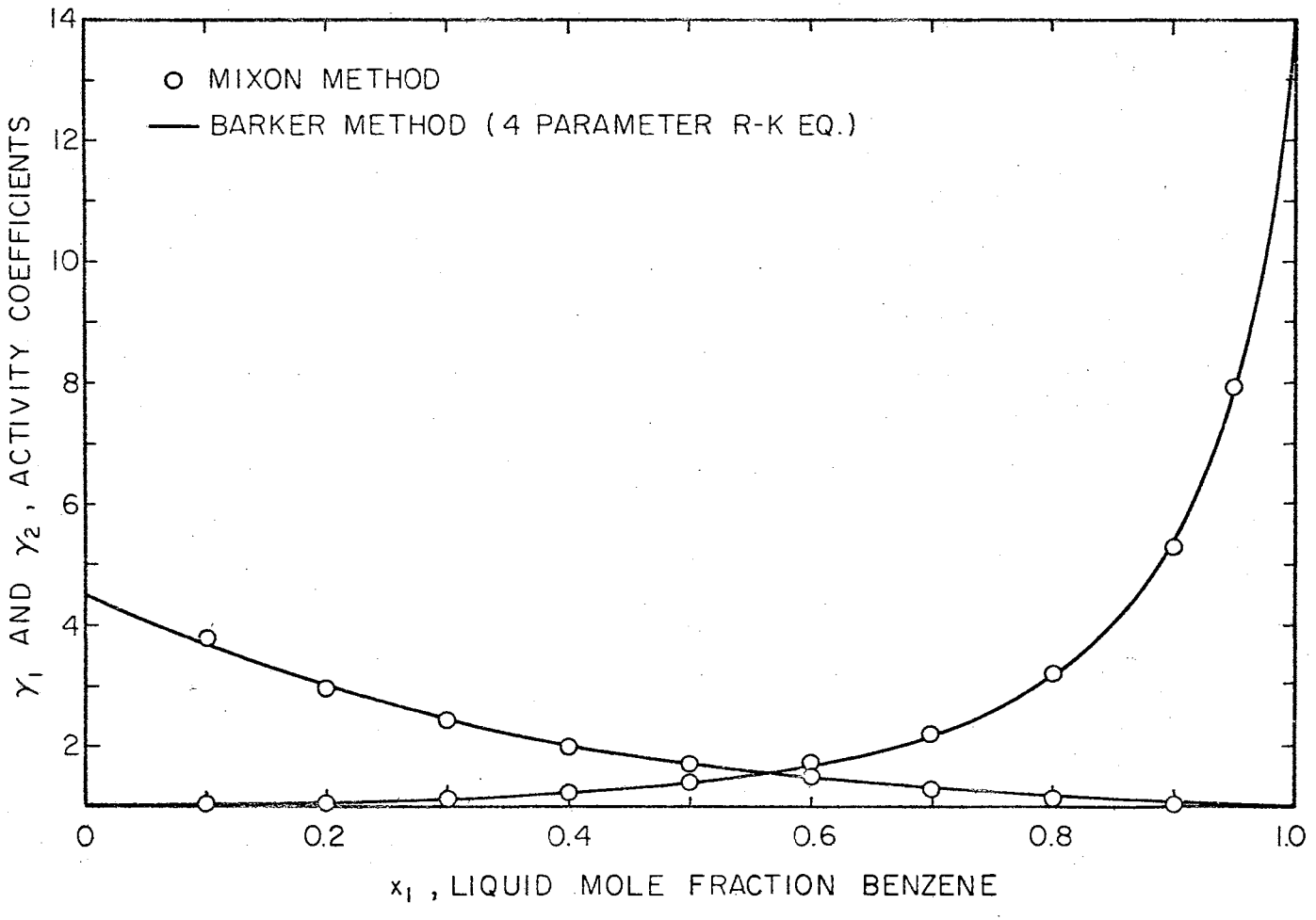

Figure 12. Activity Coefficients at 25° C for the System Benzene-Ethanol

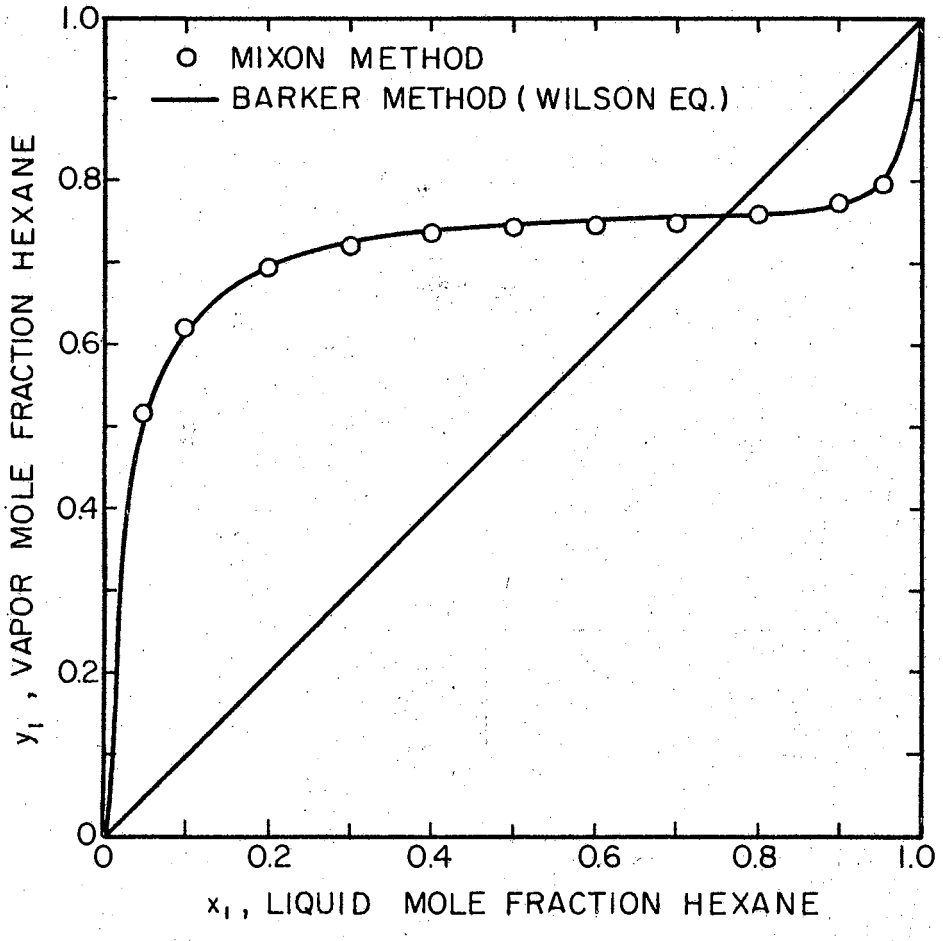

Figure 13. Vapor Composition at 25° C for the System n-Hexane-Ethanol

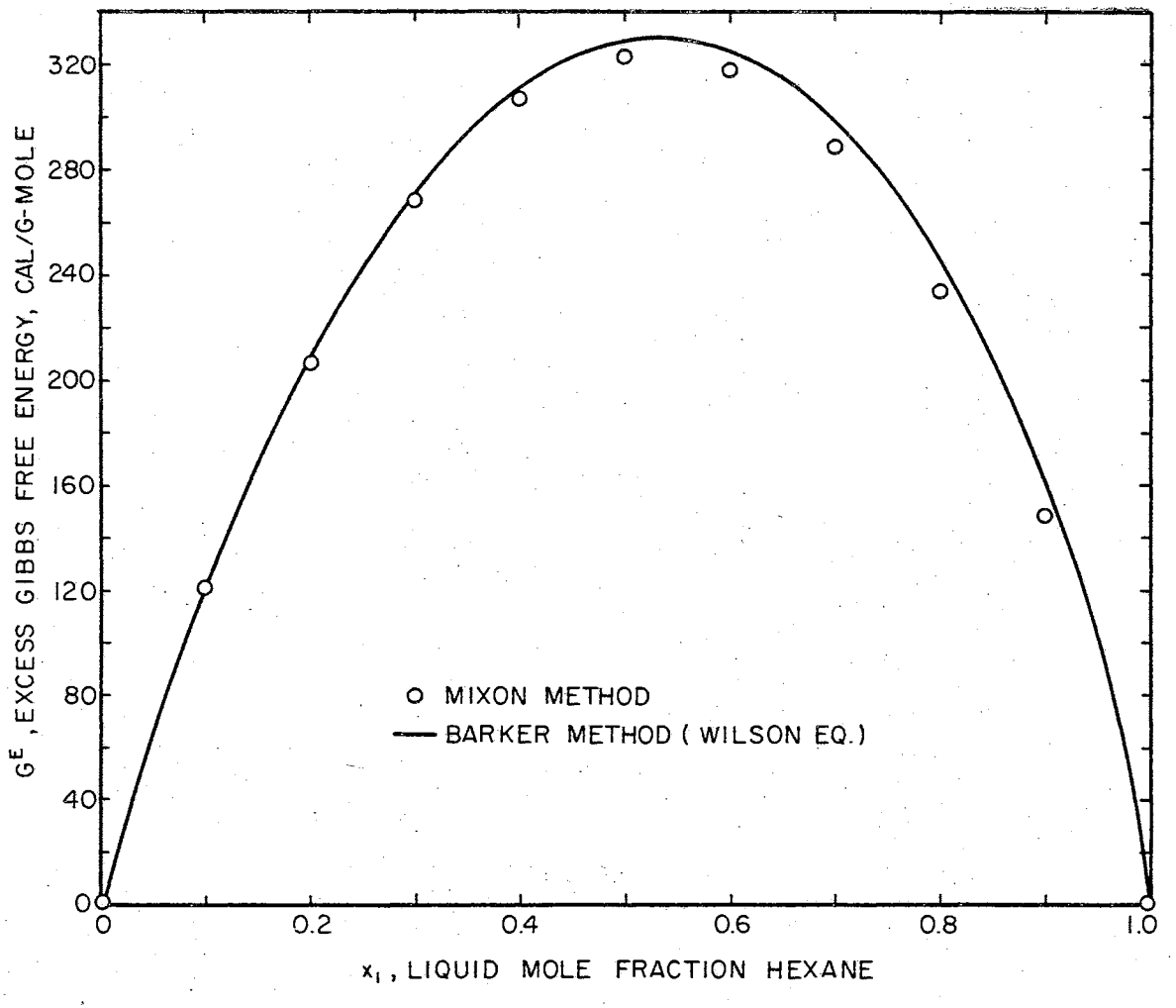

Figure 14. Excess Gibbs Free Energy at 25° C for the System n-Hexane-Ethanol

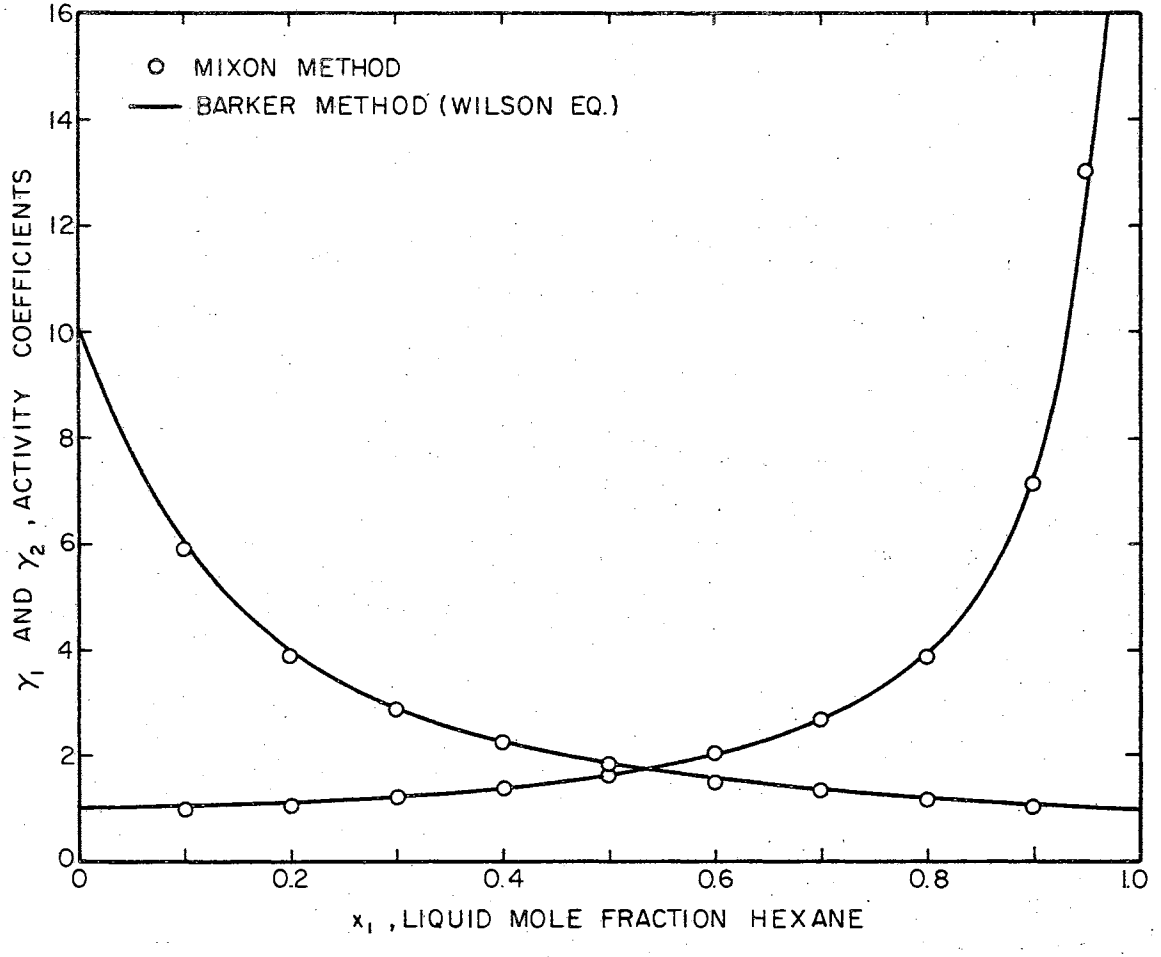

Figure 15. Activity Coefficients at 25° C for the System n-Hexane-Ethanol

$$H^M = -T^2 \left(\frac{\partial G^E/T}{\partial T} \right)_{P,x_i} \qquad \text{(V-8)}$$

This equation may be used to estimate heat of mixing when free energy data are available.

Orye and Prausnitz (24) point out that to a good approximation the quantities $(\lambda_{12} - \lambda_{11})$ and $(\lambda_{12} - \lambda_{22})$ associated with the Wilson equation may be considered to be independent of temperature. When this assumption is made, equation II-36 may be utilized in equation V-8 to give

$$H^M = x_1 \left(\frac{x_2 \Lambda_{12}}{x_1 + x_2 \Lambda_{12}} \right) (\lambda_{12} - \lambda_{11})$$

$$+ x_2 \left(\frac{x_1 \Lambda_{21}}{x_2 + x_1 \Lambda_{21}} \right) (\lambda_{12} - \lambda_{22}) \qquad \text{(V-9)}$$

Wilson parameters given in Table VII were used to calculate values of H^M at 25° C for each system. Results of these calculations are summarized in Tables XIII, XIV, and XV. Also tabulated are smoothed values of H^M determined from the experimental data of Jones and Lu (18). These data are presented graphically in Figures 16, 17, and 18. These graphs show that equation V-9 gives only a rough approximation to experimental H^M data for the systems studies. Qualitatively, the experimental and calculated curves compare quite well.

Excess Temperature-Entropy Product of Mixing

Equation II-28 rearranged for the calculation of excess temperature-entropy product gives,

TABLE XIII

HEAT OF MIXING DATA AT 25° C FOR THE SYSTEM N-HEXANE-BENZENE

Liquid Mole Fraction Hexane, x_1	Heat of Mixing*, H^M, cal/g-mole	
	I	II
0.10	44.27	96.0
0.20	71.53	160.0
0.30	86.56	194.0
0.40	92.21	211.0
0.50	90.29	211.0
0.60	82.02	198.0
0.70	68.30	171.0
0.80	49.74	128.0
0.90	26.84	72.0

*I Calculated by equation V-9
II Smoothed experimental data of Jones and Lu (18)

TABLE XIV

HEAT OF MIXING DATA AT 25° C FOR THE SYSTEM BENZENE-ETHANOL

Liquid Mole Fraction Benzene, x_1	Heat of Mixing*, H^M, cal/g-mole	
	I	II
0.10	28.52	43.0
0.20	51.95	82.0
0.30	71.19	120.0
0.40	86.75	157.0
0.50	98.80	188.0
0.60	107.02	209.0
0.70	110.32	216.0
0.80	105.65	203.0
0.90	83.66	156.0

*I Calculated by equation V-9
II Smoothed experimental data of Jones and Lu (18)

TABLE XV

HEAT OF MIXING DATA AT 25° C
FOR THE SYSTEM N-HEXANE-ETHANOL

Liquid Mole Fraction Hexane, x_1	Heat of Mixing*, H^M, cal/g-mole	
	I	II
0.10	36.16	46.0
0.20	58.50	79.0
0.30	73.43	103.0
0.40	83.80	120.5
0.50	90.93	133.0
0.60	95.35	138.0
0.70	96.86	136.0
0.80	93.89	126.0
0.90	79.93	102.0

*I Calculated by equation V-9
II Smoothed experimental data of
Jones and Lu (18)

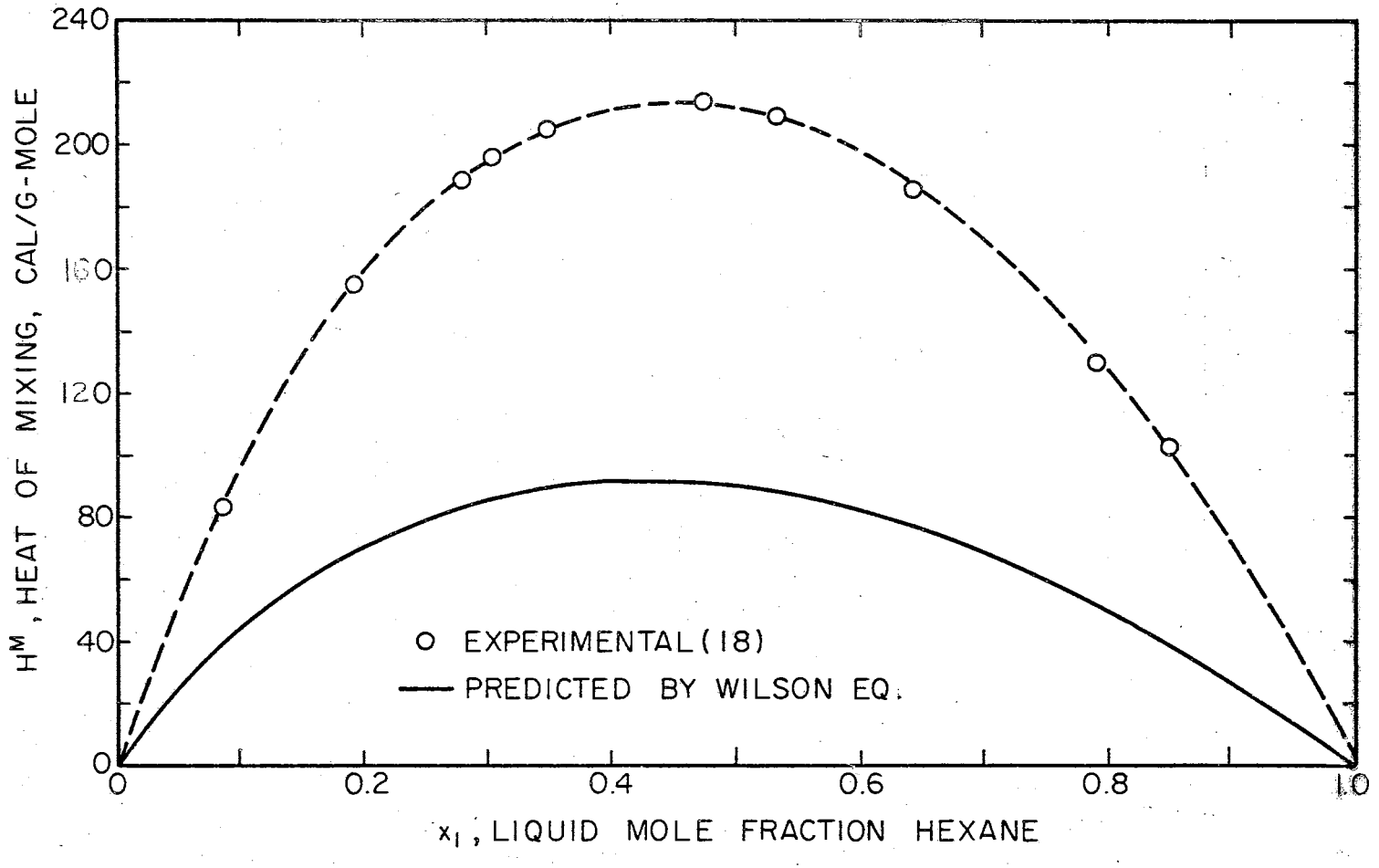

Figure 16. Heat of Mixing at 25° C for the System n-Hexane-Benzene

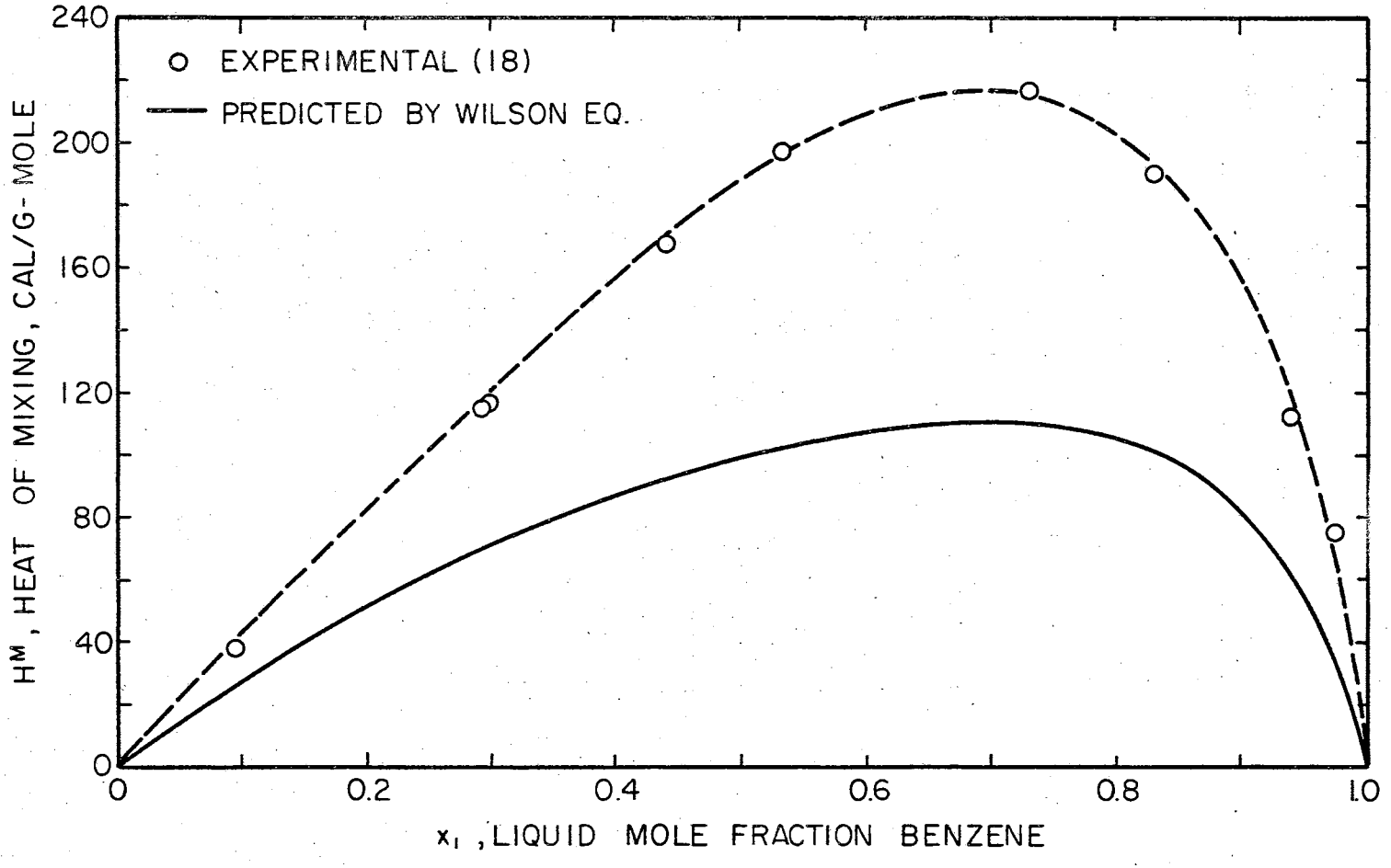

Figure 17. Heat of Mixing at 25° C for the System Benzene-Ethanol

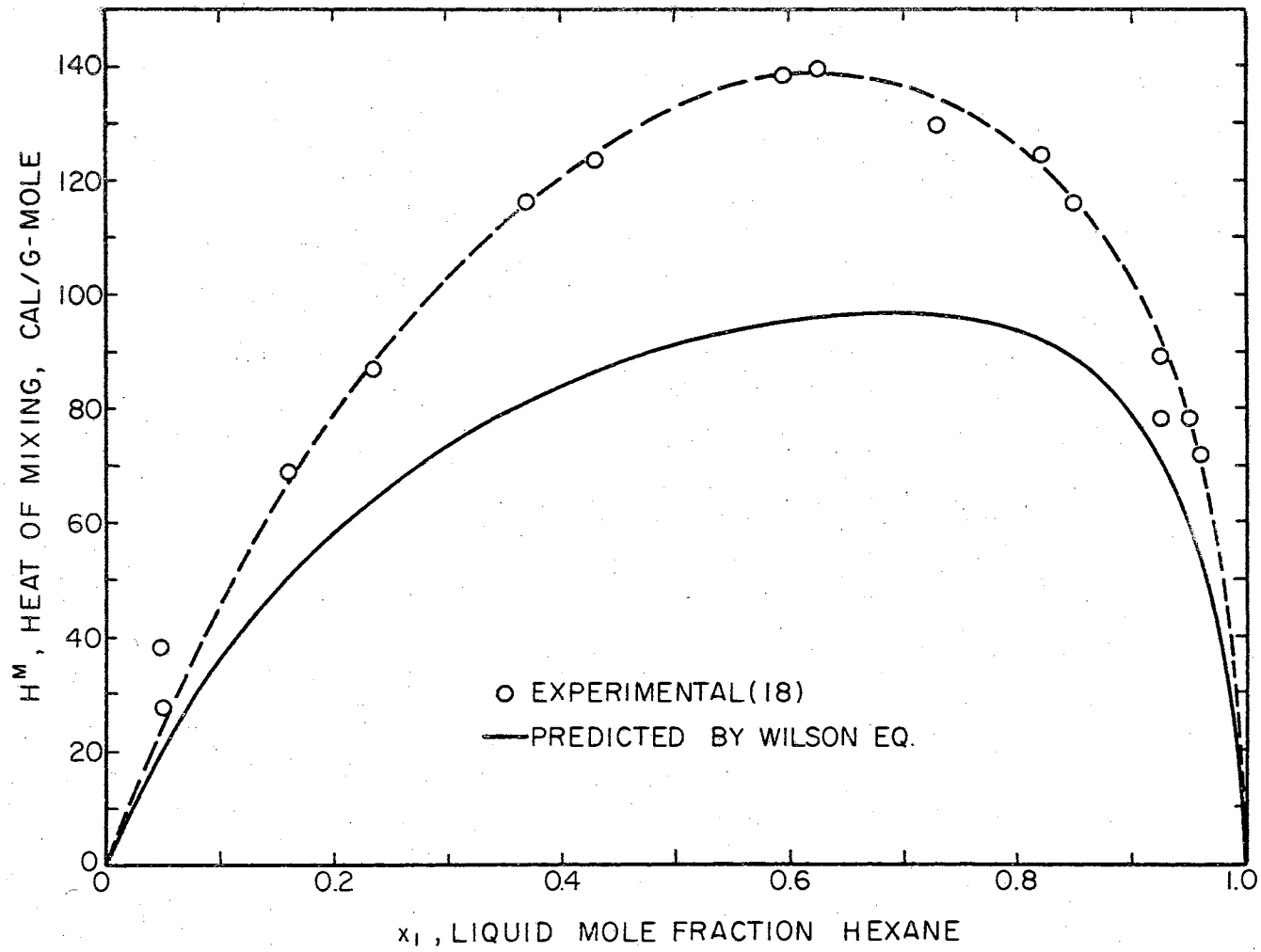

Figure 18. Heat of Mixing at 25° C for the System n-Hexane-Ethanol

$$TS^E = H^E - G^E \qquad \text{(V-10)}$$

Values of G^E calculated by Mixon's method were combined with Jones' H^M data for the calculation of TS^E. Values of H^M and G^E predicted by Wilson's equation were also used to calculate TS^E by equation V-10. Results of these calculations are presented in Tables XVI, XVII, and XVIII. Excess temperature-entropy product curves are shown for comparison with excess Gibbs free energy and heat of mixing curves in Figures 19, 20, and 21, for the systems hexane-benzene, benzene-ethanol, and hexane-ethanol respectively.

The caluclation of excess temperature-entropy product from experimental heat of mixing and excess Gibbs energy data completes the identification of pertinent thermodynamic mixing properties for each of the mixtures studied at 25° C.

Comparison With Literature Data

Since there are no previously reported VLE data at 25° C for the systems studied, the present data will be compared for mutual consistency with literature data at other temperatures.

Van Ness (37) shows that

$$d(G^E/T) = (V^M/T)dP - (H^M/T^2)dT + R \sum_{i=1}^{n} (\ln \gamma_i dx_i) \qquad \text{(V-11)}$$

where V^M = molar volume change on mixing, cc/g-mole.

For a liquid mixture with constant composition, equation V-11 may be modified to give

TABLE XVI

EXCESS TEMPERATURE-ENTROPY PRODUCT AT 25° C
FOR THE SYSTEM N-HEXANE-BENZENE

Liquid Mole Fraction Hexane, x_1	Excess Temperature-Entropy Product*, TS^E, cal/g-mole	
	I	II
0.10	0.29	50.2
0.20	-1.38	87.0
0.30	-3.29	105.8
0.40	-4.73	114.3
0.50	-5.45	115.6
0.60	-5.45	112.2
0.70	-4.78	99.4
0.80	-3.57	73.3
0.90	-1.93	39.3

*I Calculated by Wilson's Equation
II Calculated from experimental data

TABLE XVII

EXCESS TEMPERATURE-ENTROPY PRODUCT AT 25° C
FOR THE SYSTEM BENZENE-ETHANOL

Liquid Mole Fraction Benzene, x_1	Excess Temperature-Entropy Product*, TS^E, cal/g-mole	
	I	II
0.10	-56.7	-37.5
0.20	-101.9	-67.4
0.30	-135.0	-81.8
0.40	-155.5	-80.9
0.50	-162.7	-69.3
0.60	-155.7	-48.9
0.70	-133.4	-23.3
0.80	-94.9	7.2
0.90	-42.1	35.0

*I Calculated by Wilson's Equation
II Calculated from experimental data

TABLE XVIII

EXCESS TEMPERATURE-ENTROPY PRODUCT AT 25° C
FOR THE SYSTEM N-HEXANE-ETHANOL

Liquid Mole Fraction Hexane, x_1	Excess Temperature-Entropy Product*, TS^E, cal/g-mole	
	I	II
0.10	-83.6	-74.6
0.20	-149.9	-128.3
0.30	-197.8	-165.3
0.40	-227.4	-186.2
0.50	-238.6	-190.3
0.60	-230.7	-179.9
0.70	-202.3	-152.9
0.80	-151.2	-108.5
0.90	-75.0	-46.5

*I Calculated by Wilson's Equation
II Calculated from experimental data

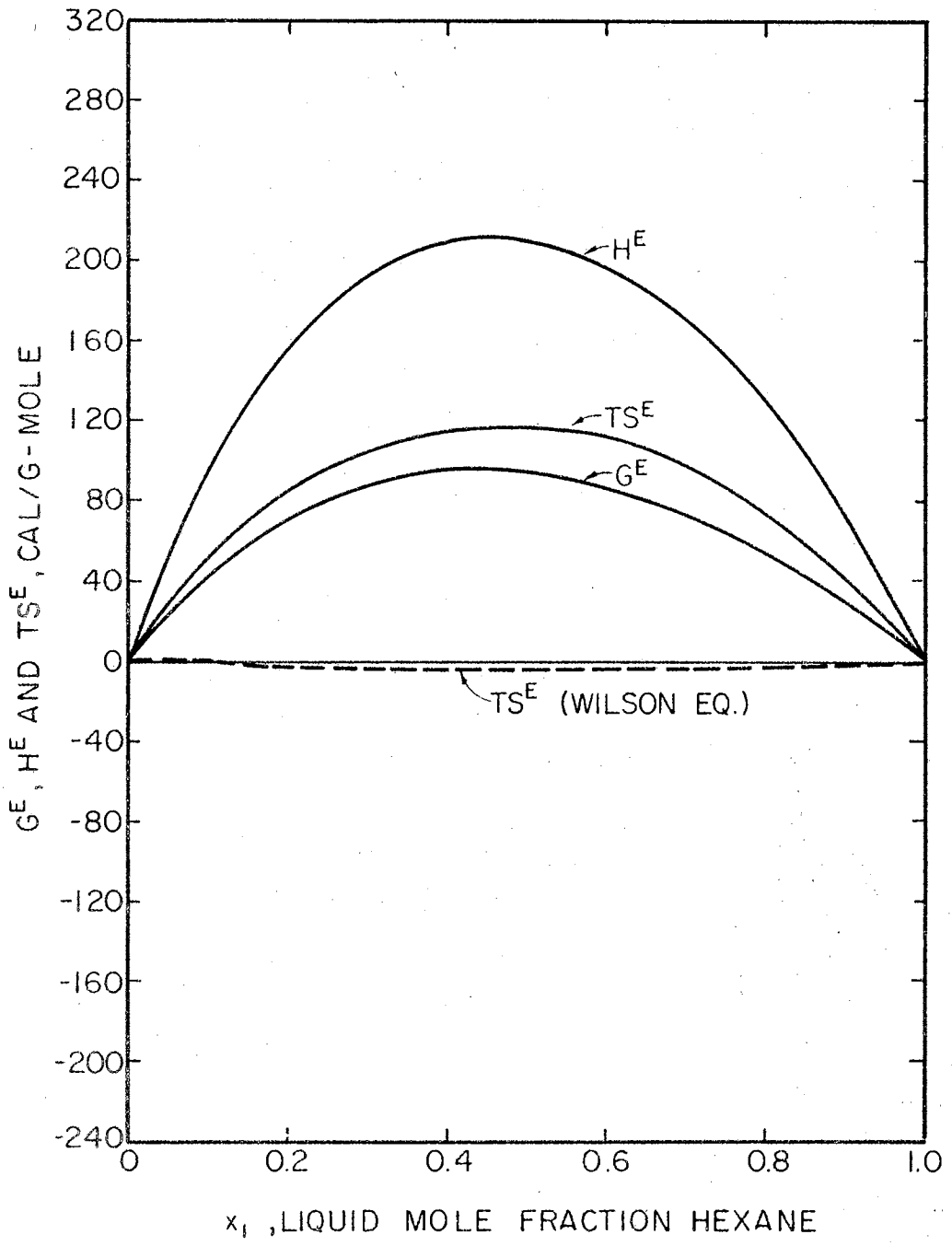

Figure 19. Excess Thermodynamic Properties at 25° C for the System n-Hexane-Benzene

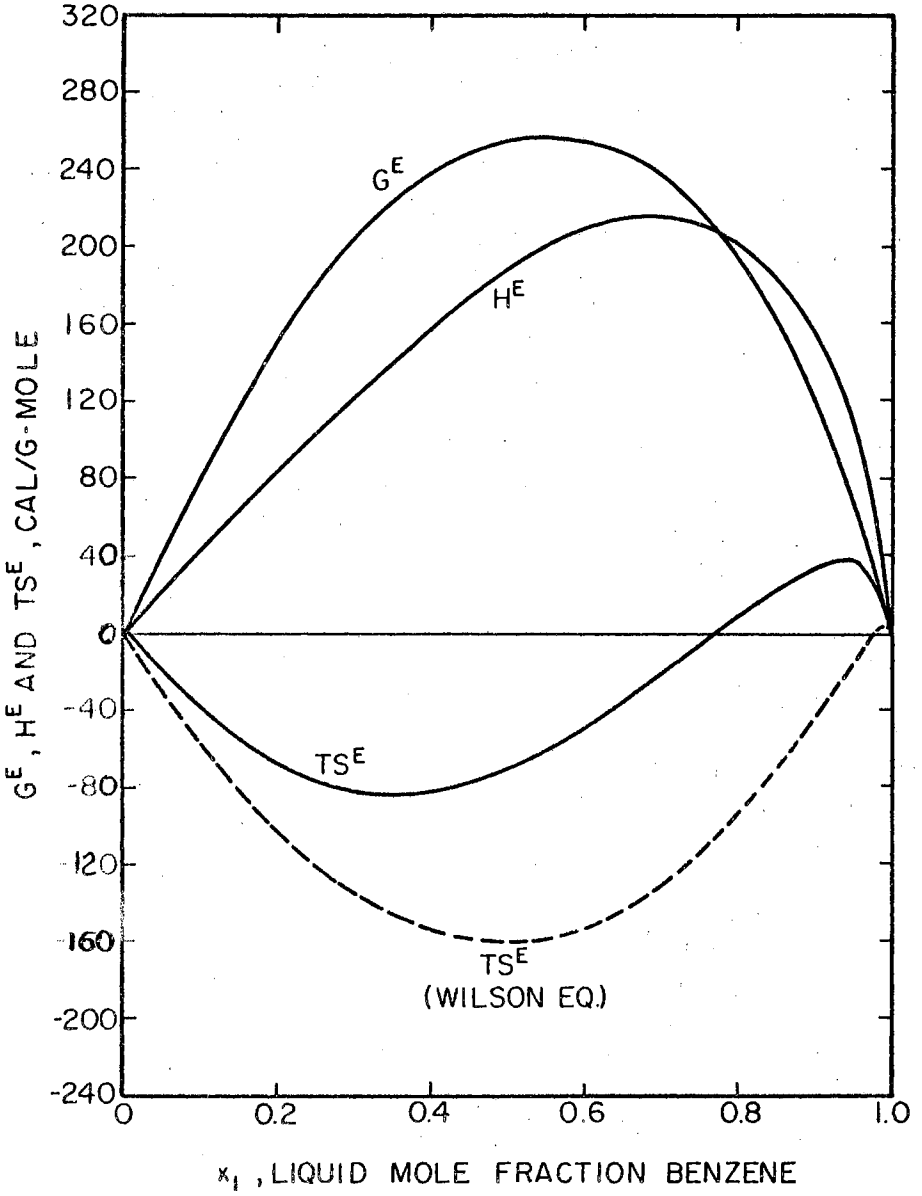

Figure 20. Excess Thermodynamic Properties at 25° C for the System Benzene-Ethanol

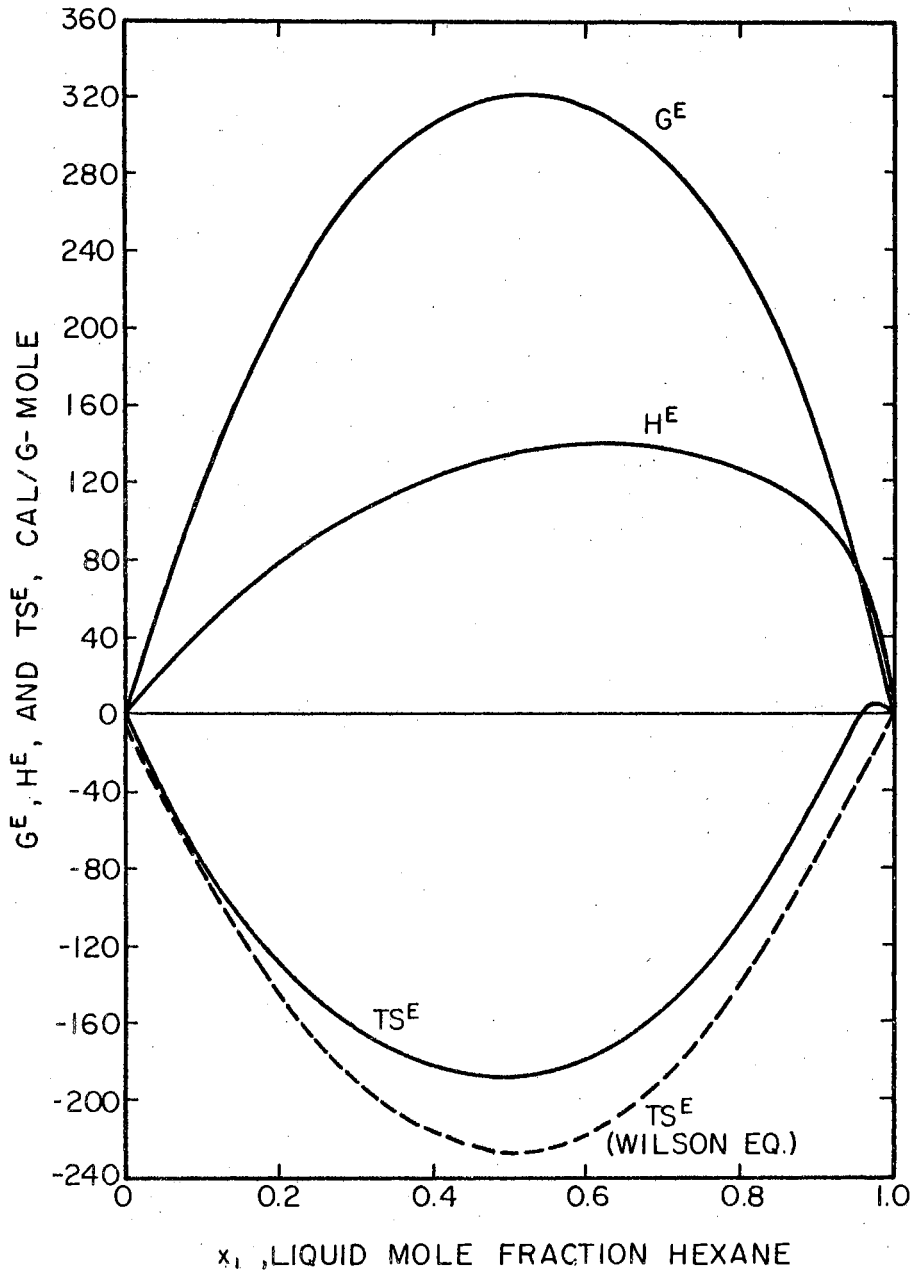

Figure 21. Excess Thermodynamic Properties at 25° C for the System n-Hexane-Ethanol

$$\int_{(G^E/T)_1}^{(G^E/T)_2} d(G^E/T) = \int_{P_1}^{P_2} (V^M/T)dP - \int_{T_1}^{T_2} (H^M/T^2)dT \qquad \text{(V-12)}$$

In Appendix B the term $\int_{P_1}^{P_2} (V^M/T)dP$ is shown to have a negligible effect on the value of G^E/T for the systems studied with small changes in P. Therefore, equation V-12 may be simplified to give

$$\int_{(G^E/T)_1}^{(G^E/T)_2} d(G^E/T) = \int_{T_1}^{T_2} -(H^M/T^2)dT \qquad \text{(V-13)}$$

Equation V-13 was used with the present 25° C VLE data and published heat of mixing data for the calculation of G^E/T data at several temperatures for the systems benzene-ethanol and hexane-ethanol. Sufficient heat of mixing data were not available for this calculation with the hexane-benzene system.

Brown and Fock (3) report H^M data for the entire composition range of benzene-ethanol at 25, 35, and 45° C. Brown, Fock and Smith (4) report H^M data at these temperatures for the hexane-ethanol mixture. Smoothed values of H^M at 0.1 increments of liquid mole fraction were read from plots of these data. Each value of H^M was divided by the square of absolute temperature. Values of $-(H^M/T^2)$ were plotted as a function of temperature for values of x_1 ranging from 0.1 to 0.9. Points were available at 25, 35, and 45° C and each plot was extrapolated to 55° C. Figure 22 shows typical plots for the system benzene-ethanol at benzene compositions of 0.1 and 0.2.

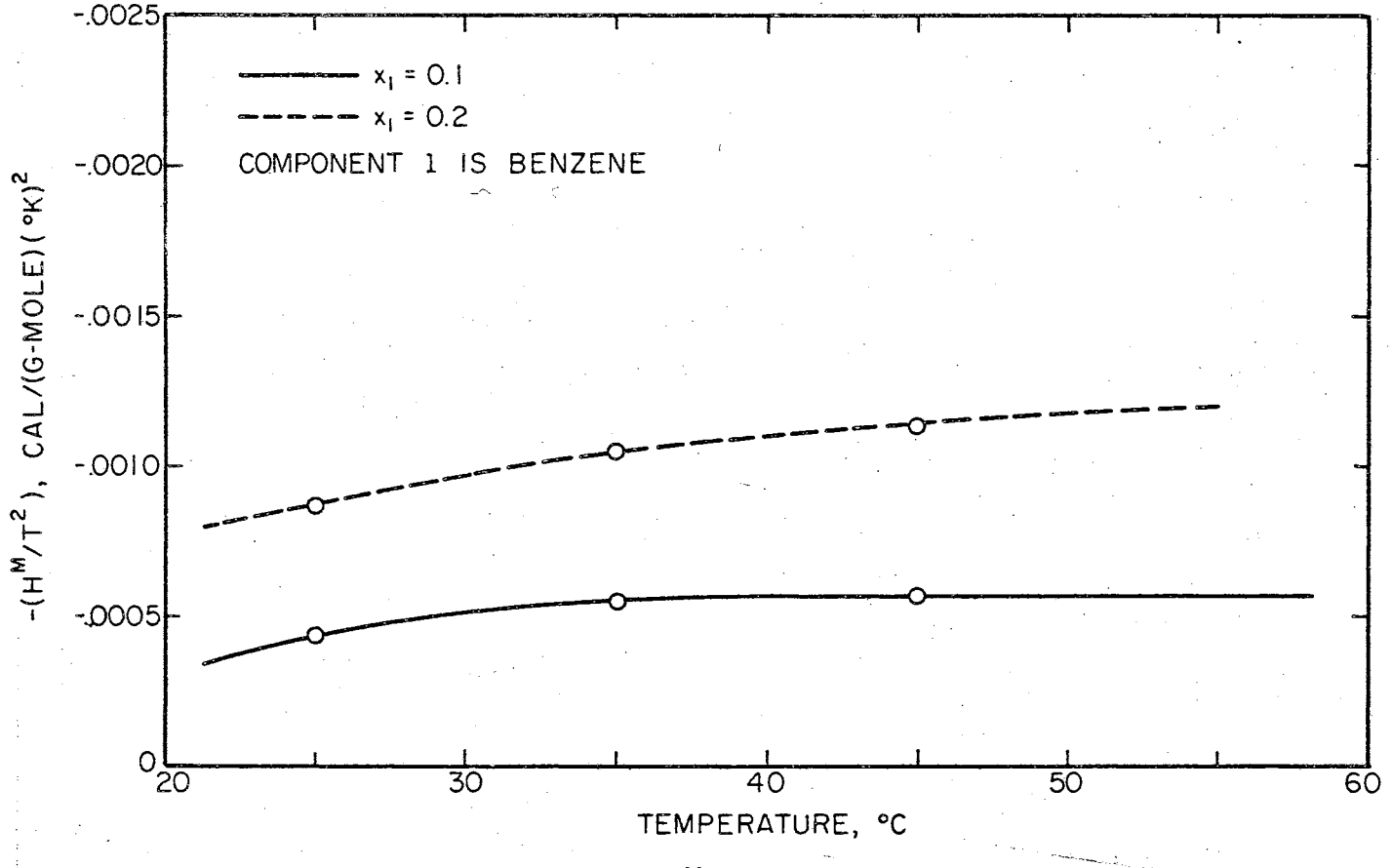

Figure 22. Typical plots of $-(H^M/T^2)$ vs. T for the System Benzene-Ethanol

Values of (G^E/T) at 25° C were calculated from "Mixon method" values of G^E given in Tables XI and XII. Graphical integration of each $-(H^M/T^2)$ curve from 25° C to the temperature of interest, T_2, led to the calculation of G^E/T at T_2 by the expression

$$(G^E/T)_{T_2° C} = (G^E/T)_{25° C} + \int_{298° K}^{T_2° K} (-H^M/T^2)dT \qquad (V-14)$$

Equally spaced predicted values of G^E at T_2 were then used as data in the computer program for the Mixon method. The program was allowed to pass through only one iteration so that predicted values of Π and y_1 could be calculated from the predicted values of G^E. (See equations II-14, II-49, and II-52). These predicted values of Π and y_1 at temperature T_2 resulted from rigorous calculations utilizing the experimental 25° C Π-x data from this study and experimental H^M data from the literature.

VLE data at 50° C are reported for the system benzene-ethanol by Zharov and Morachevskii (40) and by Udovenko and Fatkoulina (35). (The second data are also published by Timmermans (34).) For comparison with these data, values of Π and y_1 at 50° C were predicted by the method described above. Predicted Π-x data are compared with smoothed experimental values in Table XIX, and predicted y-x data are compared with smoothed experimental data in Table XX. Predicted data are compared graphically with experimental data in Figures 23 and 24 for Π-x data respectively.

Table XIX and Figure 23 show that the predicted and experimental Π-x data agree qualitatively, but that the predicted Π-x data are

TABLE XIX

PREDICTED AND EXPERIMENTAL VAPOR PRESSURES
AT 50° C FOR THE SYSTEM BENZENE-ETHANOL

Liquid Mole Fraction Benzene, x_1	Predicted Vapor Pressures, mm Hg	Smoothed Experimental Vapor Pressures*, mm Hg	
		I	II
0.10	296.2	298.0	299.0
0.20	337.7	341.0	342.0
0.30	359.5	365.0	366.0
0.40	371.7	378.0	377.0
0.50	377.3	383.0	383.0
0.60	378.5	384.5	384.5
0.70	377.9	384.5	384.0
0.80	374.2	378.0	377.5
0.90	356.1	360.0	361.0

*I Zharov and Morachevskii (40)
II Udovenko and Fatkoulina (34)

TABLE XX

PREDICTED AND EXPERIMENTAL VAPOR COMPOSITIONS
AT 50° C FOR THE SYSTEM BENZENE-ETHANOL

Liquid Mole Fraction Benzene, x_1	Predicted Vapor Mole Fraction Benzene, y_1	Smoothed Experimental Vapor Mole Fraction Benzene*, y_1	
		I	II
0.10	0.317	0.314	0.330
0.20	0.444	0.443	0.460
0.30	0.511	0.513	0.527
0.40	0.554	0.551	0.562
0.50	0.584	0.579	0.586
0.60	0.604	0.606	0.606
0.70	0.627	0.630	0.625
0.80	0.646	0.657	0.642
0.90	0.705	0.710	0.695

*I Zharov and Morachevskii (40)
II Udovenko and Fatkoulina (34)

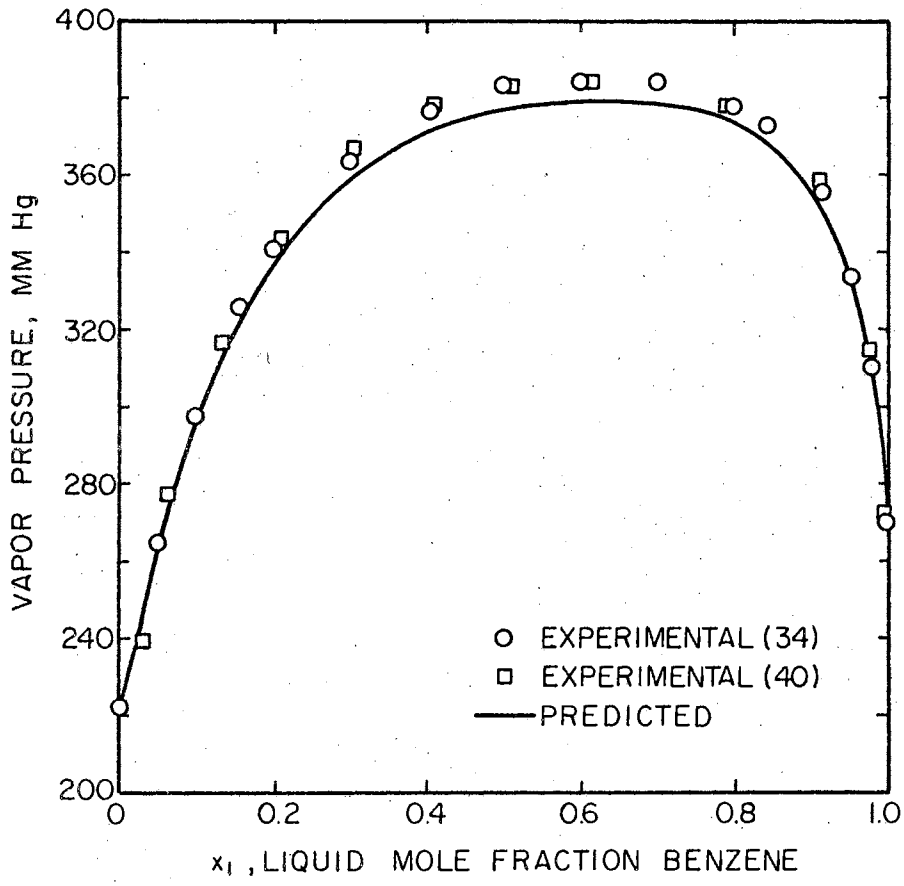

Figure 23. Predicted and Experimental Vapor Pressure at 50° C for the System Benzene-Ethanol

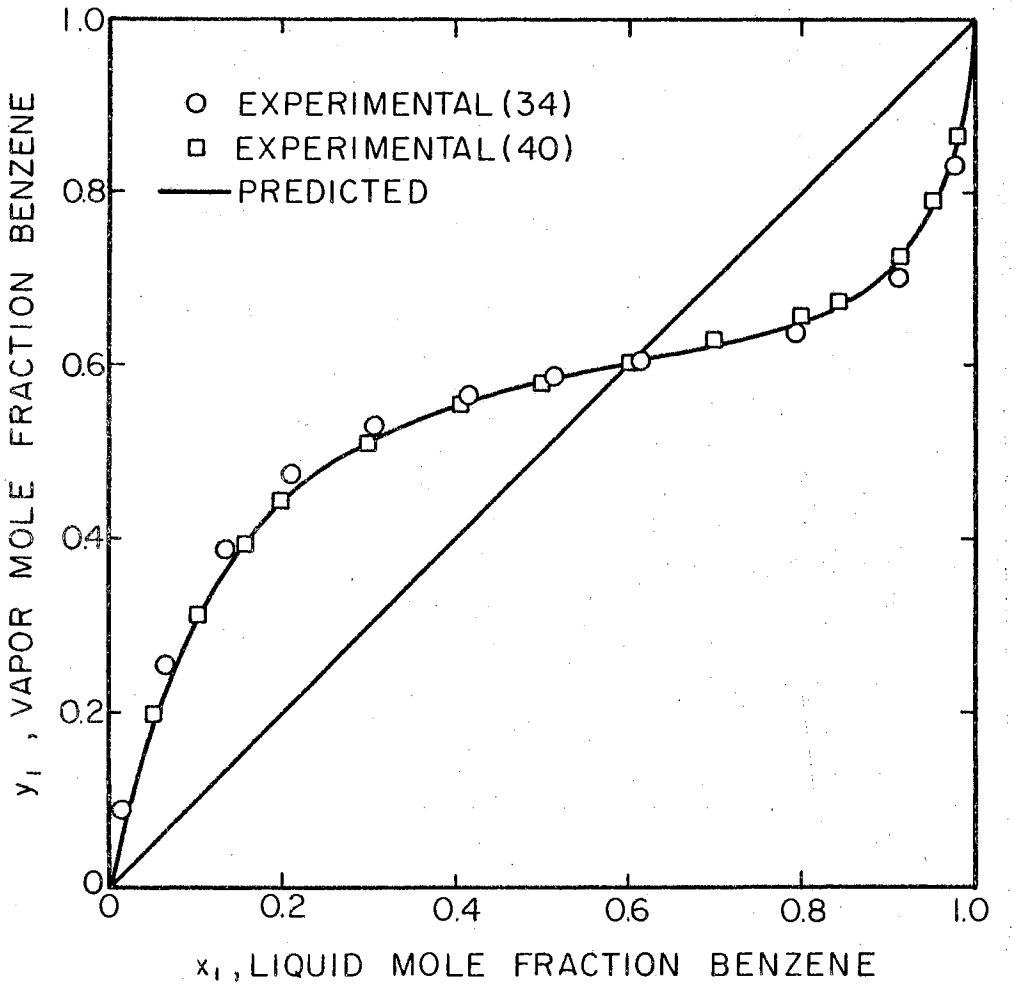

Figure 24. Predicted and Experimental Vapor Composition at 50° C for the System Benzene-Ethanol

lower than the experimental values by an average of 5 mm Hg. However, Table XX and Figure 24 show the predicted y-x data to agree with Zharov's data within an average of 0.004 in vapor mole fraction. Udovenko's y-x data deviate from Zharov's data and the predicted data by an average of about 0.015 in vapor mole fraction. The good agreement of the predicted y-x data with Zharov's data suggests that the 25° C data from this study and Zharov's 50° C data are mutually consistent. Since the predicted Π-x data and the predicted y-x data are thermodynamically consistent by the calculational method used, the disagreement in predicted and experimental Π-x data suggests that the 50° C experimental vapor pressures are high. The references for the 50° C data give no descriptions of the experimental apparatus used. However, if these authors used circulating stills which utilized gas caps for pressure control, their vapor pressures may be high.

Predicted values of Π-x data and y-x data for the system benzene-ethanol were also calculated at 55° C. The calculated values were compared with experimental data reported by Ho and Lu (16). The results of this comparison are not presented in detail since they were very similar to the results at 50° C. Again, the predicted y-x data agreed very well with experimental values, and the predicted Π-x curve was lower than the experimental curve by about 7 mm Hg.

The last temperature investigated for the system benzene-ethanol was 45° C. Predicted VLE data have been compared with experimental data reported by Brown and Smith (5). Predicted Π-x data are tabulated with smoothed experimental data in Table XXI. Predicted and smoothed experimental y-x data are given in Table XXII. Figures 25 and 26 show graphical comparisons of predicted and experimental values for Π-x

TABLE XXI

PREDICTED AND EXPERIMENTAL VAPOR PRESSURES
AT 45° C FOR THE SYSTEM BENZENE-ETHANOL

Liquid Mole Fraction Benzene, x_1	Predicted Vapor Pressures, mm Hg	Smoothed Experimental Vapor Pressures*, mm Hg
0.10	236.5	238.5
0.20	272.2	273.5
0.30	291.0	292.5
0.40	301.4	303.0
0.50	306.9	308.0
0.60	308.0	309.5
0.70	308.0	309.1
0.80	305.6	306.0
0.90	292.9	295.0

*Brown and Smith (5)

TABLE XXII

PREDICTED AND EXPERIMENTAL VAPOR COMPOSITIONS
AT 45° C FOR THE SYSTEM BENZENE-ETHANOL

Liquid Mole Fraction Benzene, x_1	Predicted Vapor Mole Fraction Benzene, y_1	Smoothed Experimental Vapor Mole Fraction Benzene*, y_1
0.10	0.335	0.327
0.20	0.464	0.463
0.30	0.529	0.530
0.40	0.571	0.570
0.50	0.602	0.598
0.60	0.620	0.618
0.70	0.641	0.637
0.80	0.659	0.660
0.90	0.712	0.715

*Brown and Smith (5)

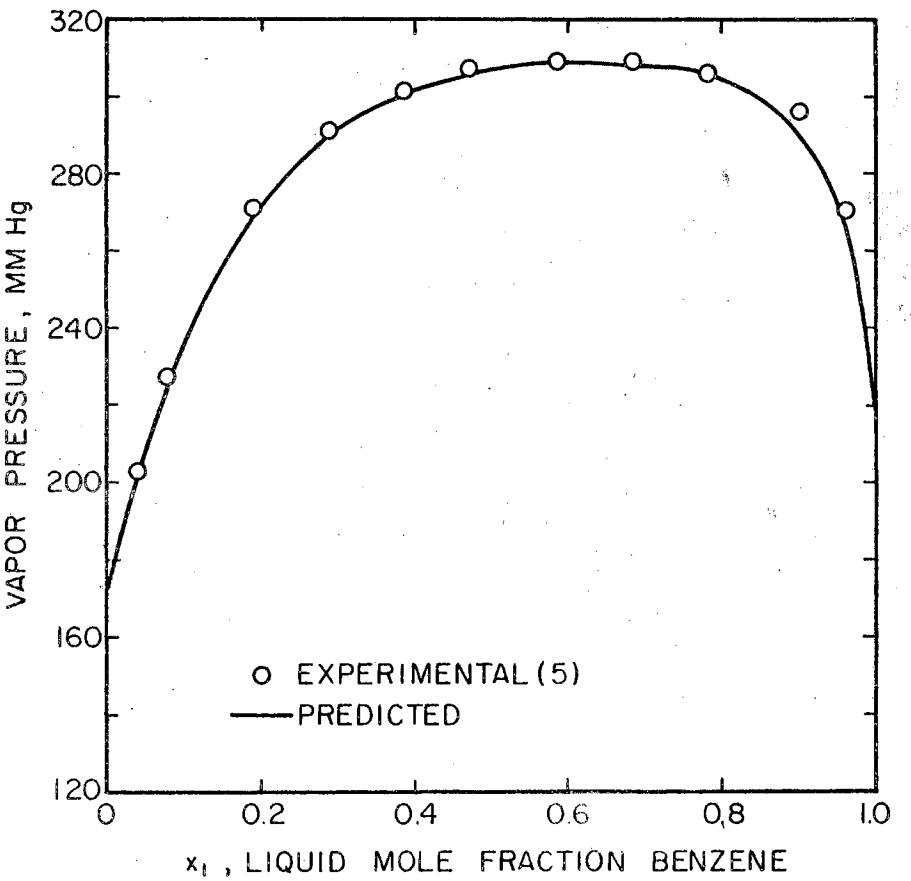

Figure 25. Predicted and Experimental Vapor Pressure at 45° C for the System Benzene-Ethanol

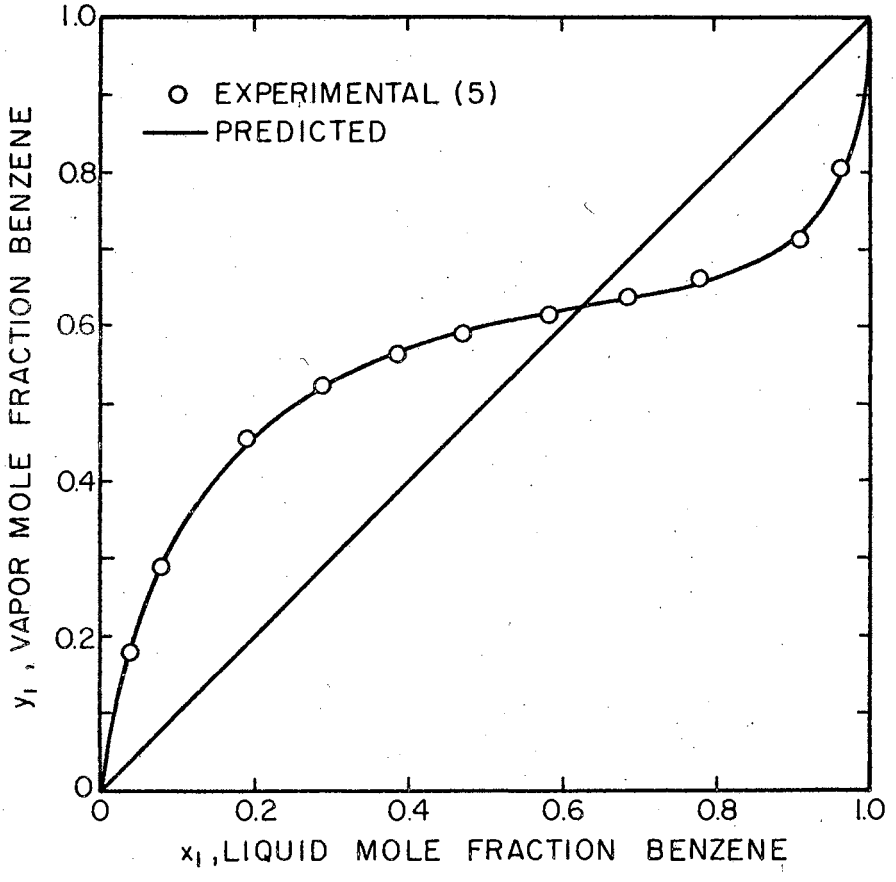

Figure 26. Predicted and Experimental Vapor Composition at 45° C for the System Benzene-Ethanol

data and y-x data respectively. Table XXI and Figure 25 show that the agreement in predicted and experimental Π-x data is much better than in the previous comparisons at 50 and 55 ° C. The predicted curve is lower than the experimental curve by an average of only 1.5 mm Hg. As in the previous comparisons, the predicted y-x data agree very well with the experimental data. In this case, predicted y-x data differ from the experimental data by an average of 0.003 in vapor mole fraction.

The good agreement in predicted and experimental VLE data at 45° C leads to the conclusion that the present 25° C Π-x data, the reported H^M data, and Brown's 45° C VLE data are mutually consistent.

The method of using the present 25° C Π-x data to predict VLE data at different temperatures was also used to analyze the hexane-ethanol data. Ho and Lu (16) report VLE data for this system at 55° C, and Kudryavtseva and Susarev (19) report VLE data at 35, 45, and 55° C. Predicted and smoothed experimental Π-x and y-x data at 55° C are given in Tables XXIII and XXIV respectively. Graphical comparison appears in Figures 27 and 28 for Π-x data and y-x data respectively. Table XXIII and Figure 27 show the predicted Π-x data to be lower than Ho's data by an average of 12 mm Hg. Kudryavtseva's vapor pressures are between the predicted curve and Ho's curve. Ho's vapor pressures may be high since he did use a circulating still with a gas cap to regulate pressure.

Figure 28 shows considerable disagreement in the two sets of experimental y-x data. At one point, the two sets of data differ by 0.07 in vapor mole fraction. The predicted y-x curve lies between the two experimental curves over most of the composition range. From this comparison, one must conclude that the two sets of experimental data are

TABLE XXIII

PREDICTED AND EXPERIMENTAL VAPOR PRESSURES
AT 55° C FOR THE SYSTEM N-HEXANE-ETHANOL

Liquid Mole Fraction n-Hexane, x_1	Predicted Vapor Pressures, mm Hg	Smoothed Experimental Vapor Pressures*, mm Hg	
		I	II
0.10	528.1	538.1	528.0
0.20	607.5	613.0	615.0
0.30	640.6	654.4	651.1
0.40	656.8	671.9	665.0
0.50	663.0	678.6	668.0
0.60	665.2	679.9	669.0
0.70	664.8	679.2	669.0
0.80	661.0	672.3	668.0
0.90	645.9	654.0	652.0

*I Ho and Lu (16)
II Kudryavtseva and Susarev (19)

TABLE XXIV

PREDICTED AND EXPERIMENTAL VAPOR COMPOSITIONS
AT 55° C FOR THE SYSTEM N-HEXANE-ETHANOL

Liquid Mole Fraction n-Hexane, x_1	Predicted Vapor Mole Fraction n-Hexane, y_1	Smoothed Experimental Vapor Mole Fraction n-Hexane*, y_1	
		I	II
0.10	0.500	0.487	0.512
0.20	0.585	0.567	0.615
0.30	0.619	0.590	0.655
0.40	0.638	0.608	0.662
0.50	0.649	0.620	0.666
0.60	0.656	0.627	0.670
0.70	0.667	0.645	0.675
0.80	0.682	0.680	0.680
0.90	0.715	0.706	0.692

*I Ho and Lu (16)
II Kudryavtseva and Susarev (19)

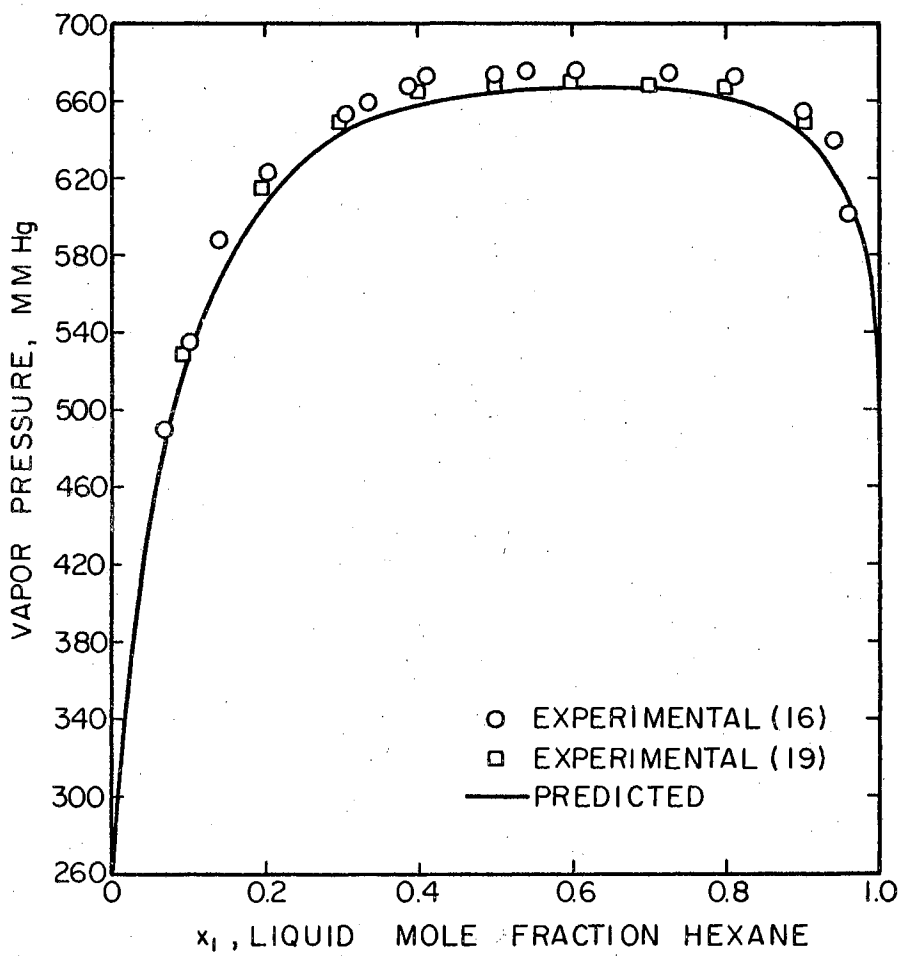

Figure 27. Predicted and Experimental Vapor Pressure at 55° C for the System n-Hexane-Ethanol

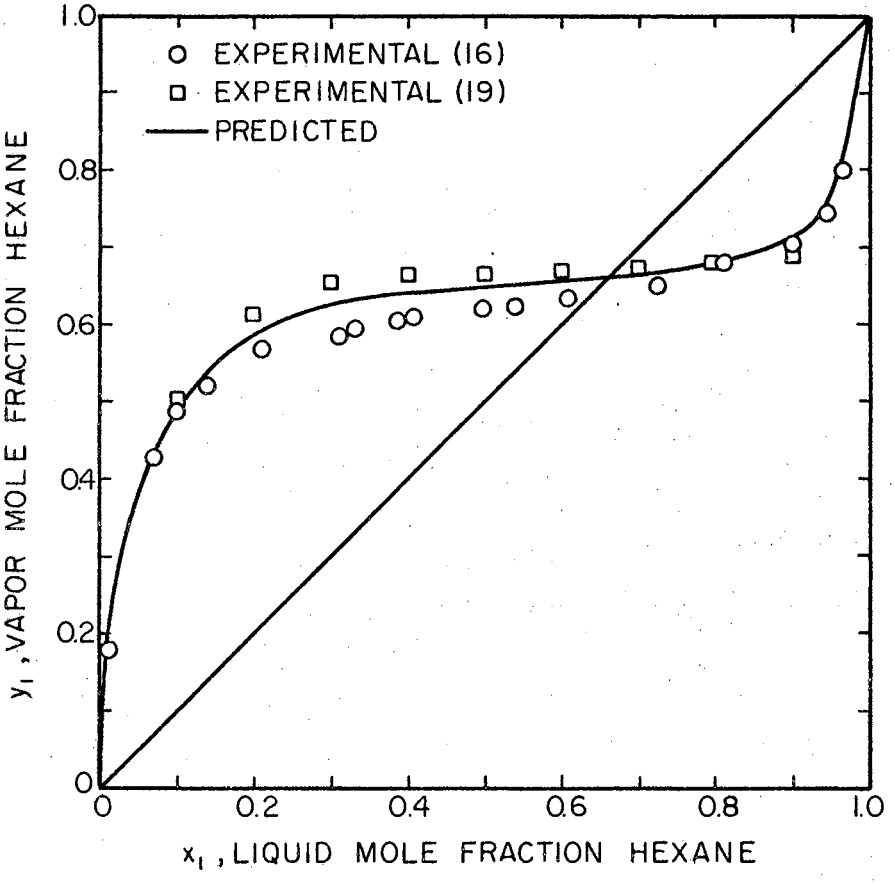

Figure 28. Predicted and Experimental Vapor Composition at 55° C for the System n-Hexane-Ethanol

mutually inconsistent. The predicted curve is not consistent with either set of experimental data since it is intermediate between the two experimental curves.

The calculations for this system were repeated for comparison with Kudryavtseva's 35° C VLE data. Details of these calculations are not presented since they resulted in a comparison qualitatively similar to the comparison with Kudryavtseva's 55° C data.

A second approach may be used to demonstrate the mutual consistency of the present 25° C data with the 55° C data reported by Ho and Lu (16). Because this second approach is dependent on an activity coefficient model, it is less rigorous than the previous approach. Recall that the Wilson parameters $(\lambda_{ij} - \lambda_{ii})$ and $(\lambda_{ij} - \lambda_{jj})$ may be assumed to be independent of temperature over a modest temperature interval. Therefore, if the 25° C and 55° C data are mutually consistent, one should be able to calculate 25° C vapor compositions using 55° C Wilson parameters.

Parameters $(\lambda_{12} - \lambda_{11})$ and $(\lambda_{12} - \lambda_{22})$ were calculated for each system using the computer program for estimation of non-linear parameters to fit Ho's 55° C Π-x data. Table XXV gives these parameters for each system. These parameters were used with equations II-37 and II-38 for calculating Λ_{12} and Λ_{21} at 25° C. Parameters Λ_{12} and Λ_{21} were then used to calculate activity coefficients and y-x data for each system. The results of these calculations are compared with 25° C y-x data from Mixon's method in Tables XXVI, XXVII, and XXVIII. Vapor compositions calculated using $(\lambda_{ij} - \lambda_{ii})$ values from the fit of the 25° C Π-x data are also tabulated.

TABLE XXV

WILSON PARAMETERS FROM HO'S 55° C
DATA FOR EACH SYSTEM

System*	$\lambda_{12} - \lambda_{11}$ cal/g-mole	$\lambda_{12} - \lambda_{22}$ cal/g-mole
Hexane-Benzene	237.68	202.59
Benzene-Ethanol	144.35	1625.63
Hexane-Ethanol	432.11	2075.36

*Component 1 is the first component listed for each system

TABLE XXVI

COMPARISON OF VAPOR COMPOSITIONS CALCULATED BY DIFFERENT METHODS FOR THE SYSTEM N-HEXANE-BENZENE AT 25° C

Liquid Mole Fraction Hexane, x_1	Vapor Mole Fraction Hexane, y_1			Differences in Mole Fractions	
	I	II	III	IV	V
0.10	0.242	0.245	0.232	-0.003	0.010
0.20	0.363	0.369	0.363	-0.006	------
0.30	0.456	0.455	0.456	0.001	------
0.40	0.529	0.527	0.532	0.002	-0.003
0.50	0.592	0.595	0.602	-0.003	-0.010
0.60	0.661	0.664	0.671	-0.003	-0.010
0.70	0.744	0.736	0.742	0.008	0.002
0.80	0.820	0.815	0.818	0.005	0.002
0.90	0.904	0.902	0.903	0.002	0.001

I Mixon Method
II Wilson Equation using parameters from 25° C data
III Wilson Equation using parameters from 55° C data
IV Difference I-II
V Difference I-III

TABLE XXVII

COMPARISON OF VAPOR COMPOSITIONS CALCULATED BY DIFFERENT METHODS FOR THE SYSTEM BENZENE-ETHANOL AT 25° C

Liquid Mole Fraction Benzene, x_1	Vapor Mole Fraction Benzene, y_1			Difference in Mole Fractions	
	I	II	III	IV	V
0.10	0.397	0.393	0.390	0.004	0.007
0.20	0.530	0.525	0.524	0.005	0.006
0.30	0.594	0.591	0.590	0.003	0.004
0.40	0.632	0.630	0.630	0.002	0.002
0.50	0.658	0.656	0.657	0.002	0.001
0.60	0.672	0.675	0.676	-0.003	-0.004
0.70	0.688	0.692	0.693	-0.004	-0.005
0.80	0.700	0.709	0.711	-0.009	-0.011
0.90	0.740	0.743	0.744	-0.003	-0.004

I Mixon Method
II Wilson Equation using parameters from 25° C data
III Wilson Equation using parameters from 55° C data
IV Difference I-II
V Difference I-III

TABLE XXVIII

COMPARISON OF VAPOR COMPOSITIONS CALCULATED BY DIFFERENT METHODS FOR THE SYSTEM N-HEXANE-ETHANOL AT 25° C

Liquid Mole Fraction Hexane, x_1	Vapor Mole Fraction Hexane, y_1			Difference in Mole Fractions	
	I	II	III	IV	V
0.10	0.620	0.618	0.628	0.002	-0.008
0.20	0.694	0.695	0.697	-0.001	-0.003
0.30	0.721	0.723	0.722	-0.002	-0.001
0.40	0.734	0.737	0.733	-0.003	0.001
0.50	0.739	0.745	0.740	-0.006	-0.001
0.60	0.744	0.751	0.745	-0.007	-0.001
0.70	0.749	0.755	0.749	-0.006	------
0.80	0.758	0.760	0.755	-0.002	0.003
0.90	0.776	0.772	0.771	-0.004	0.005

I Mixon Method
II Wilson Equation using parameters from 25° C data
III Wilson Equation using parameters from 55° C data
IV Difference I-II
V Difference I-III

Tables XXVI through XXVIII show that for each system, 25° C vapor compositions calculated using 55° C Wilson parameters are in excellent agreement with values calculated by Mixon's method. For the hexane-ethanol system, values of y_1 calculated with 55° C parameters are in better agreement with results by Mixon's method than are values of y_1 calculated with 25° C parameters.

These results suggest that the 25° C data from this study and Ho's 55° C VLE data are mutually consistent. Since 55° C Wilson parameters were successfully used to calculate y-x data at 25° C, Wilson parameters may be used for the calculation of VLE data for the systems studied at any temperature between 25 and 55° C.

CHAPTER VI

CONCLUSIONS AND RECOMMENDATIONS

This study consisted of an investigation of isothermal vapor-liquid equilibrium for the binary mixtures of hexane, benzene, and ethanol. A simplified apparatus for measuring solution vapor pressure was designed and constructed. The apparatus was tested for the mixtures mentioned at 25° C. From the experimental work and from analysis of the results of this work, certain conclusions may be summarized:

1. The results of this study successfully demonstrate that the simplified vapor pressure apparatus designed in this study may be used without appreciable sacrifice of experimental accuracy. Measured vapor pressures were estimated to be accurate within ±0.3 mm Hg.
2. The method described by Mixon for calculating vapor-liquid equilibrium data from Π-x data is more rigorous than the method presented by Barker. However, the Mixon method fails to converge for the Π-x data of some non-ideal mixtures.
3. The Wilson equation is the best 2-parameter model for expressing the excess Gibbs free energy of the systems studied. In some cases, the 3 and 4 parameter Redlich-Kister equations provided an improved fit of the experimental Π-x data.

4. Tabulation of excess Gibbs free energy and subsequent calculation of excess temperature-entropy product completes the identification of pertinent mixing properties for the mixtures studied at 25° C.
5. The data from this study have been shown to be reasonably consistent with literature data for these systems at different temperatures.

The following recommendations suggest modifications of the experimental apparatus:

1. The absolute pressure transducer should be replaced by the combination of a differential pressure cell and a highly accurate pressure gauge such as the fused quartz precision pressure gauge. This combination should result in more accurate pressure measurement.
2. The expansion (F in Figure 1) above the condenser on the equilibrium cell should be eliminated. This expansion complicated observation of the line of condensation during the boiling phase of degassing.
3. Greaseless joints should again be studied so that the use of lubricant between the equilibrium cell and the pressure measuring device could be eliminated.

With regard to future theoretical work, the following recommendation is a result of this study:

The Mixon method for calculating VLE data should be investigated from a mathematical approach to determine why the method fails to converge for some mixtures. This investigation might result in a modification of

the method which would cause the method to converge for all systems.

A SELECTED BIBLIOGRAPHY

(1) Barker, J. A. Aust. J. Chem. 6 (1953), 207.

(2) Beyer, V. W., H. Schuberth, and E. Leibnitz. Journal für praktische Chemie 4 (1965), 276.

(3) Brown, I. and W. Fock. Aust. J. Chem. 14 (1961), 387.

(4) Brown, I, W. Fock, and F. Smith. Aust. J. Chem. 17 (1964), 1106.

(5) Brown, I. and F. Smith. Aust. J. Chem. 7 (1954), 264.

(6) Chao, K. C. Unpublished Lecture Notes (1967).

(7) Chao, K. C., R. L. Robinson, M. L. Smith, and C. M. Kuo. Chemical Engineering Progress Symposium Series 63 (1968), 121.

(8) Chu, J. C. "Vapor-Liquid Equilibrium Data." Ann Arbor, Michigan, 1956.

(9) Davison, R. R., W. H. Smith, Jr., and K. W. Chun. AIChE Journal 13 (1967), 590.

(10) Dodge, B. F. "Chemical Engineering Thermodynamics." New York: McGraw-Hill Book Company, Inc., 1944.

(11) Dymond, J. and J. H. Hildebrand. I&EC Fundamentals 6 (1967), 130.

(12) Erbar, J. H. Private Communication (1968).

(13) Harris, H. G. and J. M. Prausnitz. AIChE Journal 14 (1968), 737.

(14) Hermsen, R. W. and J. M. Prausnitz. Chem. Eng. Science 18, (1963), 485.

(15) Ho, J. C. K., O. Boshko, and B. C.-Y. Lu. Can. J. Chem. Eng. 39 (1961), 205.

(16) Ho, J. C. K. and B. C.-Y. Lu. J. Chem. Eng. Data 8 (1963), 553.

(17) Hougen, O. A., K. M. Watson, and R. A. Ragatz. "Chemical Process Principles," Part II. New York: John Wiley & Sons, Inc., 1959.

(18) Jones, H. K. D. and B. C.-Y. Lu, J. Chem. Eng. Data 11 (1966), 488.

(19) Kudryavtseva, L. S. and M. P. Susarev. Zh. Prik. Khim. 36 (1963), 1471.

(20) Ljunglin, J. J. and H. C. Van Ness. Chem. Eng. Science 17 (1962), 531.

(21) Marquardt, D. W. J. S. I. A. M. 11 (1963), 431.

(22) Mixon, F. O., B. Gumowski, and B. Carpenter. I&EC Fundamentals 4 (1965), 455.

(23) O'Connell, J. P. and J. M. Prausnitz. I&EC Process Design and Development 6 (1967), 245.

(24) Orye, R. V. and J. M. Prausnitz. Industrial and Engineering Chemistry 57 (1965), 19.

(25) Prausnitz, J. M., C. A. Eckert, R. V. Orye, and J. P. O'Connell. "Computer Calculations for Multicomponent Vapor-Liquid Equilibria." Englewood Cliffs, New Jersey: Prentice-Hall, Inc., 1967.

(26) Prengle, W. W., Jr. and M. A. Pike, Jr. J. Chem. Eng. Data 6 (1961), 400.

(27) Prengle, W. W., Jr. and G. F. Palm. Industrial and Engineering Chemistry 49 (1957), 1769.

(28) Ramalho, R. S. and J. Delmas. Can. J. Chem. Eng. 46 (1968), 32.

(29) Ramalho, R. S. and J. Delmas. J. Chem. Eng. Data 13 (1968), 161.

(30) Renon, H. and J. M. Prausnitz. AIChE Journal 14 (1968), 135.

(31) Scatchard, G., G. M. Wilson, and F. G. Satkiewicz. Journal of the Am. Chem. Soc. 18 (1964), 125.

(32) Smith, J. M. and H. C. Van Ness. "Introduction to Chemical Engineering Thermodynamics." New York: McGraw-Hill Book Company, Inc., 1959.

(33) Susarev, M. P. and C. Shutzu. Russian Journal of Physical Chemistry 37 (1963), 938.

(34) Timmermans, J. "The Physio-Chemical Constants of Binary Systems in Concentrated Solutions," Interscience. New York, 1960.

(35) Udovenko, V. V. and L. G. Fatkulina. Zh. Fiz. Khim 26 (1952), 719.

(36) Van Laar, J. J. Zh. Physik. Chem. 72 (1910), 723.

(37) Van Ness, H. C. "Classical Thermodynamics of Non-Electrolyte Solutions." New York: MacMillan Company, 1964.

(38) Wiehe, I. A. and E. B. Bagley. I&EC Fundamentals 6 (1967), 209.

(39) Williamson, A. G. and R. L. Scott. J. Phys. Chem. 64 (1960), 440.

(40) Zharov, V. T. and A. G. Morachevskii. Zh. Prik. Khim. 36 (1963), 2397.

APPENDIX A

EQUIPMENT LIST

Model numbers, catalog numbers, and descriptive information for commercial components of the experimental apparatus are listed below in Table A-I. Figure numbers indicate items shown in the figures in Chapter III.

TABLE A-I

COMMERCIAL EQUIPMENT ITEMS

Figure Number	Item	Description
1-A	Stopcock	Greaseless, high vacuum 3-way stopcock. Westglass Cat. No. W-1846.
2-A	Transducer	Consolidated Electrodynamics Type 4-313, 0-20 psia absolute pressure transducer. Installed in waterproof adapter Type 4-013. Sensitivity: 21.04 mv Combined non-linearity and hysteresis: ±0.19% FR Zero Shift: +0.005% FR/°F Sensitivity Shift: -0.002% FR/°F Rated Excitation: 5 volts dc
2-B	Power Supply	Harrison Laboratories dc power supply, Model 6201 B.
2-C	Potentiometer	Tinsley Thermo-Electric Free Potentiometer. Type 3589-R.

TABLE A-I (Continued)

Figure Number	Item	Description
2-D	Galvanometer	Leeds & Northrup Model 2430-C
2-E	Power Supply	Harrison Laboratories dc power supply, Model 801 C.
2	Resistors	Leeds & Northrup 1 ohm and 2000 ohm precision standard resistors
3	Vacuum Pump	Duo Seal Model 1402. Rated vacuum: 0.1 micron
3	McLeod Gage	Curtin Cat. No. 8266Y2.
3	Manostat	Cartesian manostat. Curtin Cat. No. 13017-6.
	Pressure Gage	Fused Quartz Precision Pressure Gage. Texas Instruments Model 141A.
	Temperature Bath	Curtin Cat. No. 16532. Constant temperature bath equipped with two heaters, a cooling coil, heavy duty stirrer, and a Philadelphia Micro-Set temperature controller.
	Water Cooler	Sargent Cat. No. S-84890.
	Thermometer	Brooklyn Type 63/48. Range from 19°C to 31°C. Divisions of 0.01°C.
	Balance	Mettler Model B6 Semi-Micro, single pan balance. Rated accuracy: ±0.02 mg.
	Refractometer	Modified Abbe Precision Refractometer. Baush & Lomb Cat. No. 33-45-03-01. Rated accuracy ±0.00003 units.
	Magnetic Stirrer	Electric magnetic stirrer. Sargent Cat. No. S-76490.
	Magnetic Stirrer	Laboratory Supplies Company Cat. No. P111. Driven by tap water. May be immersed in water bath.

APPENDIX B

SIMPLIFICATION OF EQUATION V-12

In this section, the value of $\int_{P_1}^{P_2} (V^M/T)dP$ will be shown to be very small compared with the other two terms in equation V-12.

Consider an equal molar mixture of hexane and ethanol at 25° C. The volume change on mixing may be calculated as,

$$V^M = V - x_1 v_1^L - x_2 v_2^L \tag{B-1}$$

or

$$V^M \doteq V - (.5)(132) - (.5)(59)$$

$$\doteq V - 95 \text{ cc/g-mole} \tag{B-2}$$

Suppose the system exhibits a large volume change on mixing equal to about 3% of the ideal molar volume or about 3 cc/g-mole. Under these conditions,

$$V^M/T = 3/298 \doteq 0.01 \text{ cc/(g-mole)(°K)} \tag{B-3}$$

Assume that V^M/T is independent of system pressure. With this restriction,

$$\int_{P_1}^{P_2} (V^M/T)dP = (V^M/T)(P_2 - P_1) \tag{B-4}$$

Solution vapor pressures at 55° C and 25° C may be used as system pressures. For the equimolar hexane-ethanol mixture,

$$P_2 - P_1 \doteq 500 \text{ mm Hg} \doteq 0.66 \text{ atm} \qquad \text{(B-5)}$$

Equations B-3 and B-5 may be used in equation B-4 to give,

$$(V^M/T)(P_2 - P_1) = 0.0066 \frac{(\text{atm})(\text{cc})}{(\text{g-mole})(°\text{K})} \qquad \text{(B-6)}$$

Using the identity,

$$1 \text{ atm-cc} = 0.024 \text{ cal} \qquad \text{(B-7)}$$

we find that,

$$\int_{P_1}^{P_2} (V^M/T)dP = (V^M/T)(P_2 - P_1) \doteq 0.00016 \frac{\text{cal/g-mole}}{°\text{K}} \qquad \text{(B-8)}$$

For the equimolar mixture of hexane-ethanol at 298.16° K, calculations show that,

$$G^E/T = 1.1028 \text{ cal/(g-mole)(°K)} \qquad \text{(B-9)}$$

and

$$\int_{298° \text{ K}}^{328° \text{ K}} - (H^M/T^2)dT = -0.0535 \text{ cal/(g-mole)(°K)} \qquad \text{(B-10)}$$

Relative to these quantities, the value of $\int_{P_1}^{P_2} (V^M/T)dP$ given by equation B-8 is negligible. This reasoning led to simplification of equation V-12 to equation V-13.

APPENDIX C

COMPUTER PROGRAM FOR VAPOR-LIQUID EQUILIBRIUM

CALCULATIONS BY MIXON'S METHOD

As mentioned in Chapter V, a computer program was written for VLE calculations based on the method described by Mixon and co-workers (22). The program is in Fortran IV language. A block diagram, input and output information and a listing of the program are given below.

Block Diagram

The following block diagram shows the sequence of major steps in the calculation of VLE data by Mixon's method.

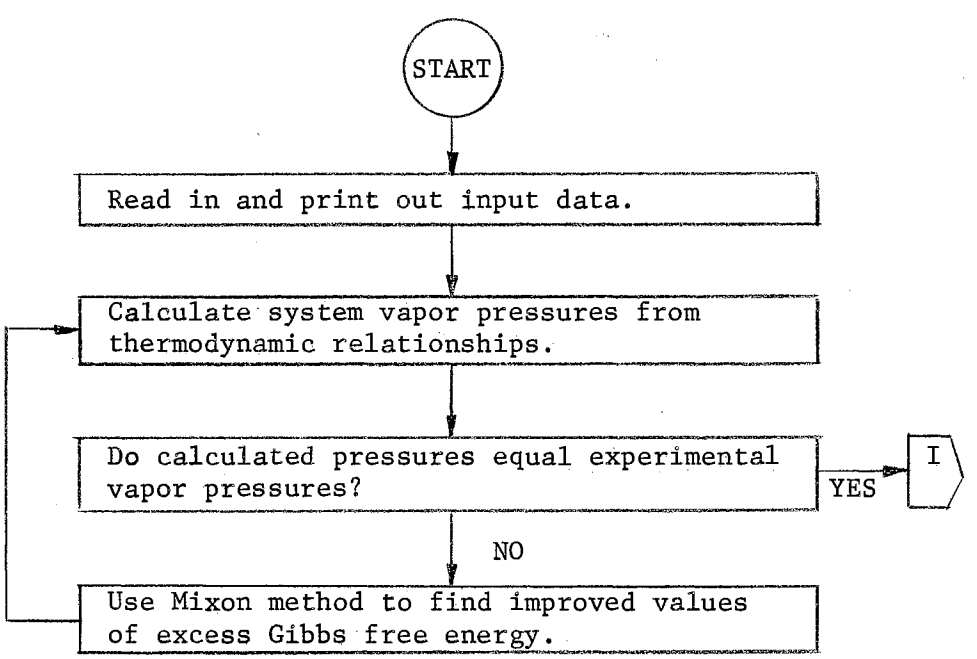

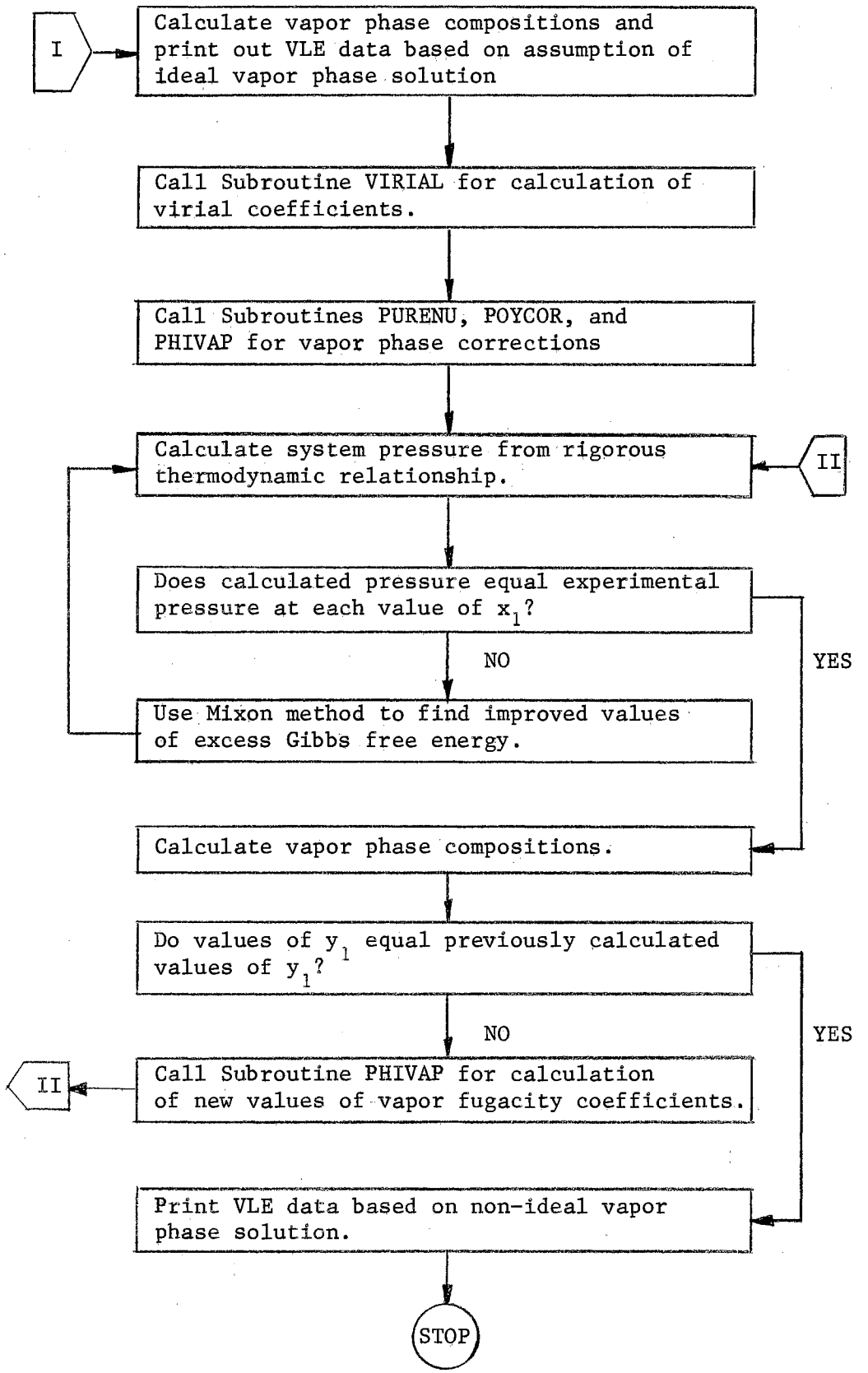
I
Calculate vapor phase compositions and print out VLE data based on assumption of ideal vapor phase solution
Call Subroutine VIRIAL for calculation of virial coefficients.
Call Subroutines PURENU, POYCOR, and PHIVAP for vapor phase corrections
Calculate system pressure from rigorous thermodynamic relationship.
II
Does calculated pressure equal experimental pressure at each value of x_1?
NO
YES
Use Mixon method to find improved values of excess Gibbs free energy.
Calculate vapor phase compositions.
Do values of y_1 equal previously calculated values of y_1?
NO
YES
II
Call Subroutine PHIVAP for calculation of new values of vapor fugacity coefficients.
Print VLE data based on non-ideal vapor phase solution.
STOP

Input Information

Required input information for operation of the program is described in this section.

Card 1

Variables: (ANAME(I), I = 1, 15)

Format: (15A4)

Comments: Card 1 identifies the run. Up to 60 spaces of alphameric information may be used.

Card 2

Variables: T, PSTAR1, PSTAR2, XINC

Format: (4F10.0)

Comments: T = system temperature, °C.
PSTAR1 = Vapor pressure of pure component 1, mm Hg.
PSTAR2 = Vapor pressure of pure component 2, mm Hg.
XINC = Increment for liquid mole fraction of component 1.

Cards 3 through NX+3

Variables: P(I), G(I)

Format: (2F10.0)

Comments: NX = 1.0/XINC
P(I) = Smoothed experimental vapor pressures, mm Hg.
G(I) = Initial guess for the values of G^E/RT.

A card corresponding to each value of x_1 is used to read in values of P(I) and G(I). Each value of G(I) may equal 0.0 if the system is one for which the calculation converges.

Card NX+4

Variables: TC1, TC2, PC1, PC2, VC1, VC2

Card NX+4 (Continued)

Format: (6F10.0)

Comments: TC1, TC2 = Critical temperature of components in °K.
PC1, PC2 = Critical pressure of components in atmospheres.
VC1, VC2 = Critical volume of components in cc/g-mole.

This card is called by Subroutine VIRIAL.

Card NX+5

Variables: WH1, WH2, DEBYE1, DEBYE2, CONST1, CONST2

Format: (6F10.0)

Comments: WH1, Wh2 - Accentric factors of components.
DEBYE1, DEBYE2 = Dipole moments of components in Debye.
CONST1, CONST2 = Empirical association constants of components.

This card is called by Subroutine VIRIAL. Dipole moments and association constants equal zero for nonpolar components.

Card NX+6

Variables: IPOLAR, JPOLAR, B11, B22

Format: (2I5, 2F10.0)

Comments: IPOLAR and JPOLAR refer to components 1 and 2 respectively. If the component is polar, enter a fixed point number. If the component is nonpolar, leave the field blank.

B11, B22 = Second virial coefficients for components 1 and 2. If experimental values are available, enter them; otherwise leave the fields blank.

Card NX+7

Variables: VLIQ1, VLIQ2

Format: (2F10.0)

Card NX+7 (Continued)

Comments: This card is called by Subroutine POYCOR. VLIQ1, VLIQ2 = Pure component molar volumes of components 1 and 2 at system temperature, cc/g-mole.

Output Information

A printout of input data preceeds the calculated results. Included in the results are VLE data based on the assumption of an ideal vapor phase. This output includes liquid and vapor compositions, experimental and calculated vapor pressures, excess Gibbs energy function, and activity coefficients.

This information is printed again after corrections for a non-ideal vapor phase have been made.

Fortran Listing

Following is a complete listing for the main program and Subroutines VIRIAL, PURENU, POYCOR, and PHIVAP.

FORTRAN LISTING OF PROGRAM FOR
VAPOR-LIQUID EQUILIBRIUM CALCULATIONS
BY MIXON'S METHOD

```
      COMMON R,TABS,U,B11,B22,B12,POYNT1,POYNT2,PSTAR1,PSTAR2,P,PURE1
      COMMON PURE2,Y,PHI1,PHI2,T,NX
      DIMENSION X)101*,P)101*,G)101*,DGDX)101*,GAMA1)101*,GAMA2)101*,
     1PRES)101*,PARP1)101*,PIDEL)101*,A)101*,B)101*,W)101*,BE)101*,F)101
     1*,GE)101*,Y)101*,BMIX)101*,PATM)101*,RAD)101*,V)101*,PLOG1)101*,
     1PLOG2)101*,POYNT1)101*,PHI1)101*,YPREV)101*,POYNT2)101*,PHI2)101*
      DIMENSION XG)50*,ANAME)15*
C
C  READ INPUT DATA FOR THE SYSTEM.
C
      IN = 1
      IO = 3
    1 READ)IN,2,END = 771*)ANAME)I*,I = 1,15*
    2 FORMAT )15A4*
      KKK = 1
      WRITE)IO,3*)ANAME)I*,I = 1,15*
    3 FORMAT )1H1,15A4*
      READ)IN,10*T,PSTAR1,PSTAR2,XINC
   10 FORMAT)4F10.0*
      WRITE)IO,4* T,PSTAR1,PSTAR2
    4 FORMAT)//22H SYSTEM TEMPERATURE = ,F6.2,22H DEGREES C.  PSTAR1 = ,
     1F8.3,10H PSTAR2 = ,F8.3*
      TABS = T + 273.16
      K = 0
      R = 82.07
      U = R*TABS
      X)1* = 1.0E-20
      NX = 1./XINC
C
C  INCREMENT MOLE FRACTION OF MORE VOLATILE COMPONENT BY XINC.
C  READ IN VALUES OF P)I* AND G)I*.  ALL VALUES OF G)I* MAY = 0.0.
C
      NX1 = NX-1
      DO 30 I = 2,NX1
   30 X)I* = X)I-1* +XINC
   25 DO 45 I = 1,NX1
      READ)IN,46* P)I*,G)I*
   46 FORMAT )2F10.0*
   45 CONTINUE
      WRITE)IO,48*NX1
   48 FORMAT )//5H THE ,I3,46H VALUES OF P)I* HAVE BEEN READ FROM DATA C
     1ARDS*
      PURE1 = 1.
      PURE2 = 1.
      DO 13 I = 2,NX
      POYNT1)I* = 1.
      POYNT2)I* = 1.
      PHI1)I* = 1.
   13 PHI2)I* = 1.
C
C  WITH THE INITIALLY ASSUMED VALUES OF EXCESS GIBBS ENERGY FUNCTION,
C  CALCULATE SOLUTION VAPOR PRESSURES AND LIQUID PHASE ACTIVITY COEFFI-
```

```
C  CIENTS AS FUNCTIONS OF LIQUID COMPOSITION.
C
  140 DO 50 I = 2,NX
      DGDX)I* = )G)I.1*-G)I-1**/)2.0*XINC*
      GAMA1)I* = EXP)G)I* .DGDX)I* -X)I**DGDX)I**
   50 GAMA2)I* = EXP)G)I*-X)I**DGDX)I**
      IF )K* 605,55,605
   55 DO 56 I = 2,NX
   56 PRES)I* = X)I**PSTAR1*GAMA1)I**PURE1*POYNT1)I*/PHI1)I* . )1.0-X)I*
     1**PSTAR2*GAMA2)I**PURE2*POYNT2)I*/PHI2)I*
C
C  COMPARE CALCULATED PRESSURE WITH EXPERIMENTAL PRESSURE.
C
  600 DO 80 I = 2,NX
      DIFF =ABS)P)I*-PRES)I**
      IF )DIFF-.001* 80,80,70
   70 GO TO 90
   80 CONTINUE
C
C  USE BLOCK RELAXATION TECHNIQUE TO FIND AN IMPROVED VALUE OF G.  USE
C  THE IMPROVED VALUE TO RECALCULATE VAPOR PRESSURE AND ACTIVITY COEFF.
C
      IF )K* 700,100,700
   90 DO 110 I = 2,NX
      PARP1)I* = X)I**GAMA1)I**PSTAR1*POYNT1)I**PURE1/PHI1)I*
      PIDEL)I* = X)I**PSTAR1
      A)I* = -1.0*))PARP1)I*-PIDEL)I**/)2.0*XINC**
  110 B)I* = PRES)I*
      W)2* = PRES)2*
      BE)2* = -)A)2*/W)2**
      F)2* = )P)2*-PRES)2**/W)2*
      DO 120 I = 3,NX
      W)I* = B)I* - A)I**BE)I-1*
      BE)I* = -)A)I*/W)I**
  120 F)I* = )P)I*-PRES)I*-A)I**F)I-1**/W)I*
      GE)NX* = F)NX*
      NXX = NX - 1
      DO 130 I = 2,NXX
      J = NX1 - I
  130 GE)J* = F)J* - BE)J**GE)J.1*
      DO 135 I = 2,NX
  135 G)I* = G)I* . GE)I*
      DO 58 I = 2,NX
   58 WRITE)IO,57* X)I*,P)I*,PRES)I*,GAMA1)I*,G)I*,GE)I*
   57 FORMAT )4F12.4,2F11.6*
      KKK = KKK . 1
      IF )KKK-10*140,1,1
C
C  AFTER THE PRESSURE CALCULATION CONVERGES TO EXPERIMENTAL VALUES,
C  CALCULATE VAPOR PHASE COMPOSITION BASED ON THE ASSUMPTION OF AN
C  IDEAL VAPOR PHASE.
C
  100 DO 150 I = 2,NX
      Y)I* = X)I**PSTAR1*GAMA1)I**PURE1*POYNT1)I*/)PHI1)I**PRES)I**
  150 YPREV)I* = Y)I*
      WRITE)IO,155*
  155 FORMAT)//89H IF ONE ASSUMES IDEAL SOLUTION BEHAVIOR FOR THE VAPOR
     1PHASE, THE VLE DATA ARE AS FOLLOWS.*
  800 WRITE)IO,160*
  160 FORMAT)/82H      X1           Y1         P EXPTL       P CALC     EXCES
     1S G/RT  GAMMA 1      GAMMA 2//*
      DO 200 I = 2,NX
  200 WRITE)IO,170*X)I*,Y)I*,P)I*,PRES)I*,G)I*,GAMA1)I*,GAMA2)I*
```

```
  170 FORMAT )3X,F6.4,6X,F6.4,6X,F7.3,6X,F7.3,5X,F6.4,5X,F7.4,5X,F7.4/*
      IF )K* 1,760,1
  760 K = K.1
C
C  USE SUBROUTINES TO MAKE CORRECTIONS FOR VAPOR PHASE NON-IDEALITIES.
C
      CALL VIRIAL
      CALL PURENU
      CALL POYCOR
  730 CALL PHIVAP
  605 DO 601 I = 2,NX
  601 PRES)I* = X)I**PSTAR1*GAMA1)I**PURE1*POYNT1)I*/PHI1)I* . )1.0-X)I*
     1**PSTAR2*GAMA2)I**PURE2*POYNT2)I*/PHI2)I*
      GO TO 600
C
C  AFTER PRESSURE CALCULATIONS CONVERGE, CALCULATE VAPOR PHASE COMPOSI-
C  TIONS.  COMPARE THESE VALUES WITH THE MOST RECENTLY CALCULATED VALUES.
C  WHEN THE DIFFERENCE IS VERY SMALL, THE CALCULATED Y'S ARE TAKEN AS
C  FINAL.
C
  700 DO 705 I = 2,NX
  705 Y)I* = X)I**PSTAR1*GAMA1)I**PURE1*POYNT1)I*/)PHI1)I**PRES)I**
      DO 710 I = 2,NX
      COMP = ABS)Y)I*-YPREV)I**
      IF)COMP-0.0001* 710,710,720
  720 GO TO 780
  710 CONTINUE
      GO TO 785
  780 DO 790 I = 2,NX
  790 YPREV)I* = Y)I*
      GO TO 730
  785 WRITE)IO,750*
  750 FORMAT)//79H AFTER CORRECTIONS FOR VAPOR PHASE NON-IDEALITIES, THE
     1 VLE DATA ARE AS FOLLOWS.*
      GO TO 800
  771 STOP
      END
C
      SUBROUTINE VIRIAL
C
C  SUBROUTINE VIRIAL CALCULATES PURE AND MIXED SECOND VIRIAL COEFFICIENTS
C  FOR THE COMPONENTS OF A BINARY MIXTURE.  THE CORRELATION OF PRAUSNITZ
C  HAS BEEN USED.  THE CORRELATION IS APPLICABLE FOR BOTH POLAR AND NON-
C  POLAR COMPONENTS.
C
      COMMON R,TABS,U,B11,B22,B12,POYNT1,POYNT2,PSTAR1,PSTAR2,P,PURE1
      COMMON PURE2,Y,PHI1,PHI2,T,NX
      DIMENSIONPOYNT1)101*,POYNT2)101*,P)101*,Y)101*,PHI1)101*,PHI2)101*
      IN = 1
      IO = 3
      READ)IN,100* TC1,TC2,PC1,PC2,VC1,VC2
  100 FORMAT )6F10.0*
      WRITE)IO,112*TC1,TC2,PC1,PC2,VC1,VC2
  112 FORMAT)//64H THE CRITICAL CONSTANTS IN DEGREES K, ATM, AND CC PER
     1G-MOLE ARE,/9H TC)1* = ,F7.2,9H TC)2* = ,F7.2,9H PC)1* = ,F7.2,9H
     1PC)2* = ,F7.2,9H VC)1* = ,F7.2,9H VC)2* = ,F7.2*
      READ)IN,110*WH1,WH2,DEBYE1,DEBYE2,CONST1,CONST2
  110 FORMAT )6F10.0*
      WRITE)IO,114*WH1,WH2,DEBYE1,DEBYE2,CONST1,CONST2
  114 FORMAT)//63H OTHER INPUT DATA FOR CALCULATION OF SECOND VIRIAL COE
     1FFICIENTS,/8H  WH1 = ,F6.3,7H WH2 = ,F6.3,10H DEBYE1 = ,F6.2,10H D
     1EBYE2 = ,F6.2,10H CONST1 = ,F5.2,10H CONST2 = ,F5.2*
C
```

```
C  IF COMPONENT 1 IS POLAR, ENTER A FIXED POINT NUMBER IN COLUMNS 1-5.
C  IF THE COMPONENT IS NON-POLAR, LEAVE THE FIELD BLANK.  DO THE SAME
C  FOR COMPONENT 2 IN COLUMNS 6-10.
C IF EXPERIMENTAL DATA ARE AVAILABLE, ENTER THE VALUES OF B11 AND/OR B22
C IF EXPERIMENTAL DATA ARE NOT AVAILABLE, LEAVE THE FIELD BLANK AND THE
C PRAUSNITZ CORRELATION WILL BE USED.
C
      N = 0
      READ)IN,120*IPOLAR,JPOLAR,B11,B22
  120 FORMAT)2I5,2F10.0*
      IF)IPOLAR* 360,370,360
  370 WRITE)IO,375*
  375 FORMAT)//26H COMPONENT 1 IS NON-POLAR.*
      GO TO 380
  360 WRITE)IO,365*
  365 FORMAT)//22H COMPONENT 1 IS POLAR.*
  380 IF)JPOLAR* 361,371,361
  371 WRITE)IO,372*
  372 FORMAT)//26H COMPONENT 2 IS NON-POLAR.*
      GO TO 390
  361 WRITE)IO,362*
  362 FORMAT)//22H COMPONENT 2 IS POLAR.*
  390 B = B11
      IF)B11* 330,392,330
  392 TRED = TABS/TC1
      GO TO 140
  150 TRED = TABS/TC2
      B = B22
      IF)B22* 320,140,320
  140 FB0 = )))-0.0121/TRED -0.1385**1.0/TRED-0.330**1.0/TRED .0.1445*
      FB1 = ))))-0.0073/TRED**5-0.097**1.0/TRED-0.50**1.0/TRED.0.46**1.0
     1/TRED.0.073*
      IF )N-1* 160,170,180
  160 IF )IPOLAR* 200,300,200
  170 IF )JPOLAR* 201,301,201
  300 W = WH1
      TC = TC1
      PC = PC1
      GO TO 302
  301 W = WH2
      TC = TC2
      PC = PC2
  302 CON = 0.0
      FUNCT = 0.0
      FATR = 0.0
  303 B = )R*TC/PC**)FB0.W*FB1.FUNCT.CON*FATR*
      IF )1-N* 310,320,330
  330 WRITE)IO,331* T,B
  331 FORMAT)//48H THE SECOND VIRIAL COEFFICIENT OF COMPONENT 1 AT,F7.2,
     112H DEGREES C =,F8.1,14H CC PER G-MOLE*
      B11 = B
      N = N.1
      GO TO 150
  200 DEBYE = DEBYE1
      TC = TC1
      PC = PC1
      W = WH1
      CON = CONST1
      GO TO 210
  201 DEBYE = DEBYE2
      TC = TC2
      PC = PC2
      W = WH2
```

```
      CON = CONST2
  210 DERED = )100000.0*DEBYE**2*PC*/)TC**2*
      IF)4.0 - DERED* 211,211,212
  212 FUNCT = 0.0
      GO TO 213
  211 FUNCT = -5.237220 .5.665807*ALOG)DERED*-2.133816*)ALOG)DERED***2*
     1.0.2525373*)ALOG)DERED***3*.)1.0/TRED**)5.769770-6.181427*)ALOG)DE
     1RED**.2.283270*)ALOG)DERED***2*-0.2649074*)ALOG)DERED***3**
  213 FATR= EXP)6.6*)0.7-TRED**
      GO TO 303
  320 WRITE)IO,321* T,B
  321 FORMAT)//48H THE SECOND VIRIAL COEFFICIENT OF COMPONENT 2 AT,F7.2,
     112H DEGREES C =,F8.1,14H CC PER G-MOLE*
      B22 = B
      N = N.1
  340 TC12 = SQRT)TC1*TC2*
      TRED = TABS/TC12
      PC12 = 4.0*TC12*)PC1*VC1/TC1 . PC2*VC2/TC2*/))VC1**0.333.VC2**0.33
     13***3*
      TC = TC12
      PC = PC12
      GO TO 140
  180 W = 0.5*)WH1.WH2*
      IF)DEBYE1*220,221,220
  220 IF)DEBYE2*222,221,222
  222 CON =)0.5*)CONST1.CONST2**
      DERED = )100000.0*DEBYE1*DEBYE2*PC12*/)TC12**2*
      IF )4.0-DERED* 211,211,223
  221 CON = 0.0
  223 FUNCT = 0.0
      GO TO 213
  310 WRITE)IO,311*T,B
  311 FORMAT)//45H THE SECOND MIXED VIRIAL COEFFICIENT, B12, AT,F7.2,11H
     1DEGREES C =,F8.1,14H CC PER G-MOLE*
      B12 = B
      RETURN
      END
C
      SUBROUTINE PURENU
C
C  SUBROUTINE PURENU CALCULATES THE PURE COMPONENT VAPOR PHASE FUGACITY
C  COEFFICIENTS AT THE SYSTEM TEMPERATURE AND PURE COMPONENT VAPOR PRES-
C  SURE.  THE VIRIAL EQUATION OF STATE TRUNCATED AFTER THE SECOND TERM
C  HAS BEEN USED.
C
      COMMON R,TABS,U,B11,B22,B12,POYNT1,POYNT2,PSTAR1,PSTAR2,P,PURE1
      COMMON PURE2,Y,PHI1,PHI2,T,NX
      DIMENSIONPOYNT1)101*,POYNT2)101*,P)101*,Y)101*,PHI1)101*,PHI2)101*
      IN = 1
      IO = 3
      PATM1 = PSTAR1/760.
      PATM2 = PSTAR2/760.
      RAD1 = 1. . )4.0*B11*PATM1/U*
      RAD2 = 1. . )4.0*B22*PATM2/U*
      VVOL1 = )1.0.SQRT)RAD1**/)2.0*PATM1/U*
      VVOL2 = )1.0.SQRT)RAD2**/)2.0*PATM2/U*
      VLOG1 = )2.0*B11/VVOL1* - ALOG)1.0.B11/VVOL1*
      VLOG2 = )2.0*B22/VVOL2* - ALOG)1.0.B22/VVOL2*
      PURE1 = EXP)VLOG1*
      PURE 2 = EXP)VLOG2*
      WRITE)IO,510*PURE1,PURE2
  510 FORMAT )//8H PURE1 =,F10.5,8H PURE2 =,F10.5*
      RETURN
```

```
      END
C
      SUBROUTINE POYCOR
C
C  SUBROUTINE POYCOR CALCULATES THE POYNTING CORRECTION FOR THE LIQUID
C  STANDARD STATE FUGACITY.  THE POYNTING CORRECTION IS A FUNCTION
C  OF TOTAL VAPOR PRESSURE.
C
      COMMON R,TABS,U,B11,B22,B12,POYNT1,POYNT2,PSTAR1,PSTAR2,P,PURE1
      COMMON PURE2,Y,PHI1,PHI2,T,NX
      DIMENSIONPOYNT1)101*,POYNT2)101*,P)101*,Y)101*,PHI1)101*,PHI2)101*
      IN = 1
      IO = 3
      READ)IN,400* VLIQ1,VLIQ2
  400 FORMAT)2F10.0*
      DO 410 I = 2,NX
      POYNT1)I* = EXP)VLIQ1*)P)I*-PSTAR1*/)U*760.0**
      POYNT2)I* = EXP)VLIQ2*)P)I*-PSTAR2*/)U*760.0**
      WRITE)IO,415* POYNT1)I*,POYNT2)I*
  415 FORMAT)2F10.5*
  410 CONTINUE
      RETURN
      END
C
      SUBROUTINE PHIVAP
C
C  SUBROUTINE PHIVAP CALCULATES THE VAPOR PHASE FUGACITY COEFFICIENT.
C  THE FUGACITY COEFFICIENT IS USED TO CORRECT THE ASSUMPTION OF AN IDEAL
C  VAPOR PHASE SOLUTION.  THE VIRIAL EQUATION TRUNCATED AFTER THE SECOND
C  TERM HAS BEEN USED.
C
      COMMON R,TABS,U,B11,B22,B12,POYNT1,POYNT2,PSTAR1,PSTAR2,P,PURE1
      COMMON PURE2,Y,PHI1,PHI2,T,NX
      DIMENSION X)101*,P)101*,G)101*,DGDX)101*,GAMA1)101*,GAMA2)101*,
     1PRES)101*,PARP1)101*,PIDEL)101*,A)101*,B)101*,W)101*,BE)101*,F)101
     1*,GE)101*,Y)101*,BMIX)101*,PATM)101*,RAD)101*,V)101*,PLOG1)101*,
     1PLOG2)101*,POYNT1)101*,PHI1)101*,YPREV)101*,POYNT2)101*,PHI2)101*
      IN = 1
      IO = 3
      WRITE)IO,520* B11,B22,B12
  520 FORMAT )3F10.2*
      DO 500 I = 2,NX
      BMIX)I*=B11*)Y)I***2*.2.0*B12*Y)I**)1.0-Y)I**.B22*))1.0-Y)I****2*
      WRITE)IO,530* BMIX)I*
  530 FORMAT)2F10.2*
      PATM)I* = P)I*/760.0
      RAD)I* = 1.0 .)4.0*BMIX)I**PATM)I*/U*
      V)I* = )1.0.SQRT)RAD)I***/)2.0*PATM)I*/U*
      PLOG1)I* = )2.0/V)I***))1.0-Y)I***B12.Y)I**B11*-ALOG)1.0.BMIX)I*/V
     1)I**
      PLOG2)I* = )2.0/V)I***)Y)I**B12 .)1.0-Y)I***B22* -ALOG)1.0.BMIX)I*
     1/V)I**
      PHI1)I* = EXP)PLOG1)I**
      PHI2)I* = EXP)PLOG2)I**
      WRITE)IO,540* PHI1)I*,PHI2)I*
  540 FORMAT )15X,2F10.5*
  500 CONTINUE
      RETURN
      END
```

VITA

Vinson Charles Smith

Candidate for the Degree of

Master of Science

Thesis: VAPOR-LIQUID EQUILIBRIUM IN THE THREE BINARY MIXTURES OF HEXANE, BENZENE, AND ETHANOL AT 25° C

Major Field: Chemical Engineering

Biographical:

Personal Data: Born in Tulsa, Oklahoma, February 28, 1945, the son of Mr. and Mrs. Charles E. Smith. Married to Anna Beth Luckinbill, Enid, Oklahoma, in May, 1968.

Education: Graduated from Edison High School, Tulsa, Oklahoma, in May, 1963; received the Bachelor of Science degree in Chemical Engineering from Oklahoma State University in 1967; completed requirements for the Master of Science degree in May, 1970.

Professional Experience: Employed as an engineer trainee with Union Carbide Corporation, Nuclear Division, Oak Ridge, Tennessee, Summer, 1966. Currently employed as a Chemical Engineer with Union Carbide Corporation Chemicals and Plastics Division, Houston, Texas. Member of American Institute of Chemical Engineers.